I. DETERMINATION OF THE QUANTUM YIELD OF THYMIDINE DINUCLEOSIDE IRRADIATED BY ULTRA-VIOLET LIGHT

II. STUDIES ON THE INACTIVATION BY ULTRA-VIOLET LIGHT OF T_4D BACTERIOPHAGE CONTAINING 5-BROMODESOXYURIDINE SUBSTITUTED DNA

Thesis by

Seymour A. Rapaport

In Partial Fulfillment of the Requirements

For the Degree of

Master of Science in Chemistry

California Institute of Technology

Pasadena, California

1962

ACKNOWLEDGEMENTS

I would like to express my gratitude to Dr. Max Delbruck and to Dr. Norman Davidson for their aid and advice in connection with the experiments described in this thesis. I found working with them a very rewarding and educational experience and am sure in subsequent years I will continue to benefit from their suggestions to me regarding approaches to and methods of doing research. Special thanks also goes to Dr. Harold Johns, Head, Department of Biophysics, Ontario Cancer Institute; it was indeed an invaluable and enjoyable experience to work beside such a competent investigator. Dr. John Smith made several suggestions that greatly facilitated the thymidine dinucleotide synthesis.

Many others also helped to make this work possible. In particular I would like to thank Drs. Robert Edgar, Ulrich Winkler (University of Frankfurt), Ann Roller, Jean Weigle, Charles Steinberg, Daniel Wolff, and the other professors and students of the Chemistry and Biology Departments at the California Institute of Technology who were of help to me. I would like to thank Zigmund Rapaport for his assistance during portions of these experiments and Phyllis Rapaport for typing portions of this thesis.

I am grateful to the Johns Hopkins Medical School for allowing me to spend my senior year of medical school on leave to Cal-tech and to the National Science Foundation for granting me a fellowship for this year.

ABSTRACT

It has been found that when frozen thymine solutions are irradiated by ultra-violet light a photoreversible steady state is formed between thymine and a thymine dimer. The suggestion has been made that such photoreversible chemical reactions might be involved in the photoreactivable mutations that occur upon irradiation of viruses with ultra-violet light. In order to give further credence to this thymine dinucleoside, TpT, was prepared and irradiated by ultra-violet light as described in Part I. A wavelength dependent photosteady state was found to be established by this, and the quantum yield of the reaction of TpT to its photoproduct determined. The existence of this steady state and the magnitude of the quantum yield (0.002) support the supposition that similar reactions may cause the photoreversible mutations in viral DNA.

Part II describes the determination of the action spectrum of inactivation of plaque forming ability of T_4 bacteriophages grown in the presence of the thymidine analogue 5-bromodesoxyuridine (5-BD). Under these conditions 5-BD is substituted into the DNA in place of thymidine. Such substituted DNA has been found to have increased sensitivity to UV light at 254 mμ. The action spectrum was determined to more precisely define this increase in sensitivity and to obtain additional information regarding the UV inactivation of DNA. It was found that 5-BD substituted T_4 was uniformly more sensitive to UV than unsubstituted T_4; this effect was most striking in the 302 to 334 mμ region where a factor of increased sensitivity up to 500 to 1000 times was noted. Furthermore, unlike unsubstituted T_4, killing of 5-BD substituted T_4 was found to follow "one hit" kinetics. The action spectrum indicated that 5-BD was directly involved in the initial steps of inactivation and was compatible with the possibility of transfer of absorbed light energy along the polynucleotide chain.

TABLE OF CONTENTS

	Title	Page
Part I		
	Introduction	1
	Synthesis of Thymidyl-(5'-3')-thymidine	2
	A. Preparation of 5'-O-Trityl-thymidine	3
	B. Preparation of 3'-O-Acetyl Thymidylic-5'-Acid	3
	C. Thymidyl-(5'-3')-thymidine Synthesis	4
	D. Separation of Thymidyl-(5'-3')-thymidine from the Reaction Mixture	5
	Monochromator Design and Calibration	7
	A. Irradiation Procedure for the TpT Solutions	8
	B. Energy Calibration	10
	Absorption Spectra	20
	Experimental Results, Kinetics, and Determination of Quantum Yields	21
	A. Results	21
	B. Kinetics	22
	C. Quantum Yields	23
Part II		
	Introduction	26
	Materials and Methods	28
	A. Media and Chemicals	28
	B. Phages	30
	C. Bacteria	31

TABLE OF CONTENTS

	Title	Page
	Monochromator and Optical Arrangements	31
	A. Apparatus for Radiation of Uncentrifuged 5-BD T_4 and T_6 and T_4 Phage Mixtures at 313 mμ and 334 mμ	31
	B. Irradiation of Ultracentrifuged 5-BD T_4	36
	Determination and Interpretation of Action Spectrum of Inactivation	37
	A. Determination of Inactivation Dose	37
	B. Interpretation of Action Spectra	38
	Results and Conclusions	44
	Summary of Propositions	49
Figures		50
Graphs		64
	Irradiations of TpT Solutions	
	Killing Curves of Ultracentrifuged 5-BD T_4	
	Killing Curves of T_6 and T_4 (313 mμ & 334 mμ)	
	Killing Curves of Uncentrifuged 5-BD T_4	
Appendix		94
References		100

INTRODUCTION

In recent years methods of chemical synthesis of nucleotides, nucleotide coenzymes, and polynucleotides have been developed (1). This has opened the way for wider physical and chemical studies of these molecules; such studies can be expected to be very fruitful in the future for the understanding of the biological functioning of these molecules in precise chemical terms. In this paper certain experiments which deal with one aspect of the chemistry of such compounds, their photochemistry, are presented.

It has long been known that irradiation with ultra-violet light (UV) is capable of bringing about mutagenic and other changes in the DNA of organisms. Two major classes of such photochemical changes have been recognized: those capable of being reversed by "visible light" (photoreactivable) and those which are irreversible by this means (non-photoreactivable). Beukers and Berends (2), Wulff and Fraenkel (3), and Wang (4) have recently demonstrated that UV irradiation of frozen thymine solutions leads to the formation of a photoreversible steady state between thymine and a thymine dimer. Wacker et al (5) have also recently demonstrated that UV irradiation of native DNA leads to the formation of thymine dimers. It thus seems possible that such photodimerization reactions might be associated with the photoreactivable mutations observed in the irradiation of native DNA. Indeed, as it turns out, the quantum yields of these photochemical reactions of thymine appear to be in the appropriate range (6). Experiments described here were carried out to further characterize such photochemical reactions in a thymine dinucleoside, thymidyl-(5'-3')-thymidine (TpT, I, Fig. 1).

The first portion of this thesis describes the synthesis of TpT and the determination of the quantum yield of the photochemical reaction which occurs when it is irradiated in solution. The second portion deals with the determination of the action spectrum of UV inactivation of 5-bromodesoxyuridine substituted bacteriophage. This is of interest because this inactivation apparently occurs at longer UV wavelengths than in unsubstituted DNA, very likely at higher quantum yields, and is entirely non-photoreactivable. These differences were more precisely defined by the experiments described, and some observations are made concerning them in view of the absorption spectrum of 5-bromodesoxyuridine.

SYNTHESIS OF THYMIDYL-(5'-3')-THYMIDINE

As early as 1952 J. D. Smith and R. Markham (7,8) described the isolation with paper chromatography and electrophoresis of several dinucleotides and dinucleosides from the deoxyribonuclease digestion of DNA. However, only "small" quantities of these substances were obtained.* The first chemical synthesis of a dinucleotide was performed by A. Todd and A. Michelson in 1955 (9) by condensing a suitable nucleoside and nucleotide.** The reactive sites of each of these reactants not involved in the formation of the 3'-5' internucleotide linkage were protected by combination with non-reactive chemical groups which were removed in the last stages of the synthesis. The synthesis and purification of these reactants were not without difficulty and side reactions

* Yields from similar experiments with RNA were less than 1% (10).
**3'-O-Acetylthymidine and Thymidine-3'-benzyl phosphorochloridate -5'-dibenzyl phosphate.

significantly reduced the dinucleotide yield. In more recent years H. Khorana and his associates have greatly simplified polynucleotide synthesis through the use of more easily obtained protected intermediates and anhydrous pyridine solutions with dicyclohexylcarbodiimide or p-toluenesulfonyl chloride for the polymerization reactions. The method described below for the synthesis of TpT uses the techniques elaborated by H. Khorana and his co-workers. Several steps were involved in the synthesis: the preparation of the intermediates, 5'-O-tritylthymidine and 3'-O-acetylthymidylic acid, the TpT synthesis per se, and the separation of the reaction products.

A. Preparation of 5'-O-Tritylthymidine (9,11,12)

1.2 g (5 mmole) of thymidine* were dissolved in 25 ml of dry pyridine**, and 1.75 g (6.4 mmole) of triphenylmethyl chloride added. The gold colored solution was allowed to remain at room temperature in a flask joined to a dehydrite drying tube for one week. It was then added dropwise to 125 ml of ice water with stirring whereupon a fine whitish precipitate was formed. This mixture was stirred in the cold for approximately 12 hours and then filtered. The residue was washed with ice water and dried at ca. 80° in a vacuum oven to constant weight. Yellow needle-like crystals were obtained by re-crystallization from a 1:9 acetone-benzene solution. M.P. 160-1° (uncorrected) Lit. M.P. 160° (11).

B. Preparation of 3'-O-Acetylthymidylic-5'-Acid (13)

A Dowex 50x4 (H^+) column was prepared and washed repeatedly

*All nucleotides and nucleosides used were obtained from Calif. Biochem. Corp.; all were Grade A.

**Dried with activated alumina and twice redistilled, 110-2° BP fraction used.

with approximately 3 N HCl and 2 N NaOH and then with 0.75 M pyridine in large excess. Next an aqueous solution of 0.16 mg (0.4 mmole) of thymidylate 2 $NH_4 \cdot 2H_2O$ was passed through the column and lyophilized to obtain the pyridinium salt of thymidylic acid. The resulting white particles were recrystallized from dry pyridine several times to give colorless crystals. These were next dissolved in 5 ml of dry pyridine, and 1.5 ml of acetic anhydride added. The solution was stirred at room temperature for about 8 hours in a stoppered flask protected from room light; after this it was cooled in an ice bath, and the reaction stopped by the addition of 10 ml of distilled water. The reactants were left at room temperature for approximately 90 minutes and subsequently lyophilized from water at 20° or less three times to give a yellow syrup. This was next lyophilized several times from dry pyridine, and the product used directly in the di-thymidine nucleoside synthesis as described below.

C. Thymidyl-(5'-3')-thymidine Synthesis (11)

Approximately 0.4 mmole each of 5'-O-tritylthymidine and 3'-O-acetylthymidylate were lyophilized several times from dry pyridine and then redissolved in 3.5 ml of pyridine to give a yellowish solution. After this 0.47 g. (2.3 mmole) N,N' dicyclohexylcarbodiimide (Cal. Biochem. Corp., Grade C) were added and the mixture kept at room temperature in room light for two days. It was next evaporated under a vacuum. Then 10 ml of 80% aq. HAc were added, and the mixture gently refluxed for 10 minutes to remove the protecting trityl groups; the mixture was then cooled and filtered. After this the filtrate was lyophilized, redissolved in a small volume of water, and maintained

with NaOH at pH 13 for about an hour to hydrolyze the 3'-O-acetyl groups. The product was thereupon passed through an Amberlite IR 120 (H^+) column and evaporated under vacuum to give transparent, colorless needles.

A small portion of the product was chromatographed on Whatman #3 paper in isopropanol: ammonia: water = 7:1:3 solvent and spots with the following R_f values were found by descending chromatography:

0.28 (Heavy Spot)
0.43 (Heaviest Spot)
0.73

These values compare well with those of Khorana et al (11):

0.25 for dithymidine-5'-pyrophosphate
0.45 for TpT
0.68 for Thymidine.

The above procedure was repeated using ca. 2 mmole of thymidylate 2 $NH_3 \cdot 2H_2O$ with corresponding scaling up of the other reactants and similar results were obtained.

D. Separation of Thymidyl-(5'-3')-thymidine from the Reaction Mixture

A 16 cm high by 4 cm diameter column of DEAE cellulose (Eastman Chemicals), prepared for use as described by Sober and Peterson (14),* was mounted on an automatic fraction collector. A portion of the TpT reaction mixture prepared above was adjusted to pH 8-9 with ammonia, applied to the top of the column, and washed in with a small volume of distilled water. Elution was begun using a linear gradient technique with triethylammonium bicarbonate.** Adequate resolution

* Spectra of aliquots of final washings showed less than 0.03 optical density units at 265 mμ.

**Triethylammonium bicarbonate has the advantage of giving only small amounts of residue upon lyophilization. It was prepared according to a method kindly communicated by M. Smith and H. Khorana: 140 ml redistilled triethylamine was added to 0.5 l water at 0°C through which

of the reaction mixture was obtained by using a linear gradient varying from 0 to 0.125 M triethylammonium bicarbonate. A typical run is shown in the automatic fraction collector tracing of eluent optical density at 254 mμ versus tube number (Fig. 2). The first of the four peaks obtained no doubt is due to thymidine. Aliquots of the third and fourth peaks were concentrated, passed through an Amberlite (H^+) column and chromatographed as above. This revealed peak 3 to be thymidylic acid and peak 4 to be TpT.

This indicated that a better resolution of the reaction mixture might have been obtained through the use of a phosphomonoesterase to convert the thymidylic acid present to thymidine. To avoid contamination of the TpT with thymidylic acid a very conservative division of the column's eluent was decided on. According to this only those tubes corresponding to the maximum optical density value registered from peak 4 and the immediate succeeding tubes were collected to prepare the TpT for the subsequent experiments. A re-run of a portion of this on the DEAE column gave only a single peak and only a single spot was noted when another aliquot was chromatographed.

Portions of this TpT solution were concentrated by lyophilization, passed through an Amberlite H^+ column and used in the experiments below.

(footnote cont'd from p. 5) carbon dioxide was bubbling; this was done for one hour. The carbon dioxide was allowed to continue to pass through the solution until the pH fell to 7.5 whereupon the volume was made up to one liter. This gave a one molar solution.

MONOCHROMATOR DESIGN AND CALIBRATION

All the irradiations described herein (except for 320 mμ) were performed with the emission lines of high pressure air or water cooled mercury vapor lamps (General Electric BH6 or AH6); these lamps emit a continuum of wavelenghts upon which the lines of the mercury spectrum are superimposed. The radiation was dispersed by a Young-Thollon monochromator (Fig. 3) formerly used by R. Dickinson (15). It consisted of two 30° natural quartz prisms 11.5 cm in width which could be simultaneously turned through equal angles by a knurled screw and two quartz collimating lenses of 11.7 cm diameter and 38 cm focal length. Different wavelengths were deviated through 45° and focused at the exit slit by the Young-Thollon system by changing the angle between the two prisms and the distances between the collimating lenses and the slits. Calibration curves for the scales involved in these operations were obtained with low pressure mercury sources (4 watt Hg lamp and a General Electric AH-4 lamp) by varying the settings of the collimating lenses and the angle between the prisms and observing the peaks of the mercury spectrum with a photocell mounted just behind the exit slit; the settings obtained with these lamps were identical to within about 1 mμ with those obtained with the AH6 or BH6 sources. Small discrepancies are probably explainable on the basis of the Stark Effect, pressure differences between lamps, and reversibility of lines. (See (16)--especially Chap. VII and Fig. 62.) The calibration curves for the linear scale used to turn the prisms paralleled a plot of index of refraction versus wavelength for quartz as it should from theoretical considerations (Appendix A); settings

for 297, 302, 313, and 334 mμ were checked with pyrex and glass filters and the setting for 404 mμ, by the color of the light. A further check on the calibration was provided with the exit slit curves obtained with a quartz spectrometer (200-500 mμ range, R. Freiss, Berlin-Steglitz, No. 502). (See below.)

The dispersion at the exit slit was measured by exposure of a photographic film at the exit slit; it was also calculated to vary at the exit slit from a maximum of 0.28 mm/mμ at 235 mμ to a minimum of 0.08 mm/mμ at 334 mμ in a way directly proportional to the change in index of refraction with wavelength for quartz. (Appendix A) The two methods of determination agreed for the shorter wavelengths but the small dispersion at longer UV wavelengths prevented accurate determinations with the film at these wavelengths.

A. Irradiation Procedure for the Thymine Dinucleoside Solutions

An air cooled BH6 mercury vapor lamp was used for these irradiations. The UV light emerging from it was focused on the entrance slit of the Young-Thollon monochromator by means of a condenser system consisting of two 5 cm plano-convex quartz lenses of 10.8 cm focal length. The entrance and exit slits were accurate to tolerances better than 0.05 mm. Slit widths were approximately 0.50 mm or less.

The exit slit assembly for these irradiations allowed continuous monitoring of the radiation intensity: A brass plate with an approximately 6x9 mm rectangular diaphragm centered relative to the UV beam emerging from the exit slit was mounted on a stand 3.5 cm behind the exit slit of the monochromator. A 1 x 1 x 4.5 cm quartz Beckman cell could be inserted behind this diaphragm so that all the radiation

passing through the diaphragm would also pass through the Beckman cell without striking its walls. The same photocell which was used throughout all the irradiation and calibration experiments to measure the radiation emerging from the exit slit could be mounted so that it was behind the space occupied by the Beckman cell (with or without the cell in place) to intercept all the radiation that passed through the diaphragm and the cell (Fig. 5). A vertically mounted mirror tilted at a 45^{o} angle to the axis of the UV beam emerging from the exit slit was placed in front of the brass plate. The mirror itself contained a hole which was arranged so as not to block the portion of the UV beam passing through the brass diaphragm and reflected to the monitoring photocell a portion of the radiation emerging from the exit slit; in this way variations of the lamp intensity (ca. about 5% or less) could be monitored. A stirring rod attached to a 3350 rpm motor extended down into the Beckman cell to a point just above the irradiated portion and provided adequate mixing of its contents.

At the beginning of each irradiation experiment about 2.5 ml* of the TpT solution were placed in the Beckman cell. The optical density of the solution was measured on a Beckman DU spectrometer at 265 mμ and at the wavelength at which the TpT was to be irradiated, the stirring motor started, and then the UV beam was permitted to pass through the diaphragm and irradiate the approximately 6x9x10 mm volume near the bottom of the Beckman cell. At intervals of 13 to 105 minutes, during which the observed variations in intensity were always less than 1.5% (except in the 297 mμ runs where they

* The volume was determined accurately by weighing and assuming a specific gravity of 1.00 for the TpT solution.

were up to 4-6%), the UV beam was interrupted by closing a shutter behind the second collimating lens of the monochromator. The optical density of the irradiated solution was then again determined at 265 mμ. The energies corresponding to the observed changes in optical density were determined by measuring the radiation incident on the TpT solution with photometer A (Fig. 5) without the Beckman cell in place each time the OD of the irradiated solution was determined. The time interval during which this radiation was allowed to fall on the solution was measured with a stop watch; appropriate corrections for the slight fluctuations in intensity were made from the observed monitor photometer (photometer B, Fig. 5) readings and the ratio of the readings of photometers A and B when the Beckman cell was not in place. In this way the energy increments reaching the TpT solutions were determined in terms of a reading on photometer A times the number of seconds this flux fell on the solution. These energy doses were expressed as "photometer-seconds" or "p-seconds." To convert them into ergs it was necessary to calibrate photometer A; because of the variation of sensitivity of the photometer with wavelength, this was done at several wavelengths.

B. Energy Calibration

Energy doses were measured with an RCA Type 935 UV phototube (A, Fig. 5) whose output was fed into an Eldorado Electronics (Berkeley, Calif.) Model PM 201 photometer that had a rated accuracy of 1%. The phototube was coated with an RCA S5 surface whose response was wavelength dependent; the phototube was most sensitive at 340 mμ, and its response fell off rapidly below 225 mμ and above 450 mμ.

UV doses were initially measured in terms of "p-seconds." The

absolute calibration in terms of ergs or quanta per p-second was obtained in two ways: (1) by the use of an actinometer substance and (2) by the use of a thermopile and standard lamp in conjunction with a sensitive galvonometer.

The monochromator arrangement for these calibrations was identical with that described above.

(1) Actinometry

Studies of Harris et al (17, 18, 19) have shown that UV in the range of 248 to 334 mμ will transform malachite green leuocyanide (MGL) into a very highly absorbing blue photoproduct with a quantum yield of 1.00. This property makes it an excellent actinometric substance for absolute energy calibrations.

In principle these calibration experiments consisted of first measuring the UV intensity at a given wavelength with the photometer, and then exposing a MGL solution of high optical density in the UV to the UV beam for a known time. The optical density of the MGL plus photoproduct solution was then determined at 620 mμ, the absorption maximum of the photoproduct. Since MGL itself does not absorb at 620 mμ, the $OD_{620m\mu}$ in conjunction with the molar extinction coefficient of the photoproduct at this wavelength, 9.49×10^4, (19) permits the number of molecules of photoproduct formed to be calculated. In the present case this number is equal to the number of quanta absorbed, since the quantum yield is known to be 1.00. This value then could be compared with the observed number of "p-seconds" measured with the photocell to obtain the desired calibration. In practice it was necessary to apply several correction factors to this method; these are described below.

(a) Materials:

Approximately 1-2 millimolar solutions of MGL* (MW 355) in 95% ethanol and 5 x 10^{-3} M HCl were prepared. The density of the solvent was determined to be 0.807 g/ml by accurately weighing 50.00 ml so that the volume could be subsequently determined by weighing. Where possible the MGL solutions in the radiation cell were kept covered to minimize evaporation losses during the course of the experiments.

(b) Irradiation Procedure:

The readings of the monitor and the photometer A (Fig. 5) were first determined without the cell in place. The cell was next filled with approximately 2 ml of an appropriate 95% ethanol-HCl dilution of the above MGL solution; the actual volume was accurately determined by weighing. The OD_{λ} **, i.e., the OD at the wavelength λ at which the irradiation was being performed, was generally about 1.5; in all cases it was greater than one and it never varied significantly in the course of the radiation. The $OD_{620m\mu}$ initially was less than 0.017 in all cases.

The MGL was next irradiated to an $OD_{620m\mu}$ of about 0.2. During this time the monitor was observed and from its readings and the previously determined ratio between its readings and those of the photometer the number of p-seconds incident on the cell during this period was obtained.

After the $OD_{620m\mu}$ and OD_{λ} had been determined, the solution

* Kindly furnished by Dr. R. Sinsheimer.
**All optical densities were determined in duplicate on a Beckman DU spectrometer whose wavelength scale calibration had been checked with the 546.1 line of a mercury arc and the 620 mμ peak of the MGL photoproduct.

was again irradiated until an $OD_{620m\mu}$ of about 0.4 was obtained; the same measurements were performed as before, and the solution was weighed to correct for volume lost by evaporation and by retention of solution on the stirrer after the cell had been removed for the first OD measurement. Except for 320 mμ the wavelengths chosen for calibration corresponded to the lines of the mercury spectrum.

(c) Correction Factors:

Since the solutions were not totally opaque (OD_λ varied from about 1 to 1.5), a small portion of the incident photons was transmitted by the MGL solution. The fraction of photons absorbed is given by $(1 - 10^{-OD_\lambda})$. However, the MGL photoproduct (PP) also absorbs photons at wavelength lambda so that only a portion of the fraction of photons absorbed by the irradiated solution are absorbed by the MGL. This effect increases as more photoproduct is formed during the course of the irradiation, but it never amounted to a correction of more than 3-4%; the proportion of photons absorbed by the MGL is given by the ratio OD_{MGL}/OD_{total}, both at lambda.

The combined effects of these two corrections is thus to reduce the number of incident photons by the following factor to obtain a measure of those photons that are absorbed by the MGL:

$$(1 - 10^{-OD_\lambda}) \frac{OD_{MGL}}{OD_\lambda} = (1 - 10^{-OD_\lambda}) \left(\frac{OD_\lambda - (OD_{pp})_\lambda}{OD_\lambda} \right)$$

$$= (1 - 10^{-OD_\lambda}) \times \left(1 - \frac{(OD_{pp})_{620}}{OD_\lambda} \times \left(\frac{\epsilon_\lambda}{\epsilon_{620}} \right)_{pp} \right)$$

since for the photoproduct $\frac{\epsilon_\lambda}{\epsilon_{620}} = OD_\lambda / OD_{620}$.

The observed values of p-seconds corresponding to the measured $OD_{620m\mu}$ values were corrected by this factor and then the observed $OD_{620m\mu}$'s were plotted as a function of these corrected p-second values. Straight lines were obtained, the slopes of which gave the number of p-seconds per unit $OD_{620m\mu}$ change at each wavelength.

Three other corrections were now applied to these values of slope to change them into quantities that correspond to the number of p-seconds incident on the front surface of the Beckman cell per unit change in $OD_{620m\mu}$:

Since the front wall of the quartz Beckman cell and the ethanol solvent both absorbed photons, it was necessary to correct for the photons "stolen" by these substances. The correction factor for the reflection and absorption that occurred at the front wall of the Beckman cell was obtained by measuring absorption spectra of the ethanol-HCl solvent in the 1 cm cell used for actinometry and in a 10 cm quartz cell.

If we let D_w be the effective optical density of the front or back wall of the cell (including diminutions of intensity due to reflections at both interfaces and absorption in the wall), U_a, the absorption coefficient of the alcohol, and D_1 and D_{10} the measured optical densities of the 1 cm and 10 cm cells respectively, then

$$D_1 = 2\ D_w + U_a$$

$$D_{10} = 2\ D_w + 10\ U_a.$$

These equations yield by subtraction

$$U_a = (D_{10} - D_1)/9.$$

This is the alcohol correction; it rose progressively from 1% at 334 mμ to 12% at 255 mμ and then more steeply to 36% at 225 mμ. The corresponding fraction of photons "stolen" from the MGL was calculated from these OD values.

Substitution of the last result in the first equation above gives

$$D_w = (D_1 - U_a)/2.$$

This is the front wall correction; it increased from about 8% at 220 mμ to a maximum of 12.6% at 240 mμ and then rapidly decreased to 4% at 270 mμ above which it remained constant at 4%.

Finally a correction was made so as to standardize all the dose rates to a total volume of 2.00 ml in the Beckman cell. In addition corrections for evaporation of the ethanol and the amount of ethanol left on the stirring rod when the cell was removed for weighing or OD determinations were included.

Next the number of quanta required to produce an OD change of 1.00 was determined from the following equations:

(1) $\Delta OD = \epsilon \Delta c \quad L$ where,

ϵ = extinction coefficient of PP at 620 mμ
L = path length of Beckman cell, 0.999 cm
c = concentration of PP in moles/liter

(2) $\Delta c = \Delta n/V\ N_o$ where,

Δn = number of molecules of PP formed from MGL
= number of quanta absorbed by substrate
V = Volume of solution, 2.00×10^{-3} l
N_o = Avogadros number

and so (3) $\Delta n/\Delta OD = N_o\ V/L\ \epsilon$

$$= \frac{6.023 \times 10^{23} \times 2.00 \times 10^{-3}}{9.49 \times 10^{4} \times 0.999}$$

$$\Delta n/\Delta OD = 1.267 \times 10^{16} \text{ quanta/OD unit.}$$

The number of photons incident on the front surface of the Beckman cell per p-second was obtained by dividing the above number by the corrected ratios of p-second/OD.

(2) Calibration with Thermopile and Standard Lamp with the Aid of a Sensitive Galvonometer

These calibrations were performed by first determining the reading of the photometer being calibrated and that of the monitor; the arrangement of the photocells was as above (Fig. 5), and the Beckman cell was not in place. Next the intensity of the UV beam emerging through the diaphragm was determined with the photometer. The photometer was then replaced by a vacuum thermopile joined to a galvonometer. The thermopile was positioned directly behind the diaphragm so that it intercepted all the light passing through it. The UV beam was interrupted a number of times by a shutter at the monochromator's entrance slit and the corresponding galvonometer deflections determined. Previously the thermopile-galvonometer combination had been calibrated with a standard lamp that emitted a known amount of power per sq. cm at a given distance; for this calibration against the standard lamp the brass diaphragm was fixed to the front of the thermopile so that the geometry relative to the thermopile's sensitive surface would not be altered. From this previous calibration and the observed galvonometer deflection due to the UV beam the flux of the latter was calculated. Observations of the monitoring photometer verified the constancy of the UV lamp intensity during the procedure. All this work was done in a darkened room so as to minimize variations in ambient heat and light sources.

(a) Materials and Equipment

Carbon Filament Standard Lamp C-966 from the National Bureau of Standards.

Rating: Amp.	Volts	Radient Flux Density at 2 m
0.300	72.19	46.5 microwatts/cm^2
0.350	83.69	65.2
0.400	95.38	86.5

John Fluke Model 803 Precision DC-AC Differential Voltmeter; accurate to 0.05% in the range of 0.1 to 500 v DC and capable of resolving 0.01 volts in the range of 50 to 500 v DC. (John Fluke Corporation, Seattle, Wash.)

Compensated vacuum thermopile from Charles M. Reeder Co. (173 Victor Ave., Detroit 3, Mich.); sensitivity approximately 0.2 μvolt/ μwatt/cm^2.

Leeds and Northrup DC Moving Coil, Reflecting Galvonometer, 2284b; Int. Res. 13.5 ohms, XDR 8 ohms, Period 6.2", Sensitivity 0.02 μv/mm.

Leeds and Northrup Standard Resistor; 1.00002 ohms to 0.005%.

(b) Arrangement of Apparatus

The arrangement of the standard lamp and the thermopile (Fig. 6) was as suggested by the National Bureau of Standards (20).

The standard lamp circuit was arranged as shown in Figure 7. The current in the circuit was determined by measuring the voltage drop across the standard resistor and the voltage across the lamp was determined directly as indicated. It was found that the current specified by the NBS was obtained when the lamp voltage was

adjusted to the corresponding specified value; because of this only the lamp voltage was monitored during most of the experiments. The approximately 100 v DC line voltage was stepped down with a variable resistor and remained sufficiently constant to allow the voltage across the standard lamp to be kept within approximately 0.04 volts of the specified NBS value.

In order to obtain reproducible results it was found necessary to use the same portion of the galvonometer scale for all deflections. This was made possible through the use of a biasing circuit in parallel with the galvonometer; the zero point of the galvonometer could be adjusted by this circuit (Fig. 8).

All the connections in the circuits connected to the galvonometer were soldered. The thermopile leads were connected directly to the galvonometer.

(c) Method

The voltage on the standard lamp was first adjusted to 95.38 v and then to 83.69 v and a series of galvonometer deflections resulting from opening and closing the shutter on the baffle board between the lamp and the thermopile obtained.

In order to correct for drifting the net galvonometer deflections were obtained by subtracting the average of two successive swings to one side from the intermediate deflection to the opposite side. Observed deflections were of the order of 15 cm. From the NBS values of the flux density at 2.00 meters and the area of the brass diaphragm (as determined with a travelling microscope) the number of microwatts reaching the sensitive surface of the thermopile was calculated and

hence the number of ergs/second/cm galvonometer deflection found. The values from two separate calibrations agreed to within 1%.

After calibration of the thermopile-galvonometer system against the standard lamp, the brass plate was removed from the thermopile and replaced to its position behind the exit slit of the monochromator. The monochromator was then set at the wavelength at which the photometer was to be calibrated and the slits adjusted to a value that would give about 15 cm galvonometer deflection.* The intensity of the radiation was then measured with the photometer. Next the thermopile was placed directly behind the diaphragm and a series of galvonometer deflections were produced by cutting off the UV at the entrance slit of the monochromator several times with a shutter. By use of the previous calibration of the galvonometer the number of ergs/sec. corresponding to the observed photometer readings was obtained.

(d) Corrections

Since the thermopile used had a quartz surface and since the standard lamp radiation was principally in the infra-red (21) while the wavelengths to be calibrated were in the UV region, a correction should be applied for the difference in reflection and absorption of the thermopile window for radiation of these different wavelengths. In order to determine these correction factors the diminution of the galvonometer deflection when a quartz plate identical to that of the thermopile** was held directly in front of the thermopile was deter-

* The slits were 0.25 mm or less in all cases.
**Kindly furnished by C. M. Reeder Co.

mined for each type of radiation the thermopile was exposed to. By this means the quartz plate was found to absorb 7.4% of the standard lamp radiation and from 7 to 11% of the UV depending on the wavelength. The net correction factors so determined were applied to the results obtained above.

The results of the calibration obtained with the thermopile agreed very closely (to the order of 1%) with the MGL calibration for wavelengths less than about 300 mμ; for longer wavelengths the thermopile calibration values were progressively greater than the values obtained with actinometry. The maximum discrepancy (10%) occurred at the longest wavelength calibrated, 334 mμ. A contributing factor to this discrepancy is the presence of scattered light of different wavelengths than those being calibrated at the exit slit of the monochromator; the absorption coefficient of MGL falls rapidly with increasing wavelength above 300 mμ so that scattered radiation of these longer wavelengths would have less effect in the MGL calibrations than in the thermopile calibrations. For the longer wavelength settings the intensity of the light above 300 mμ was probably of the order of 2 to 10% of the intensity of the mercury line at which the monochromator was set.

ABSORPTION SPECTRA

All absorption spectra were taken on continuous recording Cary spectrophotometers (Model 12 or 13) under the conditions indicated.

EXPERIMENTAL RESULTS, KINETICS, AND DETERMINATION OF QUANTUM YIELDS

A. Results

In the course of the irradiation experiments it was noted that the optical density of the irradiated TpT solution at 265 mμ progressively decreased. This was ascribed to the formation of a photoproduct (Fig. 1, II) involving the formation of an intramolecular cyclobutane ring structure akin to the thymine dimer formed by irradiating frozen thymine solutions (2,3,4). (See III, Fig. 1.)

Support for this interpretation was obtained from the demonstration of a photosteady state whose position is markedly wavelength dependent: Solutions of TpT could be irradiated at one wavelength (e.g., 265 mμ) with a progressive decrease in the optical density at 265 mμ and then irradiated at another shorter wavelength (as 235 mμ) with a subsequent increase in the optical density at 265 mμ. Repeat irradiation at the former wavelength (265 mμ) would now produce a progressive decrease in $OD_{265m\mu}$ as before. Similar wavelength dependent equilibrium states have been demonstrated in the irradiation of thymine and thymine dinucleotide solutions (6).

The molar absorption coefficients of the photoproduct of TpT are not known; however, the thymine dimer formed by irradiating frozen thymine solutions is known to have the order of 1/200th the absorption of thymine at 265 mμ and above, and it would be expected if the TpT photoproduct resulted in the loss of the conjugated ring structure as postulated above that this photoproduct should also have a very low extinction coefficient here. Thus absorption of ultra-violet light by this photoproduct should be relatively

negligible at these wavelengths.

With the use of these assumptions the decrease in the OD of the irradiated TpT solutions was taken as a measure of the quantity of TpT that had reacted photochemically. The optical density of the irradiated solution observed during the course of the experiments was plotted as a function of the total energy (Graphs 1, 2, 3).

B. Kinetics

In the course of these irradiations the amount of TpT photoproduct formed was not enough to cause an appreciable reverse reaction of photoproduct to TpT. Therefore, the reaction rate, - dc/dt, could be considered to follow a simple exponential law:

$$- dc/dt = a\ c\ I$$

where I = intensity of radiation (Einstein/cm^2 sec.)
c = molar concentration of TpT
a = constant, the actinity coeff. (cm^2/Einstein)

All the quantities on the right hand side of the above equation are uniform throughout the stirred irradiated volume except for the intensity which decreases due to absorption as the ultra-violet light travels through the solution. If D equals the optical density of the solution and L is the depth of the Beckman cell, the depth average of the intensity $I = I_o\ 10^{-Dx/L}$ is given by

$$I_{av} = (1/L)\left(\int_0^L I_o\ 10^{-DX/L}\ dX \right.$$
$$= I_o\ (1 - 10^{-D})/2.303\ D.$$

Substituting for I_o the total incident flux F (in Einsteins/sec.) as measured by the photometer divided by the cross-sectional area A of the cell, one obtains the following equation

$$I_{av} = (F/A) \times (1-10^{-D})/2.303\ D$$

and the observed average reaction rate becomes

$$(-\ dc/dt\ )_{av} = a\ c\ I_{av}$$

or $$(-\ dc/dH\ )_{av} = a\ c$$

where $dH = I_{av}\ dt$ and H equals the total average incident flux.

Plots of c vs. H were made for each experiment, and from these values of $(dc/dH)_{av}$ were obtained. TpT concentrations were determined using the value of $\epsilon_{267m\mu}$ equals 18,500 as determined by Gilham and Khorana (11); the corresponding quantum yields were obtained from the relation

$$a = 2.303 \times 10^{3}\ \phi\ \epsilon\ .$$ (See Appendix B.)

C. Quantum Yields

The quantum yields determined this way are shown below.

Wavelength	Quantum Yield
265 mμ	0.003
280 mμ	0.002
297 mμ	0.0008

The value for 297 mμ at best can only be considered an indication of the order of magnitude of the quantum yield at this wavelength because of the smallness of the observed changes in optical density and the prolonged irradiation times. It is interesting that there appears to be a gradual decrease in quantum yield with increasing wavelength as in the case of thymine and thymine dinucleotide (6).

These results together with the previously mentioned observations of a readily reversible strongly wavelength dependent steady state for UV irradiated TpT solutions seem consistent with the following

picture:

$$TpT \xrightarrow{h\gamma} \widehat{TpT}^{*} \qquad \text{Rate} = \phi_1 I_o \epsilon_{TpT}$$

$$\widehat{TpT} \xrightarrow{h\gamma} TpT \qquad \text{Rate} = \phi_2 I_o \epsilon_{\widehat{TpT}}$$

with ϕ_1 and ϕ_2 much less dependent on wavelength than are ϵ_{TpT} and $\epsilon_{\widehat{TpT}}$. At any one UV wavelength then a steady state would result from these two reactions, and due to the relative wavelength independence of the quantum yields this steady state would change dramatically with wavelength in a way predictable from the absorption coefficients of TpT and $\widehat{TpT}$. Since presumably the absorption coefficient of $\widehat{TpT}$ becomes very small compared with that of TpT for wavelengths greater than about 240 mμ, long wavelength light would tend to result in an increased proportion of molecules in the $\widehat{TpT}$ form while shorter wavelength UV would be expected to increase the proportion in the $\widehat{TpT}$ form.

These results and interpretations support the hypothesis that similar "dimerization reactions" occur in UV irradiated DNA and account for at least a portion of its photoreactivability.

---

* That is, TpT photoproduct--presumably an isomer of II, Figure 1.

PART II: STUDIES ON THE INACTIVATION BY ULTRA-VIOLET LIGHT OF T_4D BACTERIOPHAGE CONTAINING 5-BD SUBSTITUTED DNA

INTRODUCTION

Increased sensitivity to ultraviolet light and to "visible light" have been observed for bacteria (22) and viruses (23) grown in the presence of the thymidine analogue 5-bromodesoxyuridine (5-BD) or in the presence of 5-bromouracil (5-BU), an analogue of thymine. Greer (22) reported the increased sensitivity to be proportional to the extent of the 5-BD incorporation into DNA as determined by digestion with enzymes or by hydrolysis followed by chromatography. He noted a maximum increase of sensitivity to the UV from a germicidal lamp of 65 times that of unsubstituted bacteria. With "visible light" from "GE 40 watt fluorescent lamps" 1000 ft-candles reduced the viable bacteria titer by a factor of 1.5 to 2.5 in 4 hours. Stahl et al (23) also reported increasing UV sensitivity with 5-BD substitution for UV from a germicidal lamp; in this instance the degree of substitution was judged by the density of the bacteriophage as determined in an equilibrium density gradient ultra-centrifugation. For 5-BD T_2u the maximum increase in sensitivity over unsubstituted phage was 75 fold for "visible light."

Observations of increases in mutation frequency for organisms grown in 5-BD media (24,25) first suggested that 5-BD was incorporated into the DNA of these organisms. Direct chemical studies by Dunn and Smith (26,27) and by Zamenhoff and Griboff (28) subsequently showed that under the types of growth conditions used in the experiments mentioned above and described herein the 5-BD is incorporated into DNA in such a way that the mole fraction of thymine plus 5-BD per 100 DNA bases remains essentially constant for the given organism. The maximum degrees of 5-BD substitution for thymine reported are 79% (26)

and "over 80%" (unpublished results of M. Meselson et al as reported in (23).

Thus one might expect the observed increases in UV killing of such organisms to be related to photochemical changes in their 5-BD substituted DNA. On the other hand, it is conceivable that other effects of 5-BD substitution might lead to increased UV sensitivity. For example, Dunn and Smith (27) have observed small increases in 6-methylamino-purine incorporated into 5-BD substituted DNA; the data of these workers, however, simultaneously rule out any extensive substitution of such base analogues. In addition, there are several facts which suggest significant and unique photochemical events occurring in the 5-BD substituted DNA that relate to the increased sensitivity. The direct proportion which has been noted between the extent of 5-BU substitution and the degree of increased UV sensitivity suggests that the increased sensitivity is due to photochemical reactions involving the 5-BD in these organisms' DNA. Photochemical studies provide additional support for this: The lack of photoreactivation in 5-BU containing organisms (23), or its decrease (27), indicates that the photochemical changes accounting for the inactivation of these organisms differ notably from those occurring in their unsubstituted counterparts. If, as has been reported (26,27) the absorption spectrum of 5-BU substituted virus is very similar to that of unsubstituted viruses, the former's increased UV sensitivity would imply an inactivation process that proceeds with a higher quantum yield than UV inactivation of unsubstituted phage. In addition, the 5-BD absorption spectrum appears to generally parallel that of thymidine with a slight shift to longer wavelengths (Fig. 9). Between 285 and 310 mμ the ratio of the molar

absorption coefficient of 5-BD to that of thymidine under similar conditions increases progressively from 2 to over 50; also above approximately 315 mμ it shows a definite change of slope relative to thymidine. This portion of the spectrum may merely represent the tail of the absorption band centered about the 280 mμ pi to pi* band of thymidine. On the other hand, it could also be the tail end of the absorption band of another electronic transition which is not present or at least not as prominent in thymidine at these wavelengths. In this latter case it is possible that the increased sensitivity of 5-BD substituted DNA at wavelengths greater than 300 mμ is related to photochemical events proceeding from the excited state of this transition; if so, supporting evidence for another means of UV inactivation from this state might be obtained from a study of the action spectrum.

In order to test further the premise of direct involvement of 5-bromodesoxyuridylic acid in the photochemical inactivation of organisms with 5-BD substituted DNA and to clarify the nature of the sensitivity to "visible light" it was decided to determine the action spectrum of inactivation of plaque forming ability of 5-BD substituted T_4 bacteriophage. The action spectrum of T_4 bacteriophage grown under identical conditions except for the substitution of thymidine for 5-BD was determined as a control; the action spectrum of T_6 bacteriophage, which served as an internal dosimeter in some of the radiations, was also determined. This information should also be of interest in certain other experiments concerning the functioning of DNA in view of the possibility of selectively inactivating 5-BD portions of DNA genetically incorporated into an organism with an otherwise unsubstituted DNA.

MATERIALS AND METHODS

A. Media and Chemicals

5-BD--California Biochemical Corporation, Grade A (i.e., "no detectable organic impurities"); California-Biochemical reported no substance used in the preparation could account for the absorption observed about 300 mμ. MP sharp at 179-180° vs. 181-183° reported by Barbos et al (29). Chromatography in a butanol system (Cal-Biochem.) and in isopropanol: NH_3: H_2O = 7:2:1 indicated no impurities when viewed with 254 mμ and 320 mμ light; subsequent spectrum of the eluted spot again showed the long wavelength shoulder.

Thymidine--Cal-Biochem., Grade A.

Bottom Agar--Per liter demineralized water: 10 g bacto-agar (Difco), 13 g bacto-tryptone, 8 g NaCl, 2 g sodium citrate, 1.3 g glucose. Top layer agar identical except 3 g glucose and 6.5 g bacto-agar used per liter.

Tryptone Broth (TB)--Per liter of demineralized water: 10 g bacto-tryptone, 5 g NaCl; pH adjusted to 7.4 with NaOH.

Hershey Broth (HB)--Per liter of demineralized water: 8 g nutrient broth, 5 g bacto-peptone, 5 g NaCl, and 1 g Glucose; pH adjusted to 7.2-7.4 with NaOH.

Phosphate Buffer (BU)--Per liter of demineralized water: 7 g Na_2HPO_4, 3 g KH_2PO_4, 2 g NaCl.

Medium I of Stahl--Per liter of demineralized water: 7 g Na_2HPO_4, 3 g KH_2PO_4, 1 g NH_4Cl added before autoclaving and 1 ml M $MgSO_4$, 2 ml 25% (w/v) NaCl, 10 ml 10% glucose, 0.2 ml 0.5 M $CaCl_2$, and 10 ml 5% vitamin-free casein hydrolysate added after autoclaving.

Medium II of Stahl--Medium I plus 25 mg Xanthine and 10 mg Uracil

per liter added before autoclaving and 10 mg aminopterin, 200 mg 5-BD, and 10 mg gelatin per liter added after autoclaving.

Platings and phage titers were done according to the methods outlinted by Adams (30). All work with 5-BD substituted phage and all platings were done under yellow light.

B. Phages

Several phage stocks were used: The T_6 stock was from a HB culture diluted at least 1/100 into buffer prior to irradiation; it was necessary to prepare a higher titer stock from this original one for the long wavelength T_6-T_4 radiations. This latter stock was also diluted at least 100 fold from a HB medium prior to irradiation. 5-BD T_4 stocks were prepared according to Method I of Stahl et al (23). An action spectrum was determined using an uncentrifuged preparation of these phages in Medium I of Stahl from which they were diluted by at least 1/44 into buffer before irradiation; the OD_{max} of a 1 cm path length of these phage mixtures was 0.06. Four hundred ml of another 5-BD preparation made by the same method from T_4 os^r r^+* were concentrated and separated from debris by three centrifugations in a Model L Spinco centrifuge and then spun in a CsCl gradient at a density of 1.507 g/ml initially; the resulting density gradient distribution was collected in 5 drop fractions into separate tubes (Fig. 10). Fraction number 13 seemed to be the heaviest fraction with sufficient titer to determine an action spectrum, and a portion of it together with a T_6 marker phage was rebanded in another density gradient at 30,000 rpm for 18 hrs. At the start of the run the density was adjusted to 1.525 with CsCl.

* That is, os^r: osmotic shock resistant and hence capable of ultracentrifugation in a CsCl density gradient; r^+: plaque type mutant.

This distribution is shown in Figure 11 from which it is apparent that the half-maximum-titer band widths are of comparable size for the T_6 and ultra-centrifuged fraction 13 5-BD T_4.* This would argue for a relatively homogeneous amount of total 5-BD substitution in the 5-BD phages centrifuged. Another T_4 os^r r^+ stock was prepared as a control stock as in Method I of Stahl (23) except for the substitution of an equivalent amount of thymidine for the 5-BD; these were kept in the corresponding Medium of Stahl and diluted by at least 1/100 prior to irradiation.**

C. Bacteria

Platings were done on S/6 and B/4, mutant derivatives of E. Coli B. Log phase cells were used for all platings.

MONOCHROMATOR AND OPTICAL ARRANGEMENTS

Some modifications in the optical system described above were made for the irradiation of uncentrifuged and ultra-centrifuged 5-BD phage:

A. Apparatus Used for Irradiations of Uncentrifuged 5-BD Phage and T_6 and T_4 Phage Mixtures at 313 mμ and 334 mμ.

Irradiations were performed using a water cooled AH6 for the uncentrifuged 5-BD phage and a BH6 bulb for the T_6 and T_4 (unsubstituted) irradiations; this arrangement was used for the latter irradiations

* The distribution curves are asymmetrical about the peak due to heavy phages which stick to the walls--or stay in layers close to the walls-- of the tube that they are spun in, and subsequently emerge through the pin-hole of the bottom of the centrifuge tube. For this reason the half-width was determined by doubling the difference in abscissas between the maximum and the half-maximum titer point to its left.

**The aid of Drs. Ann Roller and Jean Weigle in the preparation of the ultra-centrifuged stocks is gratefully acknowledged.

because it allowed energy to be delivered at more rapid rates. A pre-dispersing element was placed in front of the entrance slit of the monochromator. This consisted of a 30^{o} quartz prism and two 5 cm plano-convex quartz lenses of 10.8 cm focal length arranged as a condensing system with one lens on either side of the prism; the radiation passing through the pre-dispersing element was focused on the entrance slit of the monochromator. Different entrance and exit slits were used for these irradiations only; they had tolerances accurate to better than 0.125 mm. Slit widths for all radiations were set to 0.4mm or less. For irradiations above 297 mμ pyrex and/or glass filters with optical density curves as shown in Fig. 12 were placed either between the radiation vessel and the exit slit or between the pre-prism and the entrance slit. This was done as a safe-guard against possible artifacts from scattered short wavelength UV; these would have been especially misleading in the case of the radiations above 297 mμ due to the rapid decline in virus sensitivity at these wavelengths. A simple test that inactivation observed above 300 mμ was not due to shorter wavelength light was performed by adding an extra pyrex filter during one of the irradiations at 313 mμ. This caused no change in the observed killing rate. Similar procedures with glass plates in the 313-334 mμ range had no effect on the action spectrum.

Spectra of the light emerging at the exit slit were taken under the same conditions as those under which the irradiations were performed (except filters were not used) with a quartz spectrometer tilted so that its entrance slit crossed the exit slit of the monochromator (Fig. 13 a and b); a photomultiplier mounted at the exit slit of the

spectrometer measured the relative intensity of the light at various wavelengths. The wavelength calibration of the spectrometer only roughly corresponded to that of the monochromator due to the fact that the center of its slit did not coincide with that portion of the monochromator exit slit which was admitting light to it--only the relative intensities of the peaks and the other unwanted radiations are relevant. Consideration of these results in view of the optical density curves of the filters used (Fig. 12) and the observed differences in viral sensitivity with wavelength (Fig. 14) indicate that these sensitivity differences cannot be attributed to the effects of scattered light.

The exit slit assembly was also different for the irradiations of the uncentrifuged phage: A total of 0.55 ml of the diluted phage suspension was placed in a 2.5 cm high cylindrical quartz cell of 0.5 cm internal diameter. The cell was mounted about 0.7 cm behind the exit slit and was rotated by a 125 rpm motor. Vertical mixing was accomplished by a fixed stirring rod that extended down one side of the cell to its bottom. Tests with ink showed that the mixing was adequate.

The cell intercepted essentially all of the radiation that emerged from the exit slit; the incident radiation was measured by the calibrated photocell mounted directly behind the irradiation cell. Prior to irradiation intensity checks showed the lamp intensity to be constant to within 10% in all cases. Intensities measured (without the radiation cell in place) before and after the irradiation varied less than 10% except for one killing curve at 265 mμ and one at 280 mμ where the difference was about 12% and for which linear corrections were applied.

The UV dose was controlled by a shutter in front of the exit slit of the monochromator, and the radiation time intervals were measured with a stop watch calibrated to 0.2 sec. These times were generally of the order of 60 seconds (minimum, 20 sec., maximum, 13 min. at the 313 mμ line where filters were also used). Dose was measured in units of photometer reading times seconds of radiation ("p-seconds") and subsequently changed to quanta/cm^2.

A variation of intensity with height was found to exist at the exit slit. The <u>average</u> intensity incident depends therefore on the volume and care must be taken that this volume does not change significantly in the course of any irradiation experiment. Samples of the phage suspension were removed for assay with 10 lambda or larger pipettes into appropriate tryptone broth dilution tubes. A total of 110 lambda was generally removed from the cell in the course of the killing curve irradiations. For one of the curves at 265 mμ and at 280 mμ 180 lambda were removed; for one curve at 320 mμ 125 lambda were removed.) The variations due to volume changes in the UV flux received by the phage suspension did not exceed about 10%. This can be seen from Table 1:

Table 1: Relative Intensities at Indicated Wavelengths and Heights in Quartz Radiation Cell

Height from Base of Quartz Cell (mm)	Wavelengths (mμ)							
	235	245	255	265	275	285	295	305
0	18	45	44	34	16	40	21	18
5	35	61	64	48	24	51	33	27
10	55	73	79	63	34	60	41	37
15	61	65	70	59	36	49	38	35
20	54	52	57	49	30	38	31	24
25	42	39	40	36	20	30	24	14
Average Intensity over Entire Cell	44	55	66	48	26	44	31	25
Average Intensity over Lower 20 mm of Cell	49	58	70	51	28	45	34	28

At least two killing curves were determined to within 10% reproducibility at each wavelength irradiated; there was generally of the order of 10 to 30% variation in the rate of delivery of the radiation between the separate determinations.

B. Irradiation of Ultracentrifuged 5-BD T_4

The air cooled BH6 mercury vapor lamp was used for these irradiations. The UV emerging from it was focused on the entrance slit of the Young-Thollon monochromator using the condensor lenses described above but without the pre-prism. The entrance and exit slits were the same as used in the TpT experiments, and the exit slit assembly was the same as described in Part I (Fig. 5) except for the absence of the monitor photocell (B) and mirror. For irradiations above 297 mμ glass and pyrex filters were used as before to remove any stray short wavelength UV. The monochromator exit slit spectra in these experiments can be considered to be about as good as or better than those in Figure 13 due to the improved entrance and exit slits, the omission of the pre-prism*, and the use of slit widths of comparable or smaller widths. Slit widths were less than 0.15 mm for radiations below 300 mμ but were adjusted up to 0.48 mm for some radiations above 300 mμ.

At the start of each killing curve measurement 3.4 ml of the diluted phage suspension was placed in the Beckman cell. The stirring motor was started, and then the UV beam was allowed to pass through the diaphragm and irradiate the Beckman cell. At intervals of 25 seconds or longer the UV beam was interrupted by closing a shutter behind the second

* The pre-prism actually only served to significantly reduce scattered visible light as the dispersion produced by it was not sufficient to prevent substantial amounts of UV light of other than the desired wavelength from passing through the entrance slit. Its two air-quartz interfaces served to add to the scattered UV and visible light.

collimating lens of the monochromator and a 0.050 ml or larger sample was withdrawn from the Beckman cell. Occasionally the intensity was rechecked with the photometer without the sample cell in place; also during certain long irradiations the photocell was kept in place behind the Beckman cell as a continuous monitor of the irradiation. The samples withdrawn were subsequently diluted in buffer or tryptone broth and plated as noted above. Appropriate corrections were made for the change in volume during the course of the irradiation as a result of removing the samples. Total UV dose was again measured in terms of "p-seconds" and then converted to quanta/cm^2.

DETERMINATION AND INTERPRETATION OF ACTION SPECTRUM OF INACTIVATION

A. Determination of Inactivation Dose

The logarithm of the fractional survival of phage was plotted against the cumulative total quanta/cm^2 allowed to reach the cell. (See Killing Curves in Graph Section.) These latter values were corrected by the factor V/V_t where V is the volume of the phage suspension that is receiving radiation and V_t is the total volume of the phage suspension placed in the cell; this factor takes account of the fact that each phage particle spends only the fraction V/V_t of time in the beam. The slopes of the straight line portions of these curves were determined. These slopes were used to find that dose in quanta/cm^2/hit which would leave active the fraction e^{-1} of the phage, i.e., the reciprocal of the "cross-section of inactivation."*

* A slight complication was introduced because the geometry used for the irradiation of the 5 BD uncentrifuged phage varied from that used for the calibration measurements. In order to determine the relation between the p-seconds measured in this somewhat ill-defined cylindrical cell geometry used during the earlier experiments and that of the rectangular Beckman cell used for the irradiations of the centrifuged 5-BD

B. The Interpretation of Action Spectra

The purpose of measuring an action spectrum of some biological effect is to make inferences about the absorption spectrum of the substance involved in the first step of the series leading to the effect. Under certain ideal conditions the action spectrum may reflect this absorption spectrum faithfully, at least over a limited range. Sufficient conditions for this faithfulness, and, failing these, the principal causes for the distortion of this relation are the following:

(1) A single species of molecule absorbs the effective light.

(2) This species undergoes only one type of photochemical reaction.

(3) The quantum yield of the reaction is independent of wavelength.

(4) There is no screening by irrelevant pigments or by the receptor pigment itself and scattering and reflection are insignificant or essentially wavelength independent.

(5) The extent of the photochemical reaction occurring is independent of the rate at which equal increments of energy are delivered. (Reciprocity law holds.)

When all these conditions are fulfilled then the rate of the

(Cont'd from p. 37) T_4 and the calibration experiments killing curves of T_6 were done at 235, 265, and 280 mμ in both geometries and the cross sections determined in each case. The results are indicated below and were calculated in the manner discussed above.

	Quanta/cm^2/hit for T_6		
	Cylindrical Geometry	Rectangular Geometry	Rectangular Geom. / Cylindrical Geom.
235 mμ	4.53×10^{14}	4.55×10^{14}	1.004
265 mμ	2.02	2.01	0.995
280 mμ	3.00	3.05	1.017
			Av. 1.01

primary photochemical reaction is strictly proportional to the absorption coefficient of the receptor substance. Thus, whatever the relation between this rate and the biological effect, equal effects will be produced for different wavelengths if the intensities are related so as to make the photochemical rates equal, i.e., if the intensities are inversely proportional to the absorption coefficients. The intensities at different wavelengths must be compared as quantum fluxes (not as energy fluxes), because the quantum flux multiplied by the absorption coefficient determines the quanta absorbed, and thus the rate of the primary photochemical reaction. Thus, under these conditions the inverse of the quantum fluxes producing equal effects at different wavelengths plotted versus the wavelength (the "equal effect" action spectrum) will be strictly proportional to the absorption spectrum of the receptor substance.

Let us now discuss the conditions enumerated above with reference to the effect studied here, i.e., the loss of plaque forming ability of the T-even phages, with and without the substitution of 5-bromouracil for thymine in their DNA:

(1) The "single species" condition is violated in several respects: (a) There is absorption by protein in addition to absorption by DNA. The aromatic amino acids, tyrosine, phenylalanine, and tryptophane have absorption maxima with absorption coefficients of the same order of magnitude as those of the nucleotides in the 265 to 280 mμ region, while the absorption of amino acids in general is known to be large at the shorter UV wavelengths. Near the absorption peak of DNA this protein absorption is not significant, but near the shortest and longest wavelengths studied here the protein absorption, though still slight, is

not negligible relative to that of DNA. Herriott and Barlow (31) in studying the absorption spectrum of the protein coats or "ghosts" of T_2 found a curve showing a relative maximum at 275-280 mμ, a relative minimum near 250 mμ, and a sharply rising limb for wavelengths shorter than this. At 280 mμ the OD of the ghosts was about 8 to 10% of that of the intact virus, while at 240 mμ the protein coats suspension's optical density was about 20% of that of the intact virus. The action spectrum of T_1 (32) shows a sharp change in slope in the 275-280 mμ region while that of B. megatherium phage (33) has a relative minimum at about 272 mμ and a relative maximum at 255-260 mμ and at 280 mμ; in both cases, the change in slope and the second peak at 280 mμ, protein absorption has been considered to be the cause of the distortion. Using the fact that proteins are less sensitive to UV light at low temperatures and the apparent temperature independence of nucleic acid sensitivity, Setlow and Doyle (34) have ascribed about one-half of the UV inactivation of T_1 at 280 mμ to absorption of photons by proteins. In addition, electron microscope studies have shown that UV irradiation also leads to structural lesions in the "head" and "tail" of bacteriophages, and it is thus very probable that a portion of the UV light absorbed by the phage protein leads to inactivation through photochemical changes unrelated to DNA (36).

(b) In DNA there is also absorption of UV by bases other than thymine and 5-bromouracil. It is believed that the purines are not photochemically altered (35); nevertheless, it is quite likely that quanta absorbed by purines may travel as excitons along the polynucleotide chains and thus act as photosensitizers for reactions involving the pyrimidines. In view of this mechanism it may be more reasonable, to a first approxi-

mation, to consider as the receptor molecule a fictitious "average nucleotide" having the absorption spectrum of DNA per nucleotide rather than one or both of the pyrimidines. Differences between the action spectrum and the absorption spectrum of DNA could then be indicative of non-ideal exciton travel.

(2) The single reaction condition is certainly not satisfied in our case: It is known that there occur at least two classes of reactions, the photoreactivable and the non-photoreactivable. From the point of view just defined which considers the "average nucleotide" as the receptor molecule these two classes occur in the same molecule, but they may or may not involve the same bases. The fact that the relative rates of the two classes appear to be nearly independent of wavelength may be a reflection of the mechanism of transport rather than of the identity of the base involved.

(3) The condition of constancy of quantum yield with wavelength may or may not be fulfilled. There is no general a priori reason that it should be fulfilled. Experimentally there is evidence from studies with model substances (mono- and dinucleotides) suggesting that the quantum yield may be approximately constant. (See Part I and (6).) Similarly, by reasoning backwards from the general similarity of the observed action spectrum of the killing actions of UV to the absorption spectrum of DNA one may infer that the quantum yield does not vary greatly with wavelength. However, it must be one of the purposes of more refined studies of the action spectrum to discern small variations of quantum yield with wavelength, possibly differing for the different reactions, and therefore leading to variations with wavelength of relative yields of these

reactions.

(4) Screening and self-screening effects distorting the action spectrum are appreciable in large organisms. In bacteriophage experiments, fortunately, these effects are quite negligible, or can be fully accounted for by measurements of optical densities combined with adequate stirring. The phage suspensions used in these experiments were essentially transparent to UV, and these effects and those of scattering and reflection were negligible.

(5) Previous studies of action spectra of viruses (See references below.) have shown the reciprocity law to hold, and, indeed, in these experiments 10 to 30% variations of the rate of delivery of the UV radiation to the uncentrifuged 5-BD phage suspensions had no detectable effect on the killing curves.

A review of the literature of action spectra of viruses shows that characteristically one had obtained the type of curve shown in Fig. 14 (T_4) with a relative minimum at about 235 mμ, a steeply climbing limb for wavelengths less than 235 mμ, a relative maximum at approximately 265 mμ, and a rapidly descending limb for wavelengths greater than about 280 mμ. Such curves have been found for S. aureus bacteriophage (37), "vaccine virus" (38), influenza A virus (39), B. megatherium bacteriophage (33), T_1 and T_2 (32), TMV* (40), Rous sarcoma virus (41), and T_4 (36). Pertinent aspects of these action spectra are indicated in Table 2, p. 43. The relatively rapid decrease in sensitivity for wavelengths greater than 290 mμ in all these action spectra is especially noteworthy in regards

*The action spectrum for TMV differs from the type cited as typical above in the shallowness of the relative minimum and its rapid decline for wavelengths greater than 260 mμ.

Table 2. Virus Action Spectra

(References as above. $\bar{\sigma}$ = (const.) x (cm^2-hit/energy))

Organism	Wavelength of Rel. Max.	Wavelength of Rel. Min.	$\frac{\bar{\sigma}_{max}}{\bar{\sigma}_{min}}$	$\frac{\bar{\sigma}_{297}}{\bar{\sigma}_{max}}$	$\frac{\bar{\sigma}_{302}}{\bar{\sigma}_{max}}$
S. aureus phage	265 mμ	238 mμ	3.2	0.1	
Vaccine virus	265	238	3.2	0.1	0.01
Influenza A virus	265	230	3.1	0.1	
B. Megatherium phage	265	255-260	2	0.1	
Rous sarcoma virus	265	248	2.5	1/6	
T_1	265	238	2	0.1	ca. 0.01
T_2	265	238	2	0.1	ca. 0.01
TMV	265	248	1.2	$\frac{\bar{\sigma}_{280}}{\bar{\sigma}_{max}}$ = 0.1	
T_1 (Ref. 32)	265	243	2.5	ca. 1/8	
T_4	265	235	3.5	0.05	0.006

to the findings which follow.

Studies indicating inactivation of bacteriophages by visible light have been reported by Wahl et al (42, 43). Using a Tungsten lamp with glass filters he found inactivation of S_{13} and C_{16} bacteriophages up to the green region of the visible spectrum; yellow and red light were ineffective, and the effectiveness of the light decreased progressively with increasing wavelengths (greater than 365 mμ). In all cases the viruses were 10^3 to 10^5 times less sensitive to these longer wave-

lengths than for the shorter wavelength UV. One hit inactivation curves were obtained for the visible light and since S_{13} was noted to be more sensitive than the larger C_{16} phage, unlike the situation at the shorter UV wavelengths*, it was thought that different photochemical processes were involved in the visible light inactivation.**

RESULTS AND CONCLUSIONS

The killing curves for the 5-BD substituted T_4, T_4, and T_6 bacteriophages from 235 to 334 mμ are shown in the graph section; other experiments indicated no significant differential increase in sensitivity of 5 BD T_4 at 365 and at 404 mμ. The fractional survival is plotted against cumulative UV dosage in quanta/cm^2. The typical curve has a initial shoulder and subsequently descends as a straight line. From the slope of the straight line portions of the graphs, as determined by least square analysis on those points not in the region of a possible initial shoulder, the quanta/cm^2 required to produce one hit--i.e., inactivate($1-e^{-1}$) of the phage--was found. The reciprocals of these values were used to obtain the action spectrum (Fig. 14). The quanta/cm^2-hit and y-intercepts of the lines fitted by least square analysis are given in Table 3.

The y-intercepts of the unsubstituted T_4 killing curves are generally greater than those found for the 5-BD substituted phage and are between 1 and 2. It is noteworthy that in 5-BD T_4 phage this intercept is to within experimental error ca. 1.0 except possibly near 235 and

*The point of equal sensitivity was between 313 and 365 mμ.
**The value Wahl gives for the energy/cm^2/hit at 254 mμ is much larger than the accepted values for this figure for other bacteriophages; the relative energy requirements given for different wavelengths are presumed valid.

289 mμ--i.e., the killing curves are simple "one hit" exponential curves.

The action spectra of the ultracentrifuged 5-BD T_4 and the unsubstituted T_4 are shown in Fig. 14; those for T_6 and the uncentrifuged

Table 3. Characteristics of the Killing Curves

	Ultracentrifuged 5-BD T_4		T_6	
Wavelength	Quanta/cm^2/hit	y-intercept	Quanta/cm^2/hit	y-intercept*
235 mμ	2.25×10^{14}	1.3	4.55×10^{14}	1.24
248			2.46×10^{14}	
254	2.05×10^{14}	1.2	2.59×10^{14} 2.22×10^{14}	
265	1.33×10^{14}	1.2	2.02×10^{14}	1.14
275	1.84×10^{14}	0.88		
280	2.16×10^{14}	1.15	3.05×10^{14}	1.6
289	3.38×10^{14}	1.4	3.64×10^{14}	
297			$3 \text{ to } 5 \times 10^{15}$	
302	7.53×10^{14}	1.33		
313	7.29×10^{15}	0.88	8.2×10^{17}	
320	$3.0_6 \times 10^{16}$	1.07		
334	$7.2_9 \times 10^{17}$	0.9	3.8×10^{19}	1.2

*Due probably to geometrical complications the y-intercepts of killing curves obtained with the earlier cylindrical cell irradiation vessel could not be reproduced generally (cf. Graph Section) and so were not obtained accurately. This effect might have been due to inadequate stirring of the phage suspension in the upper portions of the irradiation cell from which the early samples of each killing curve was obtained.

and ultracentrifuged 5-BD T_4 are shown in Fig. 15.* From the latter figure it is evident that the ultracentrifuged 5-BD T_4 is more sensitive than the uncentrifuged 5-BD T_4 throughout the range of UV investigated; this is more marked in the region above 300 mμ where it varies from about a factor of 3 to about 30 at 334 mμ.** About 289 mμ the difference between the two curves is quite small and the data do not really justify a more definite comparison of the relative sensitivities. Below 289 mμ there again appears to be some increase in sensitivity of the ultracentrifuged 5-BD T_4 over the uncentrifuged 5-BD T_4. This result is consistent with previous observations of increasing UV sensitivity with increasing 5-BD substitution (22), since the ultracentrifuged phage are more heavily substituted than the average of the uncentrifuged phage killed by the UV light. Furthermore, the ratio of the sensitivities at 254 mμ (= 1.3) agrees well with the value found by Stahl et al (= 1.26, Fig. 4, Reference 23).

A comparison of the ultracentrifuged 5-BD and T_6 curves in Fig. 15 shows that the 5-BD T_4 is generally more sensitive at the wavelengths studied; again the observed difference about 289 mμ does not justify an unequivocal statement that the 5-BD substituted virus is the more sensitive. For wavelengths above 289 mμ the factor of increased sensitivity of the ultracentrifuged 5-BD T_4 to T_6 rises to a maximum of 110-130 in the 315 mμ region and then progressively falls to about 50 at 334 mμ.

* The action spectrum of unsubstituted T_4 was determined by H. Johns and U. Winkler for wavelengths less than 313 mμ.

** It should be noted that the value at 325 mμ for the uncentrifuged 5-BD T_4 is not as well known as the other points, since it is based on only four points in a single determination; in addition, there is more uncertainty in the actual wavelength at which the experiments nominally labelled 316, 320, and 325 mμ were performed because of the lack of peaks in the emission spectra of the mercury arc at these wavelengths.

For wavelengths below about 280 mμ the factor of increased sensitivity appears to be about 1.2 to 2. While this is not very great, there are several things that imply that it is real: (1) The T_6 killing curves in this region were done in the presence of 5-BD substituted T_4 so that each phage served as an internal dosimeter for the other. Reference to these killing curves in the Graph Section shows that survival of T_6 noted at any given total dose was in all but a very few cases greater than the corresponding survival of 5-BD substituted phage at that dose. (See, for example, pages 68, 69, and 70 and compare pages 84 and 75, 85 and 76, etc. which represent separate graphs for the killing curves of uncentrifuged 5-BD T_4 and T_6 simultaneously determined.) (2) The fact that T_6 appeared to be less sensitive than the uncentrifuged 5-BD T_4 would argue for its still greater resistance relative to the more heavily 5-BD substituted ultracentrifuged T_4 because of the established increase in UV sensitivity with increase in 5-BD substitution.

Fig. 14 shows that there is a relatively large difference in sensitivity between the ultracentrifuged 5-BD T_4 and the unsubstituted T_4 phages. For wavelengths less than 289 mμ this amounts to a factor of about 4 to 5, while for wavelengths longer than this the factor rises very rapidly to a maximum of about 500 to 1000 near 313 mμ before falling again about 334 mμ. It is interesting that the ratio of the absorption coefficient of 5-BD to that of thymidine increases rapidly for wavelengths greater than 280 mμ. Thus this increase in sensitivity above 289 mμ argues for the direct involvement of 5-BD in the primary step of the photochemical process leading to the inactivation of plaque forming ability in the 5-BD T_4.

The closeness of the various action spectra at 289 mμ is also note-

worthy; this could conceivably be due to significant killing mediated by a factor(s) that does not vary significantly among the phages considered (as, for example, killing through changes induced in proteins); conceivably this might also be the result of systematic error, although the several experimental designs involved would seem to make this unlikely.

It is seen that there is no secondary peak in the action spectrum corresponding to the long wavelength "tail" seen in the 5-bromodesoxyuridine absorption spectrum; killing curves obtained at 316 mμ and 325 mμ in an effort to demonstrate such a peak gave cross-sections whose values fell roughly along the curve shown in Fig. 15. This suggests that if there indeed does exist another electronic transition in this region it is not capable of very much more efficient inactivation of the virus than the extinction giving rise to the pi to pi* transition.

It is interesting that the maximum sensitivity for the ultracentrifuged 5-BD T_4 is at 265 mμ. Certainly the action spectrum above 300 mμ implies direct participation of the substituted 5-BD in the inactivation reactions in this region. It seems reasonable to extend this and ascribe the significantly increased sensitivity below 300 mμ to photochemical reactions involving 5-BD. Yet, if this is the case and if indeed at least 80% of the thymidine has been replaced by 5-BD, why is not the maximum UV sensitivity about the 5-BD absorption peak at 280 mμ instead of at 265 mμ? A number of different explanations can be readily given for this. One of these, which does not seem to involve unreasonable assumptions, is the hypothesis of exciton travel--i.e., that the energy of UV light absorbed at one portion of the polynucleotide chain can be transmitted along the chain and cause inactivating reactions in other portions--in the present case, for example, in the 5-BD nucleotides.

It is reasonable to assume, as the data of Dunn and Smith (27) on the absorption spectrum of 5-BD substituted phage suggest, that the absorption maximum of 5-BD substituted DNA is 265 mμ. If this were the case and if exciton travel occurred, then one would expect to observe the maximum sensitivity of 5-BD substituted phage at 265 mμ.

SUMMARY OF PROPOSITIONS

(1) The ultracentrifuged 5-BD T_4 killing curves approximate "one hit" simple exponential curves except possibly about 235 and 289 mμ.

(2) The ultracentrifuged 5-BD T_4 phages are approximately 4 to 5 times more sensitive to UV light at wavelengths between 235 and 289 mμ than unsubstituted T_4; this relative sensitivity increases very rapidly with increasing wavelength above 289 mμ to a maximum of approximately 500 to 1000 near 313 mμ before beginning to fall again.

(3) The increase in sensitivity of 5-BD substituted T_4 bacteriophages at longer wavelengths appears to be significant only within the 300 mμ to approximately 350 mμ range and is attributable to the effects of the incorporated 5-BD in the primary photochemical steps leading to the inactivation.

(4) There is no definite evidence of significant UV inactivation in 5-BD substituted DNA via an electronic transition corresponding to the long wavelength tail observed in the 5-BD absorption spectrum (Fig. 7).

(5) The data are compatible with the assumption that exciton travel occurs in the inactivation of plaque forming ability of T_4 by UV light.

FIGURES

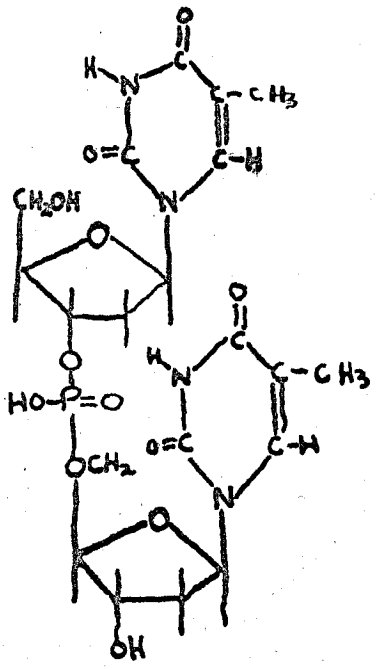

I

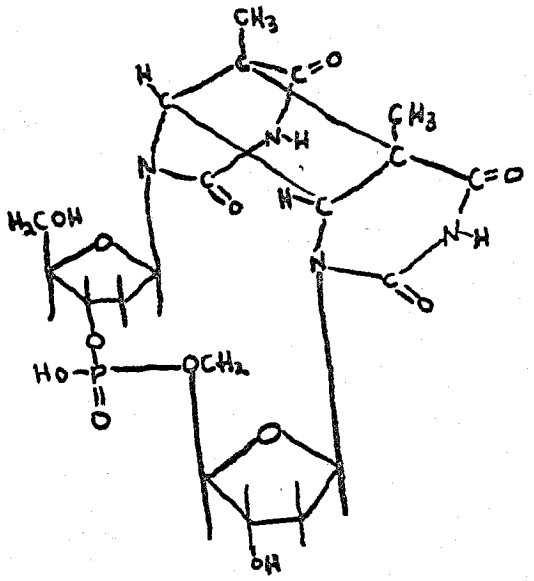

II

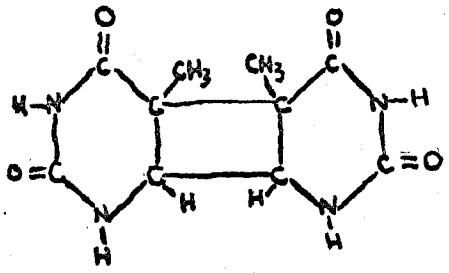

III

Fig. 1. I, Thymidyl-(5'-3')-thymidine, TpT
II, Possible Photoproduct Formed by Irradiation of TpT with Ultra-Violet Light
III, One of the Possible Isomers of the Dimer Formed by Irradiation of Frozen Thymine Solutions

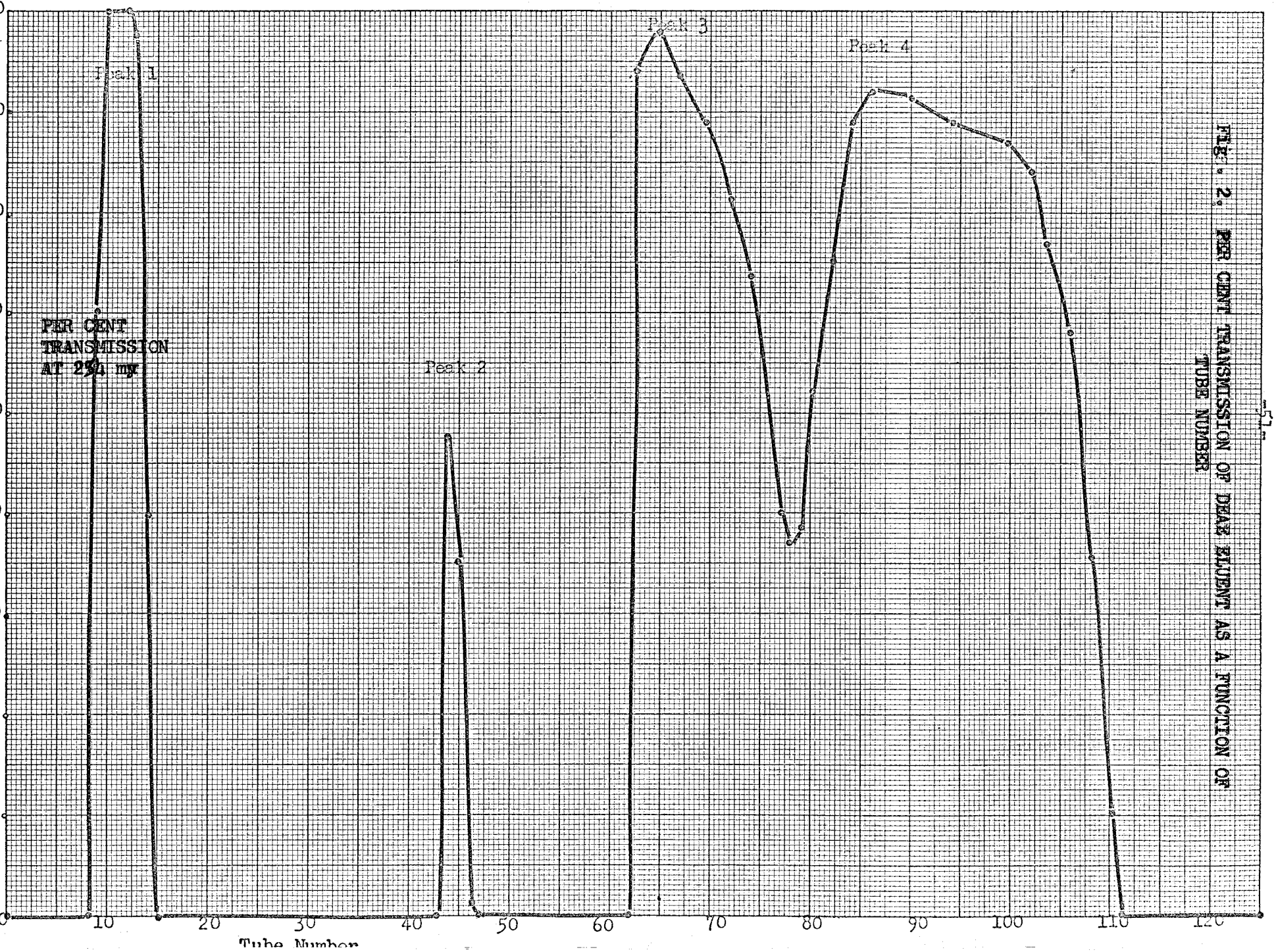

Fig. 2. PER CENT TRANSMISSION OF DEAE ELUENT AS A FUNCTION OF TUBE NUMBER

Fig. 3. OPTICAL SYSTEM OF YOUNG-THOLLON MONOCHROMATOR

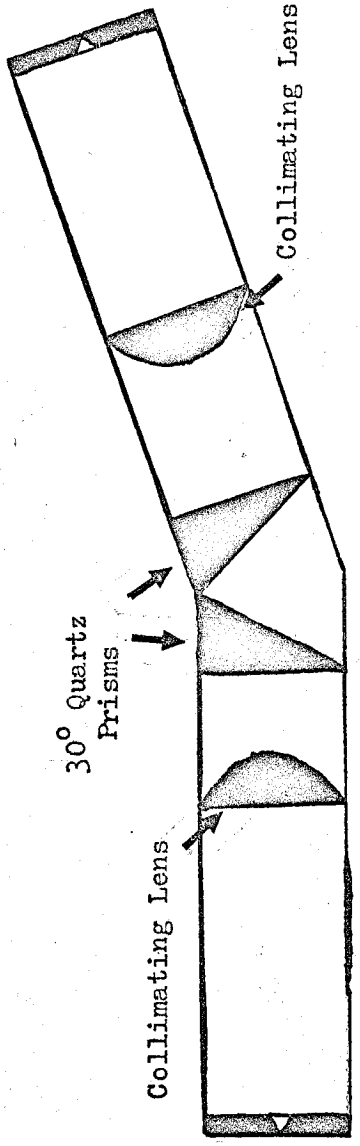

Fig. 4. ABSORPTION SPECTRUM OF THYMIDYL-(5'-3')-THYMIDINE; pH 2.5, ROOM TEMPERATURE

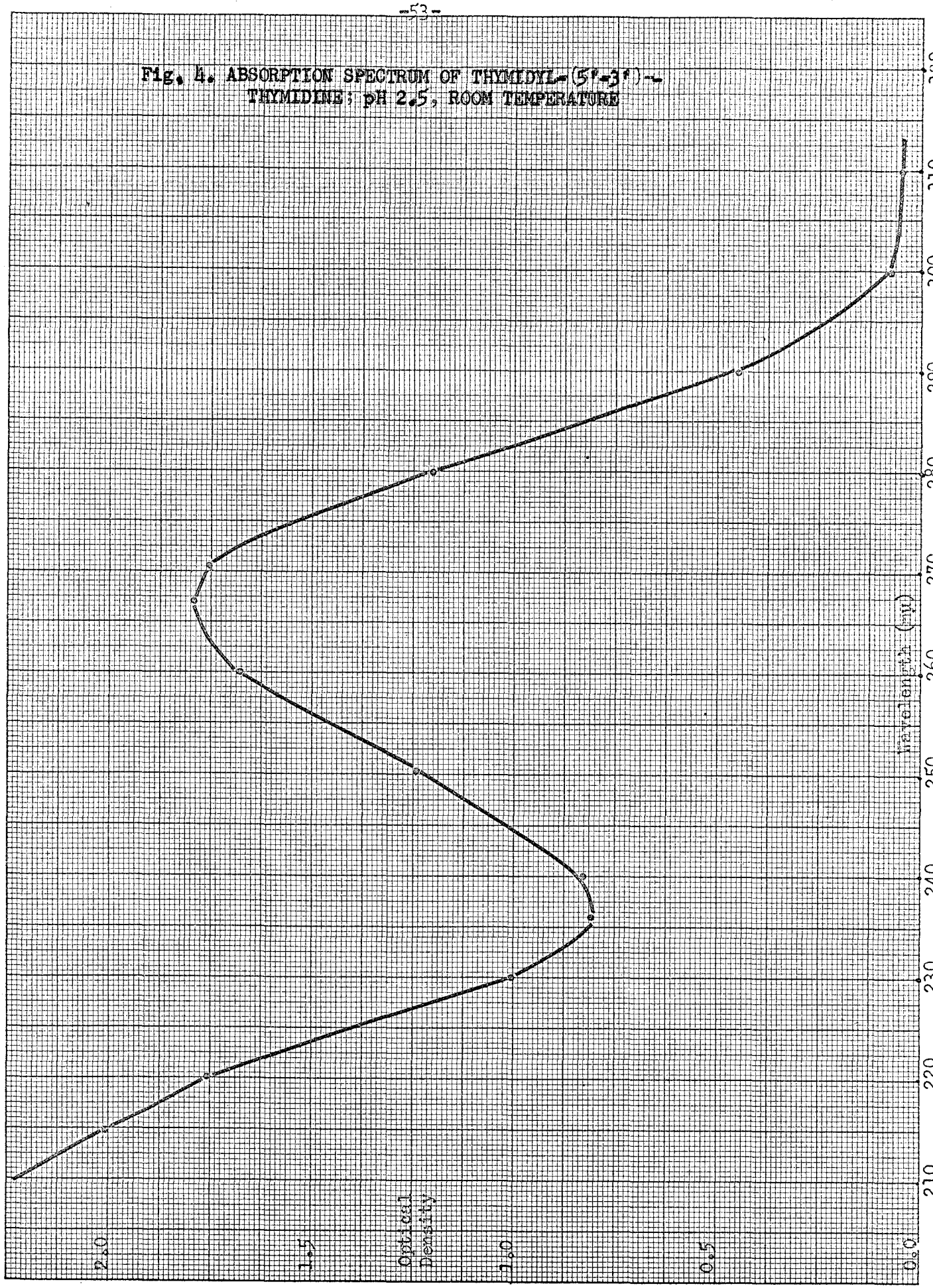

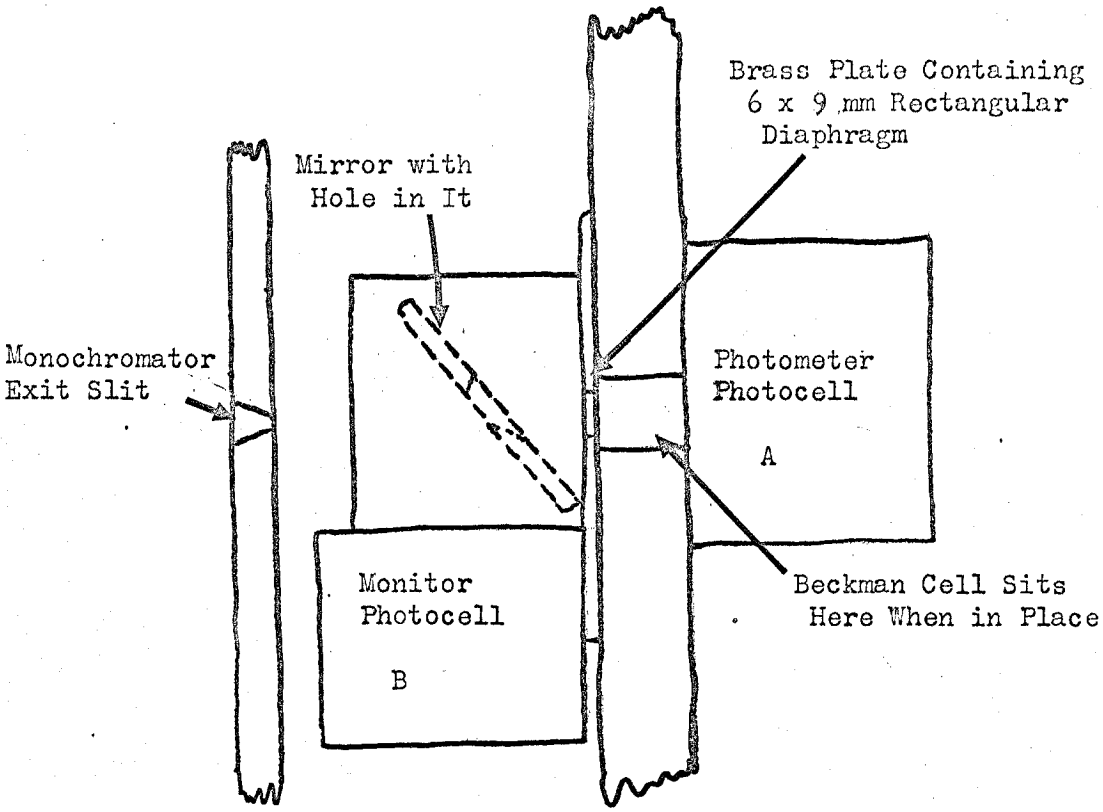

Fig. 5. Top View of Exit Slit Assembly Showing Monitor Photocell & Photometer Photocell

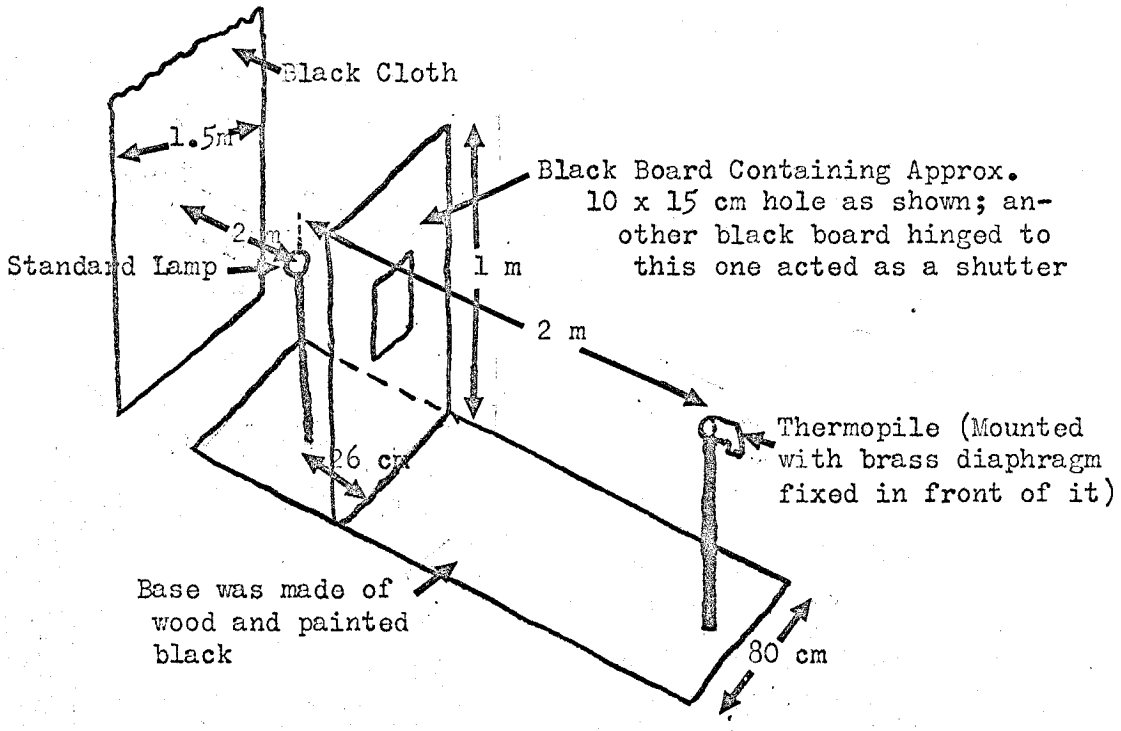

Fig. 6. Set Up Used to Calibrate Thermopile & Galvonometer Against Standard Lamp

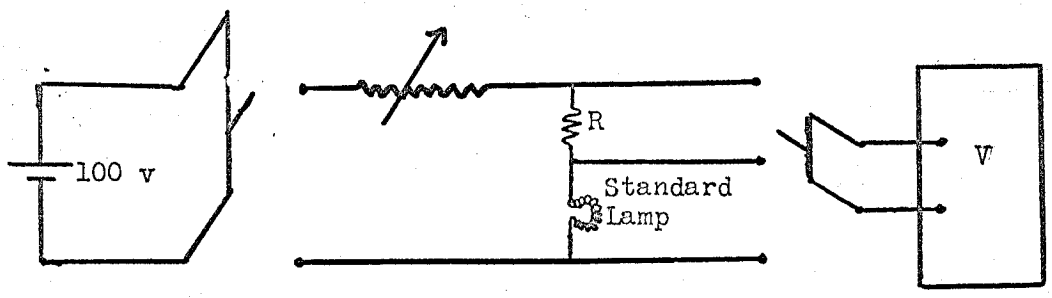

Fig. 7. Standard Lamp Circuit.
R = 1.000 ohm Standard Resistance
V = John Fluke Voltmeter

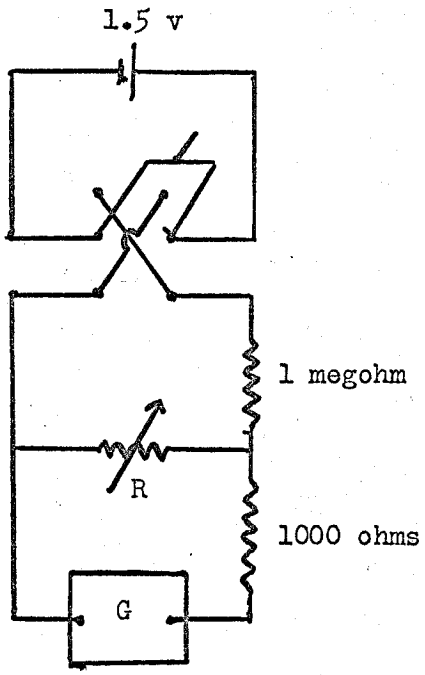

Fig. 8. Galvonometer Biasing Circuit
R = 1 to 1000 ohm Variable Resister
G = Galvonometer

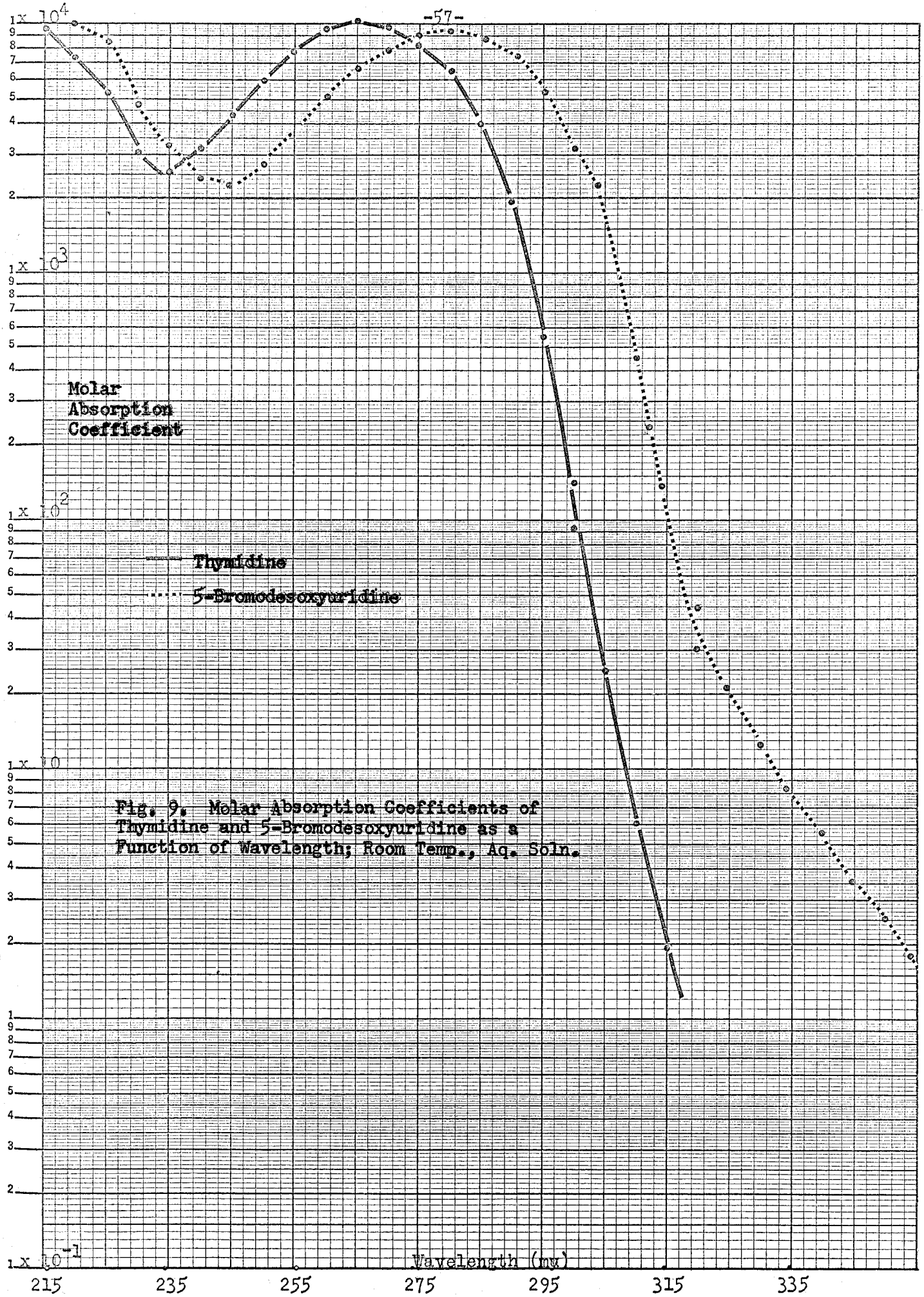

Fig. 9. Molar Absorption Coefficients of Thymidine and 5-Bromodesoxyuridine as a Function of Wavelength; Room Temp., Aq. Soln.

Fig. 10. PRELIMINARY DENSITY GRADIENT ASSAY OF S-BD T_4 (Each tube used to collect 5 drops)

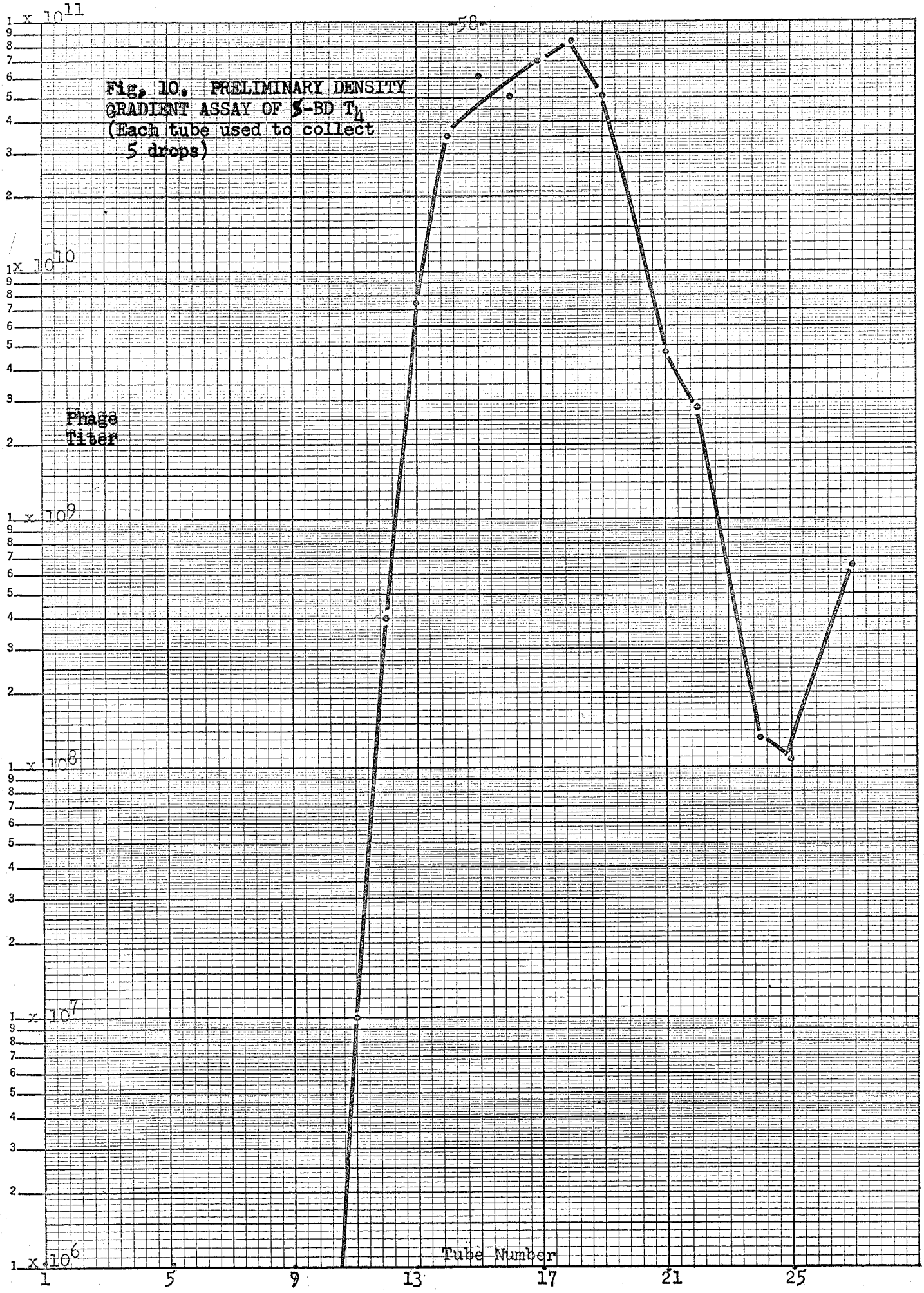

Fig. 11. DENSITY GRADIENT DISTRIBUTION OF FRACTION #13 5-BD T_4 FROM PRELIMINARY GRADIENT RUN TOGETHER WITH T_6 AS A MARKER

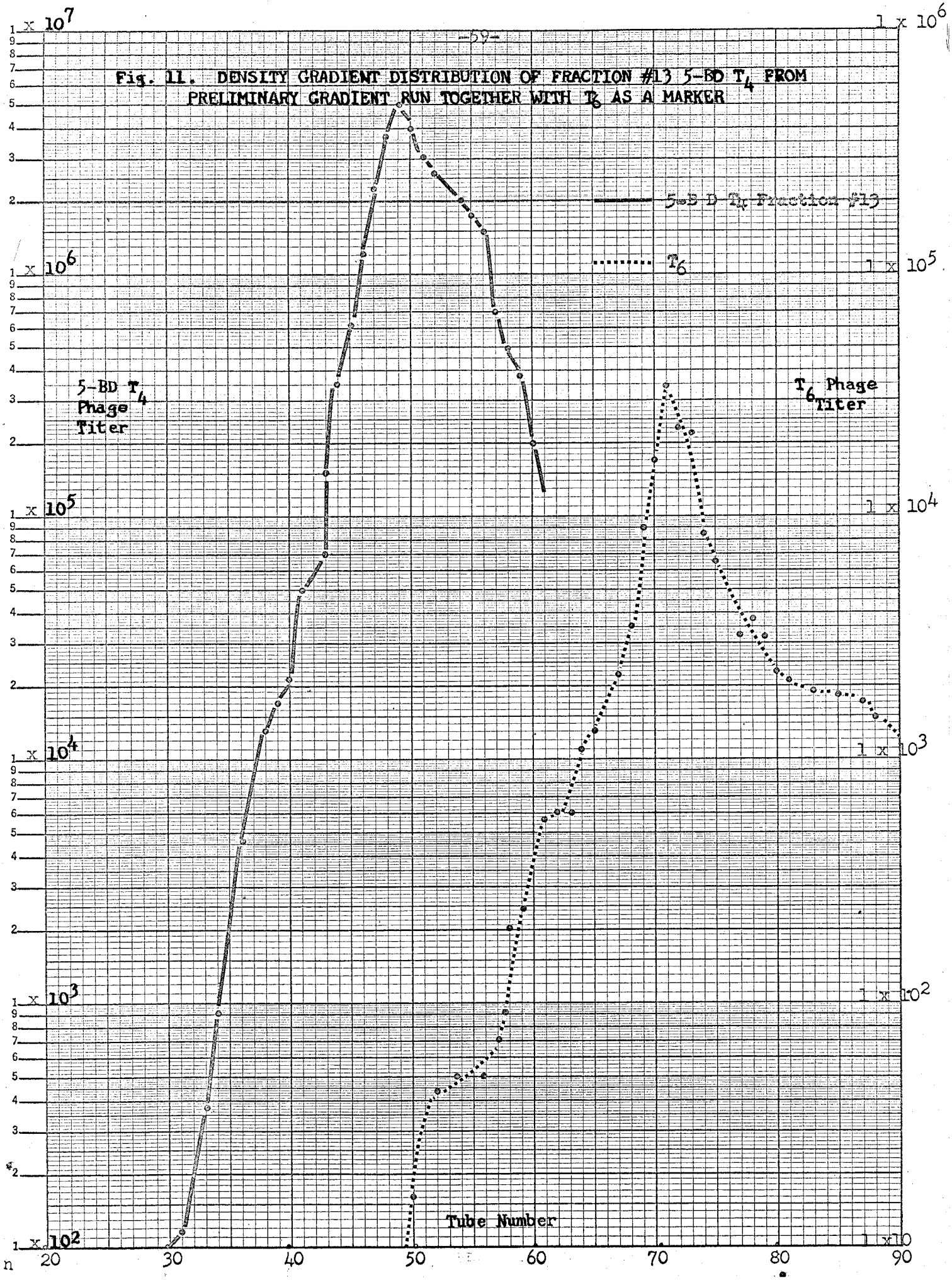

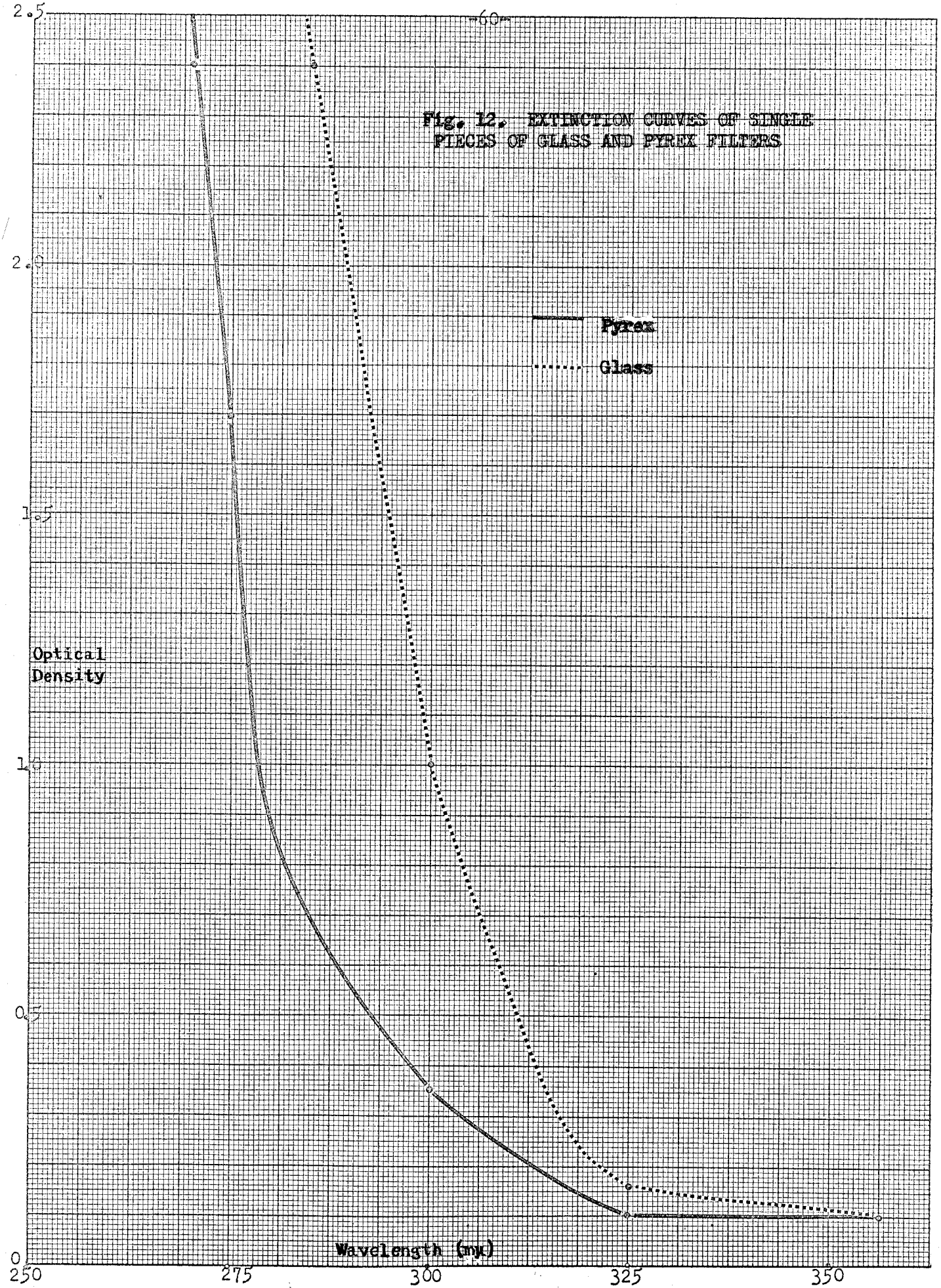

Fig. 12. EXTINCTION CURVES OF SINGLE PIECES OF GLASS AND PYREX FILTERS

Fig. 13a. SPECTRA OF MONOCHROMATOR EXIT SLIT LIGHT USED IN THE RADIATIONS AT THE INDICATED WAVELENGTHS

FIG. 13b. SPECTRA OF MONOCHROMATOR EXIT SLIT LIGHT USED IN THE RADIATIONS AT THE INDICATED WAVELENGTHS

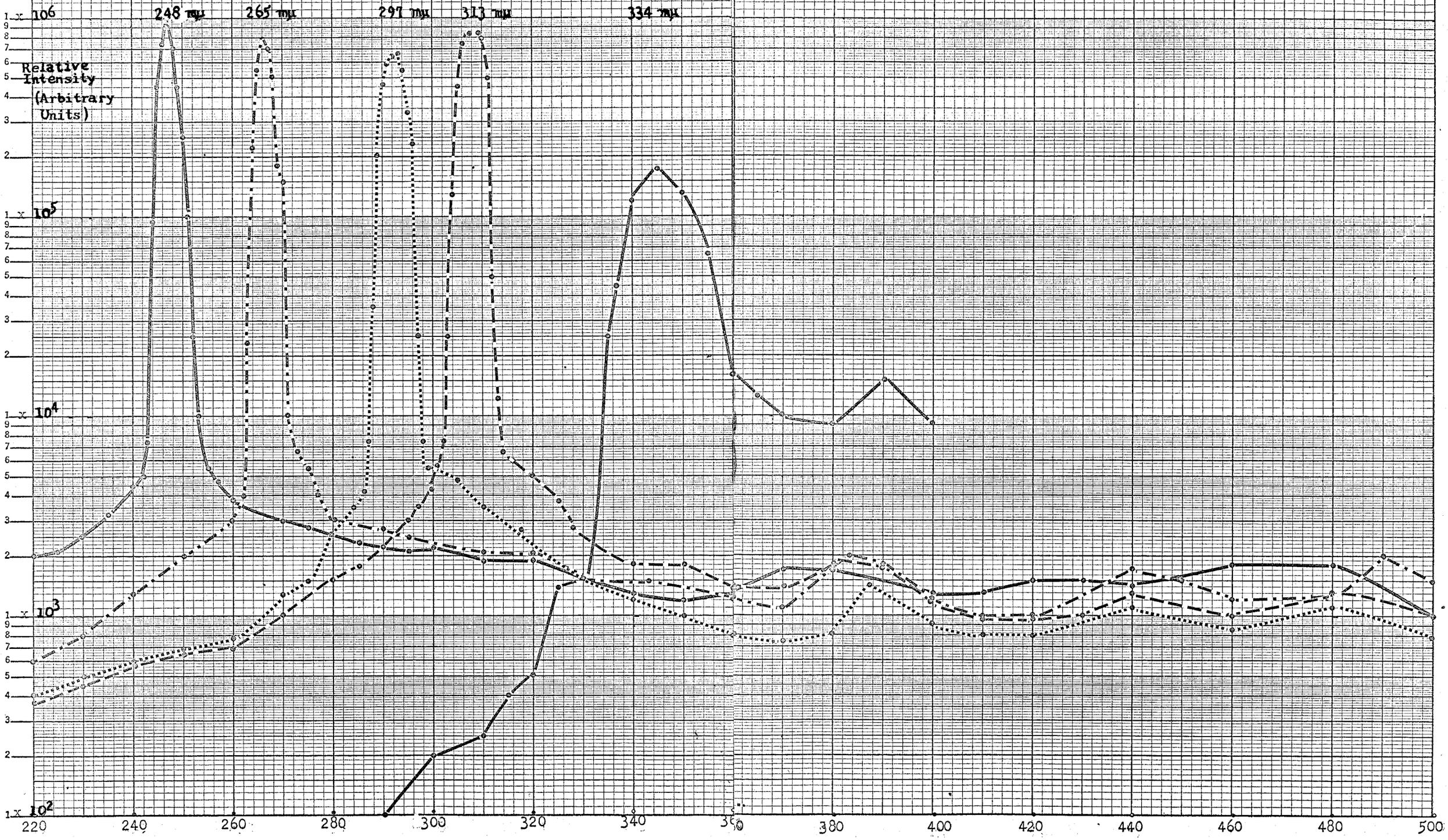

Fig. 14. ACTION SPECTRA OF UV INACTIVATION OF PLAQUE FORMING ABILITY OF ULTRACENTRIFUGED 5-BD T_4 AND UNSUBSTITUTED T_4 PHAGE

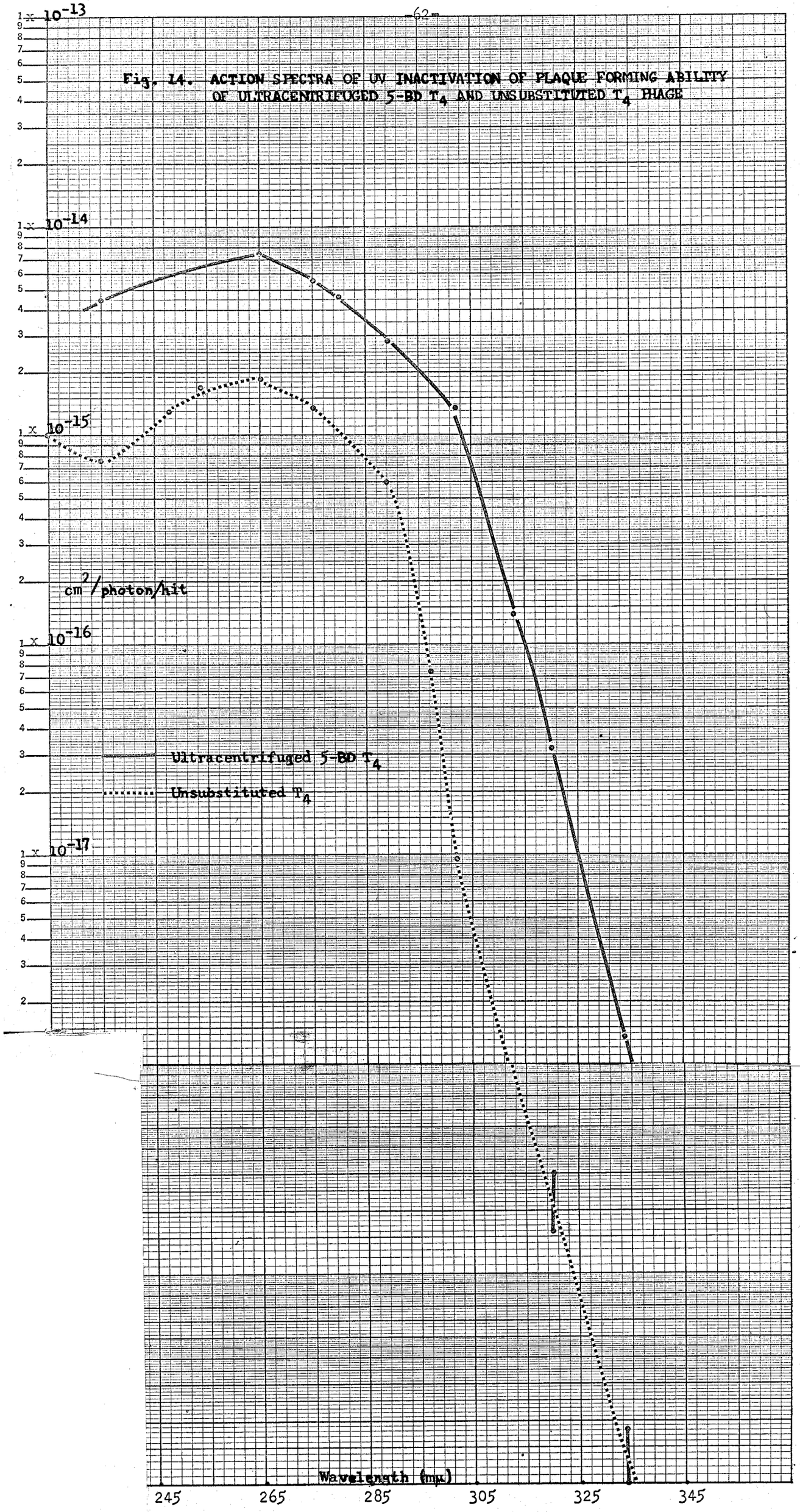

Fig. 15. ACTION SPECTRA OF UV INACTIVATION OF PLAQUE FORMING ABILITY OF ULTRACENTRIFUGED 5-BD T_4, UNCENTRIFUGED 5-BD T_4, AND T_6

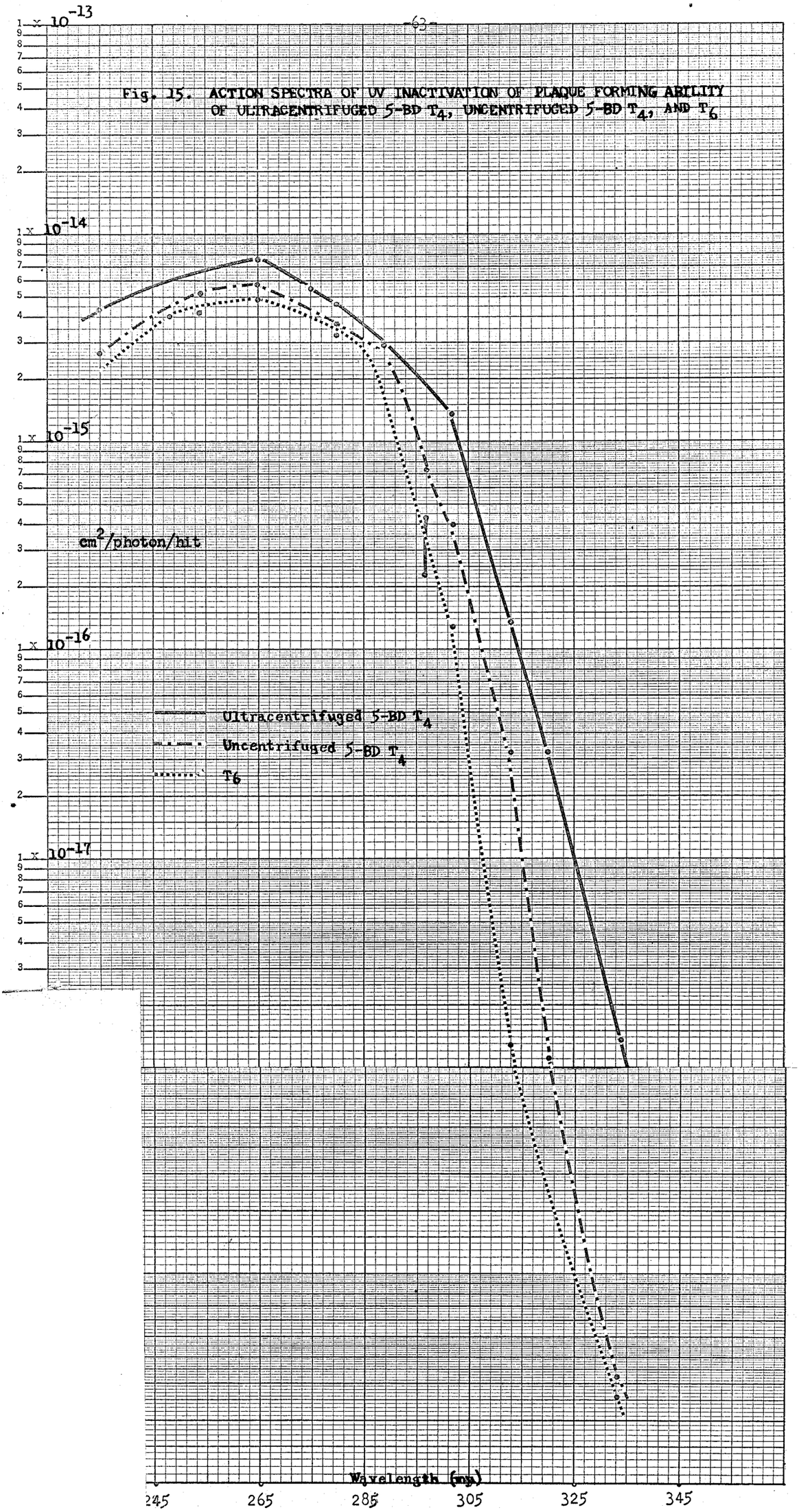

GRAPH SECTION

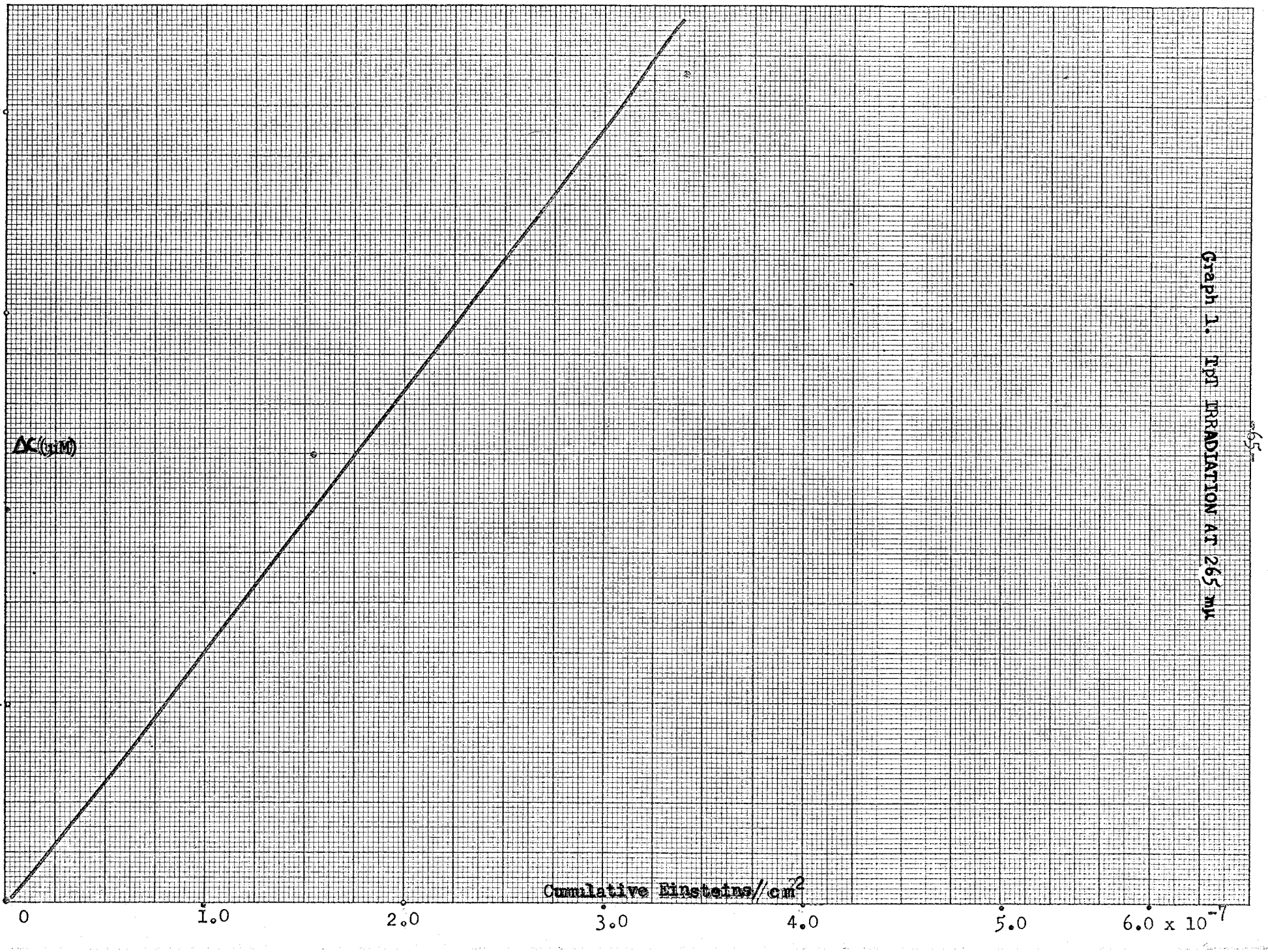
Graph 1. TpT IRRADIATION AT 265 mμ
ΔC (μM)
0
1.0
2.0
3.0
4.0
5.0
6.0 x 10⁻⁷
Cumulative Einsteins/cm²

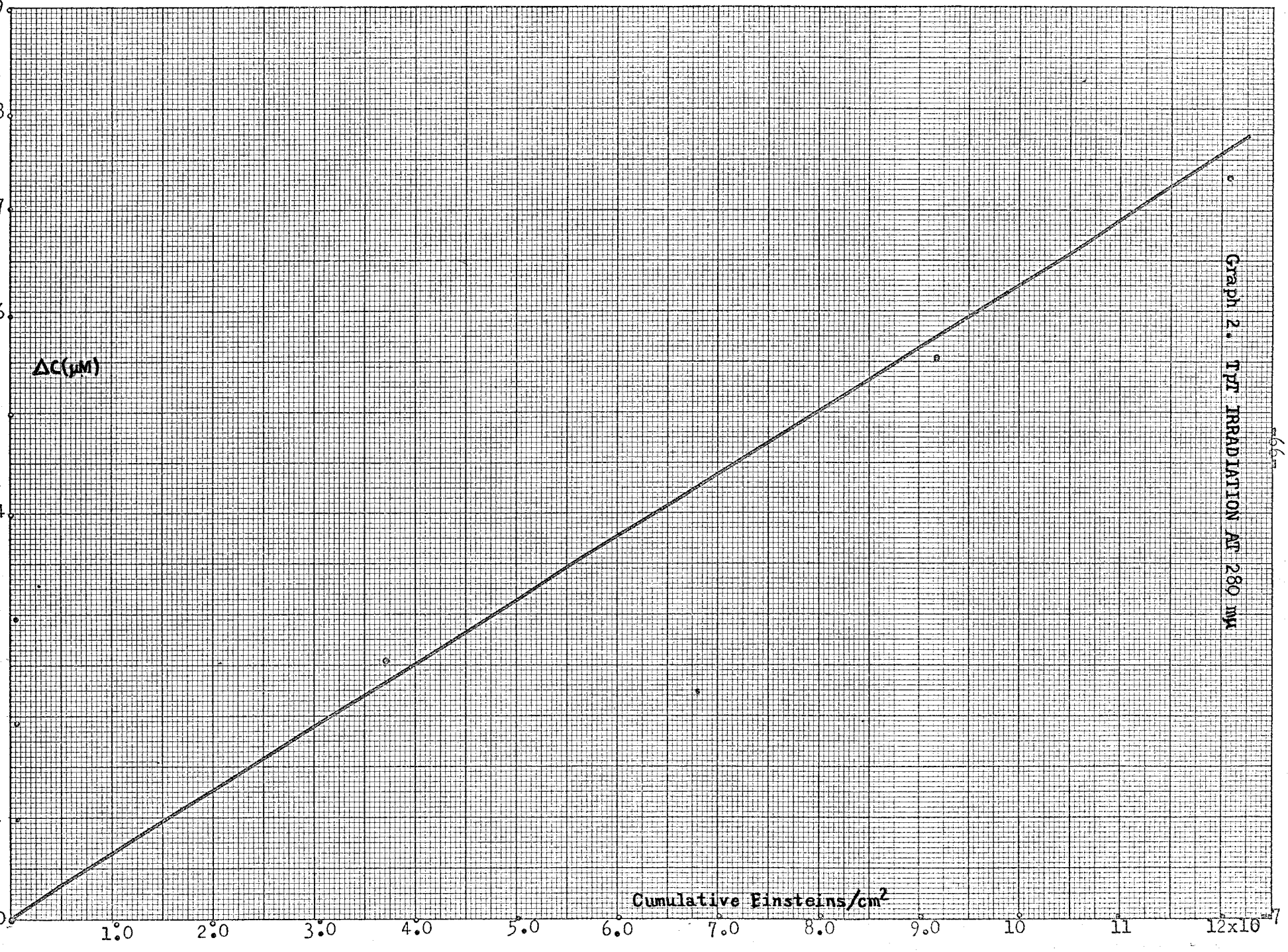

Graph 2. TPT IRRADIATION AT 280 mμ

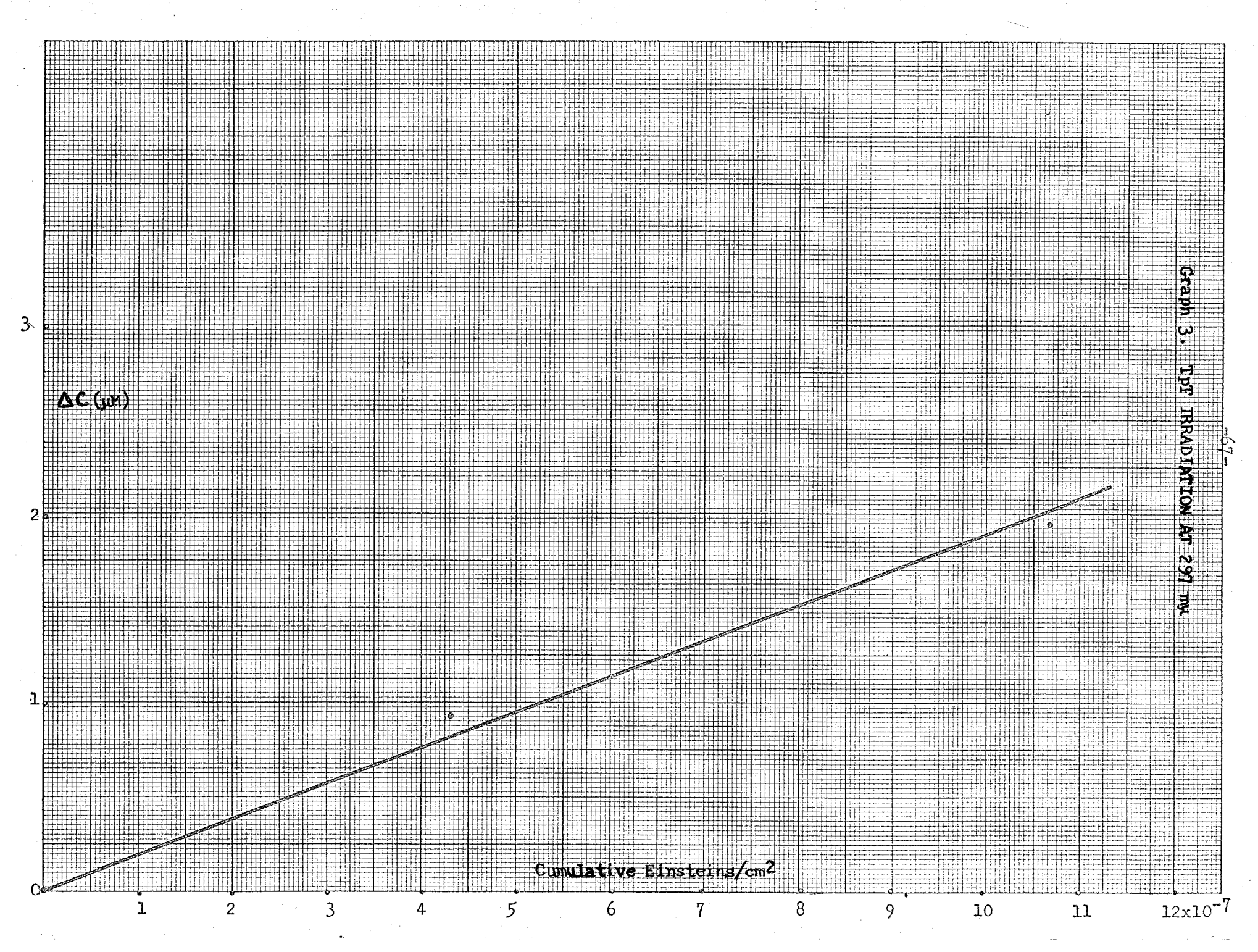
Graph 3. TpT IRRADIATION AT 297 mμ
ΔC (μM)
3
2
1
0
1
2
3
4
5
6
7
8
9
10
11
12x10⁻⁷
Cumulative Einsteins/cm²

SIMULTANEOUSLY DETERMINED KILLING CURVES FOR ULTRACENTRIFUGED 5-BD T_4 AND T_6 BACTERIOPHAGES AT 235 mμ

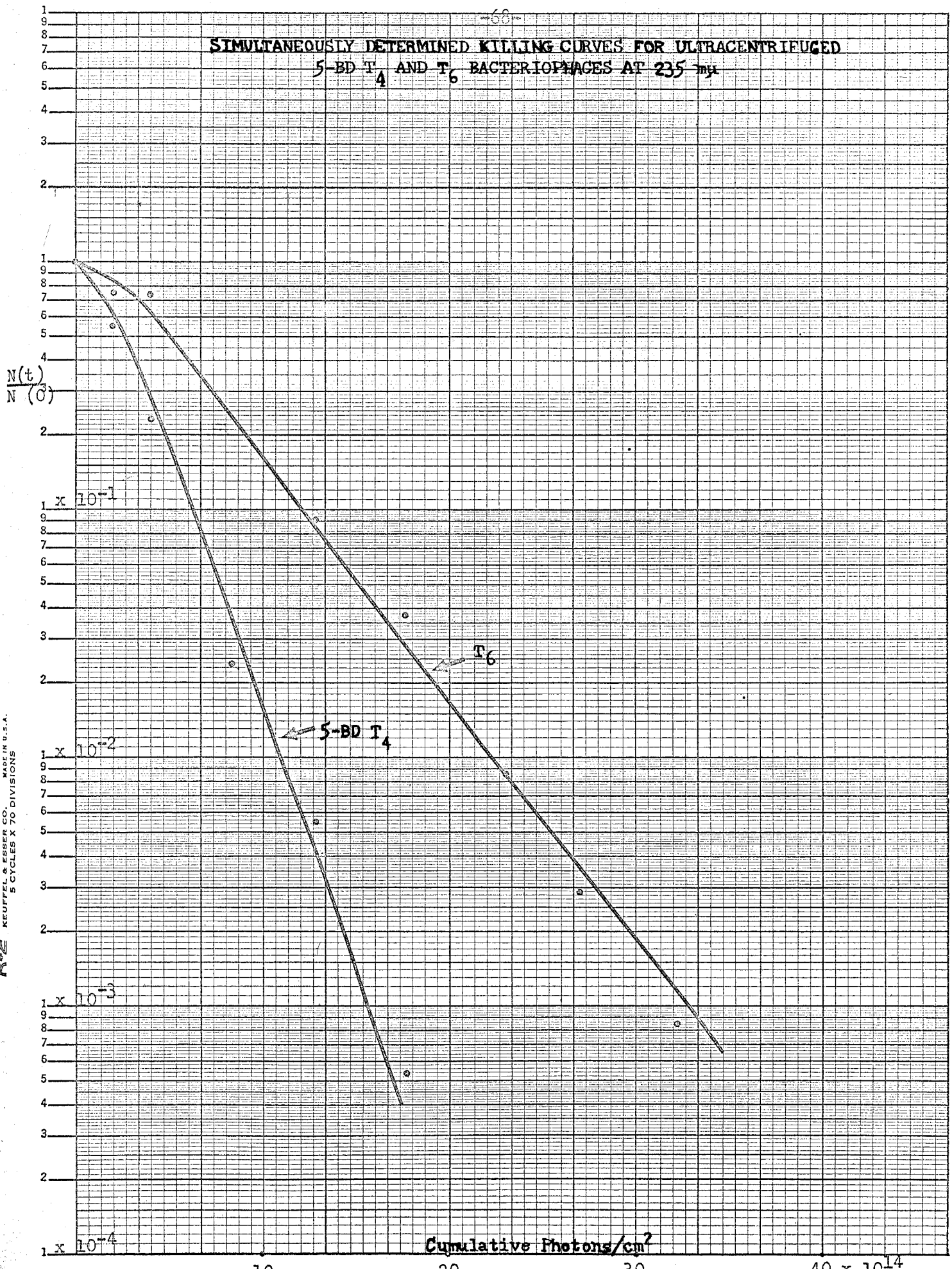

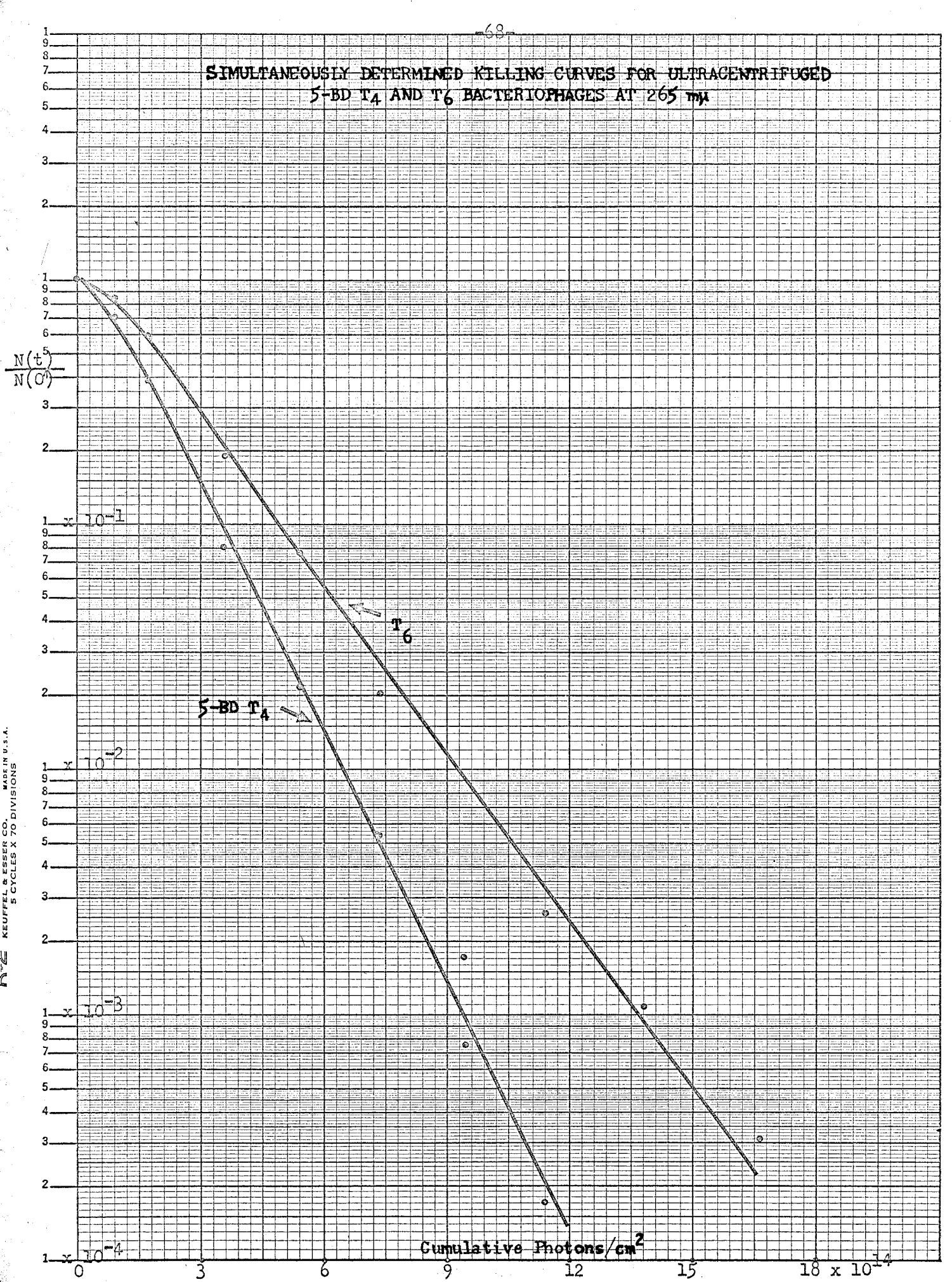
SIMULTANEOUSLY DETERMINED KILLING CURVES FOR ULTRACENTRIFUGED
5-BD T4 AND T6 BACTERIOPHAGES AT 265 mμ
N(t)/N(0)
T6
5-BD T4
Cumulative Photons/cm2
0
3
6
9
12
15
18 x 10-14
1 x 10-1
1 x 10-2
1 x 10-3
1 x 10-4
KEUFFEL & ESSER CO. MADE IN U.S.A.
5 CYCLES X 70 DIVISIONS

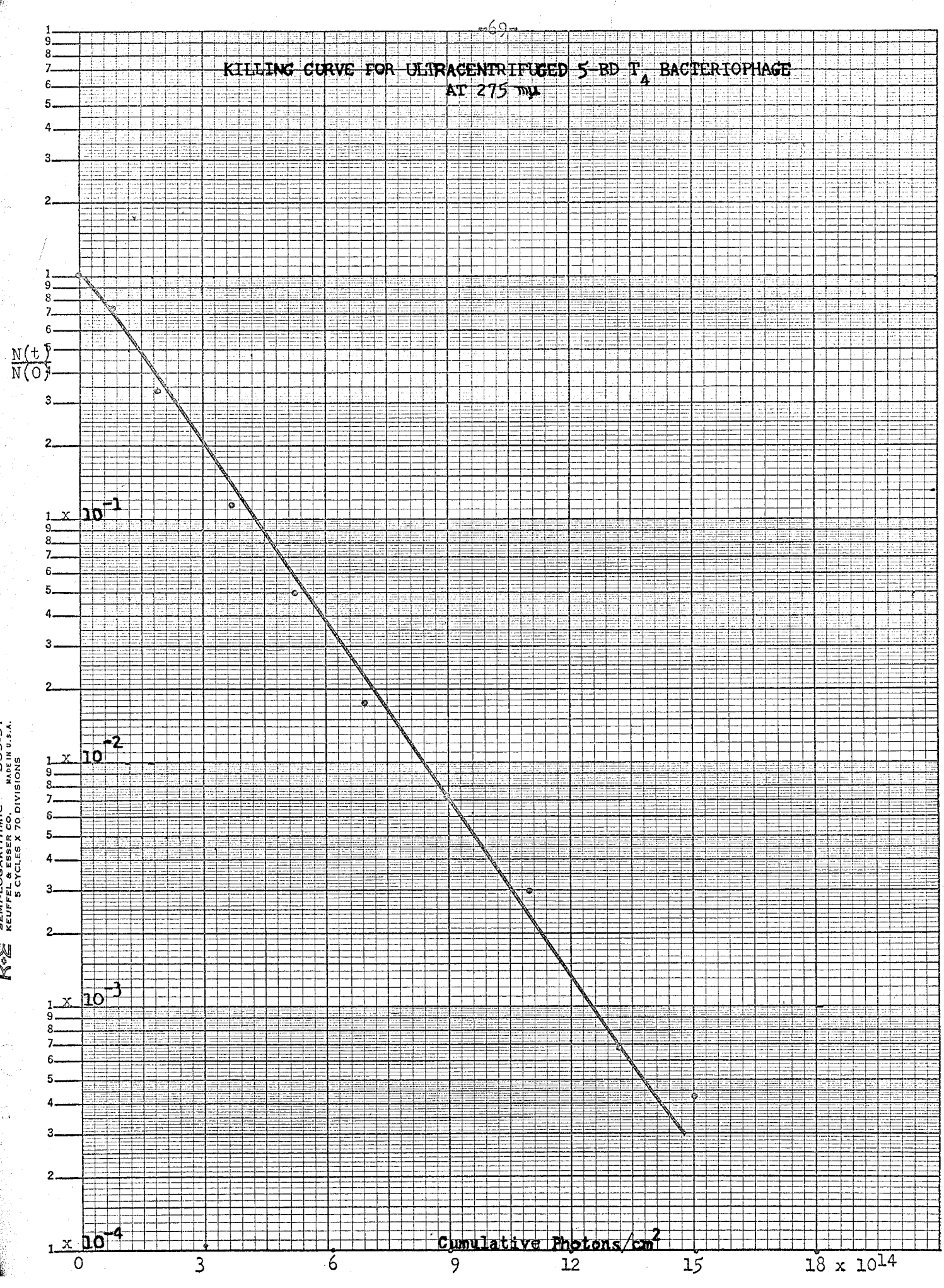

SIMULTANEOUSLY DETERMINED KILLING CURVES FOR ULTRACENTRIFUGED 5-BD T_4 AND T_6 BACTERIOPHAGES AT 280 mμ

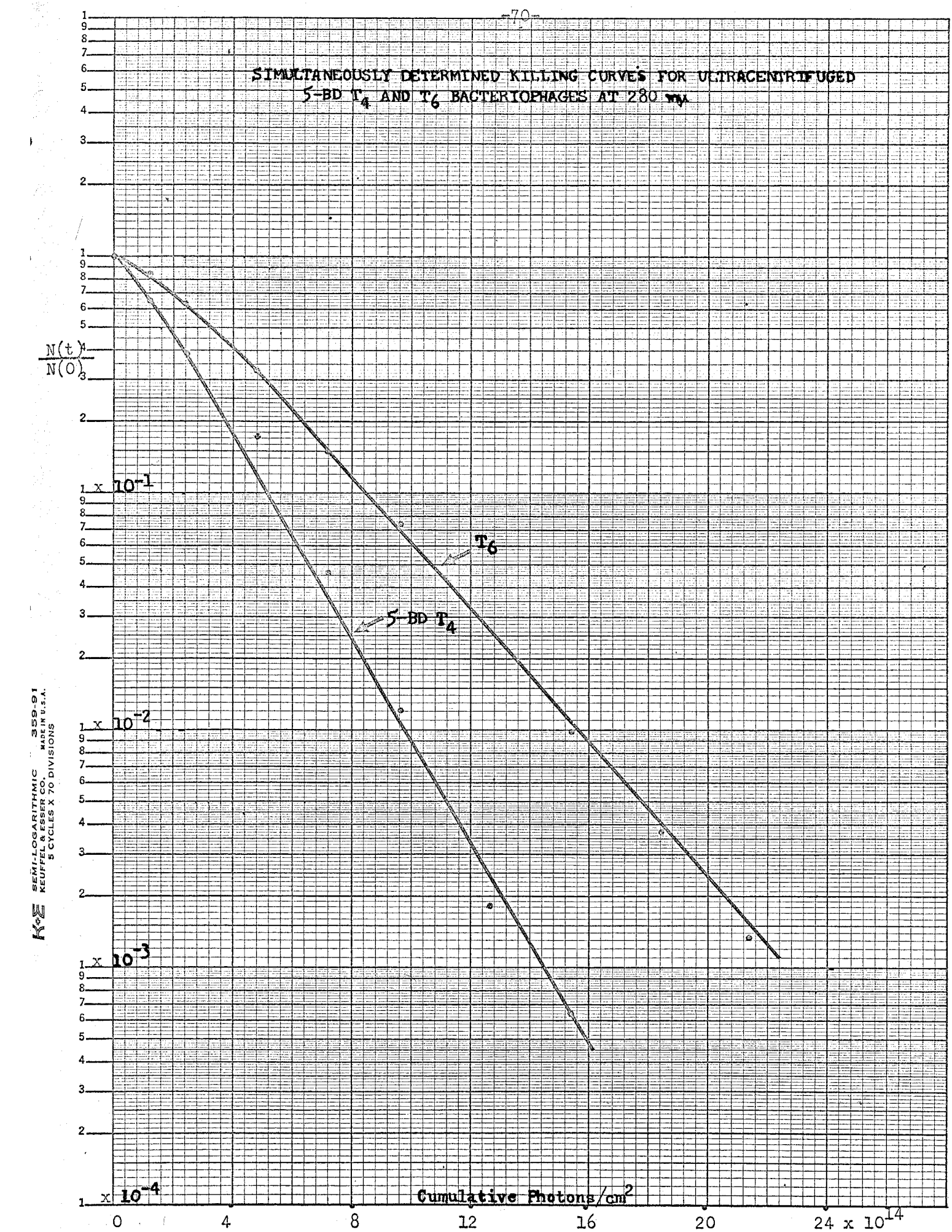

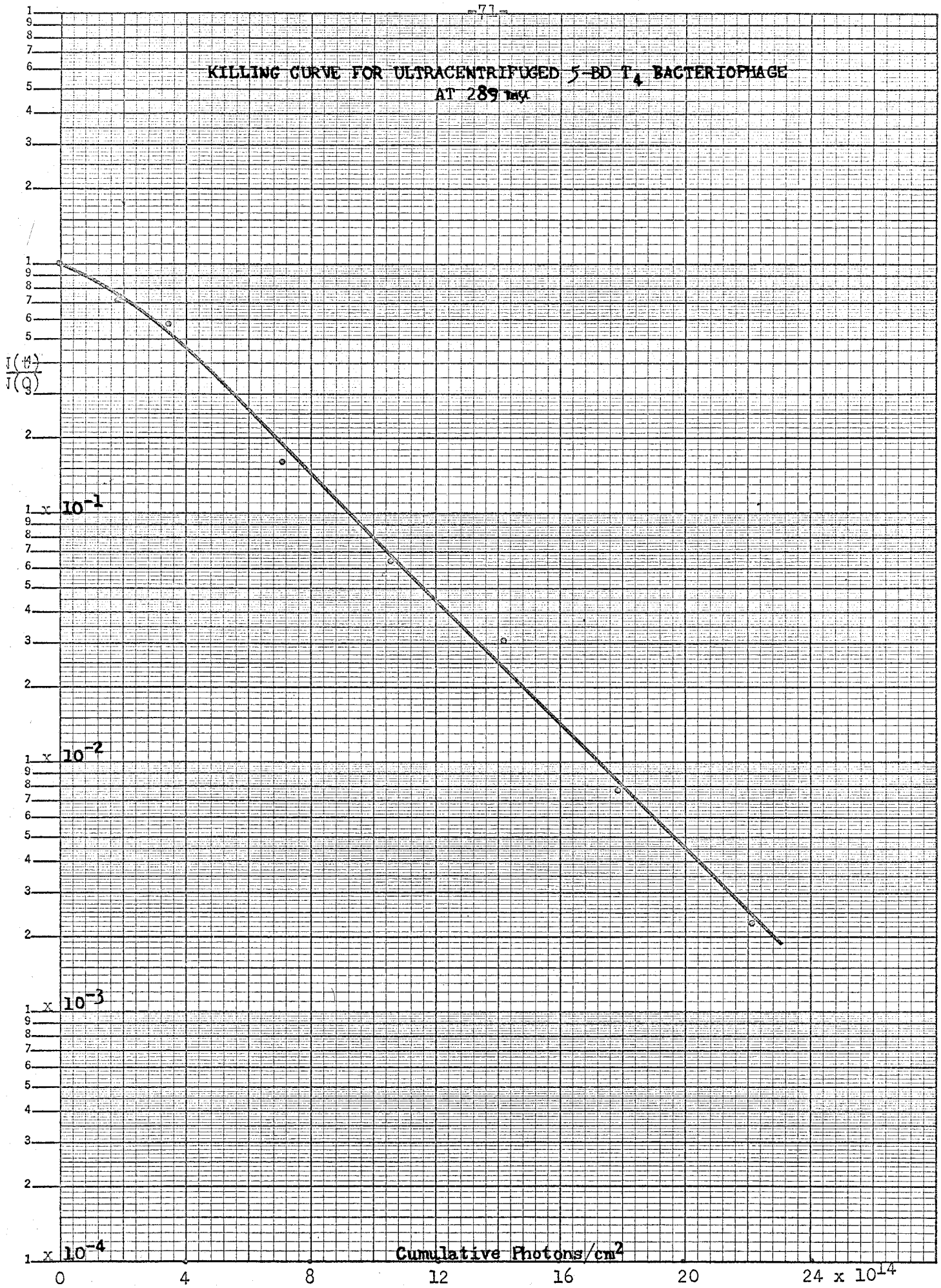
KILLING CURVE FOR ULTRACENTRIFUGED 5-BD T_4 BACTERIOPHAGE
AT 289 mμ
J(t)/J(0)
1 x 10^-1
1 x 10^-2
1 x 10^-3
1 x 10^-4
Cumulative Photons/cm^2
0
4
8
12
16
20
24 x 10^14

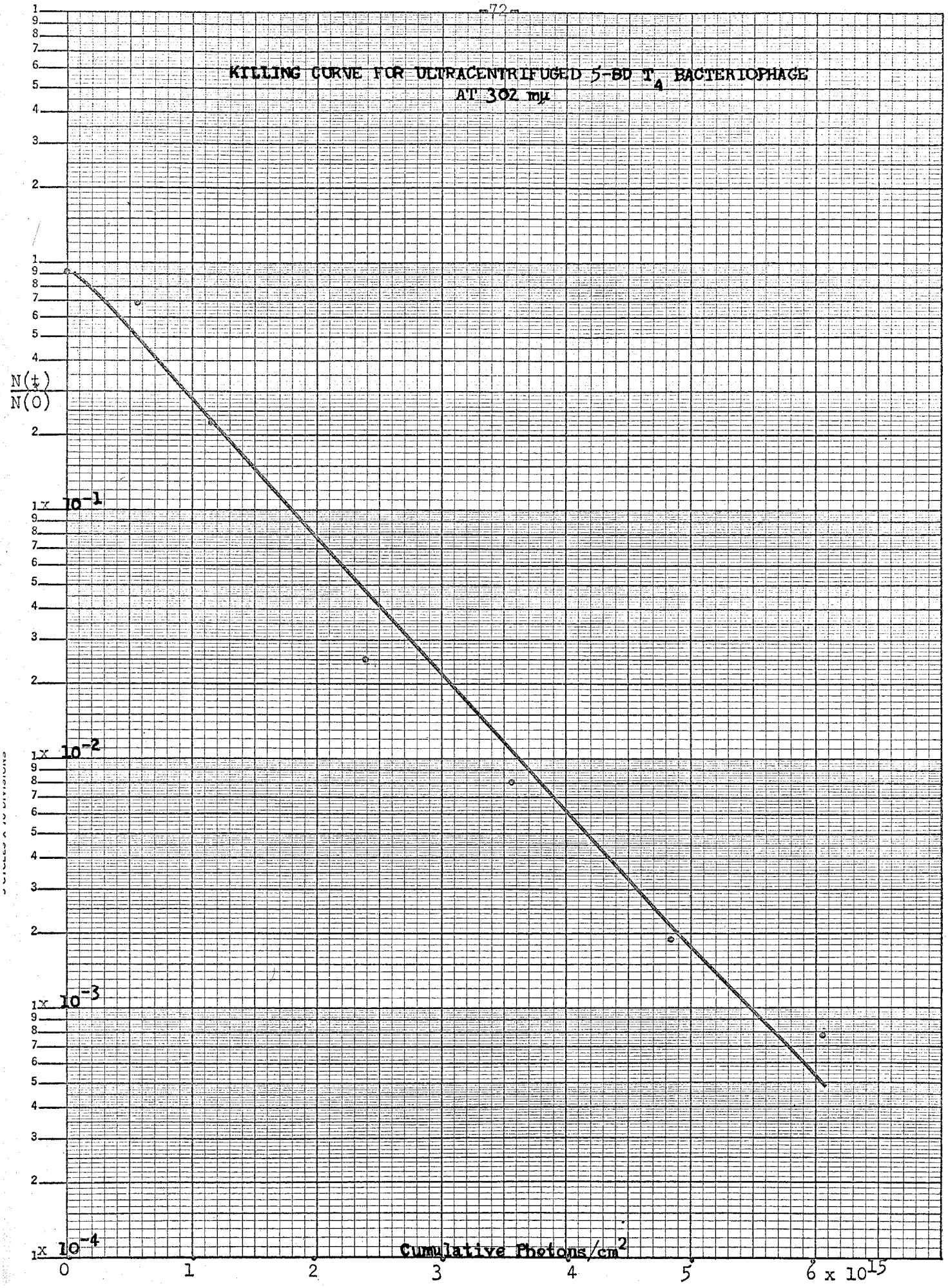
KILLING CURVE FOR ULTRACENTRIFUGED 5-BD T_4 BACTERIOPHAGE
AT 302 mμ
$\frac{N(t)}{N(0)}$
1 x 10^{-1}
1 x 10^{-2}
1 x 10^{-3}
1 x 10^{-4}
0
1
2
3
4
5
6 x 10^{15}
Cumulative Photons/cm^2

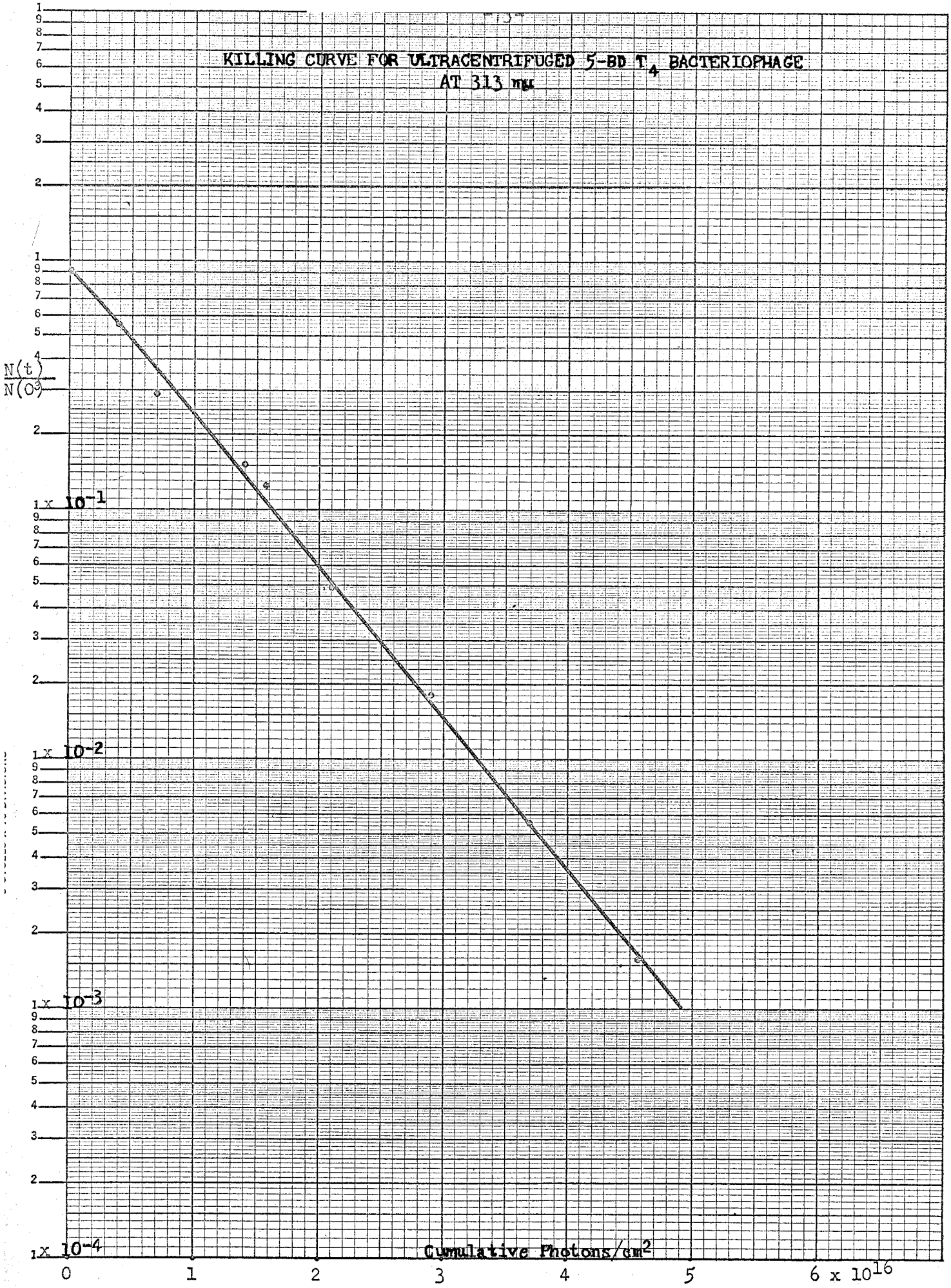
KILLING CURVE FOR ULTRACENTRIFUGED 5-BD T_4 BACTERIOPHAGE
AT 313 mμ
$\frac{N(t)}{N(O)}$
1 x 10⁻¹
1 x 10⁻²
1 x 10⁻³
1 x 10⁻⁴
Cumulative Photons/cm²
0
1
2
3
4
5
6 x 10¹⁶

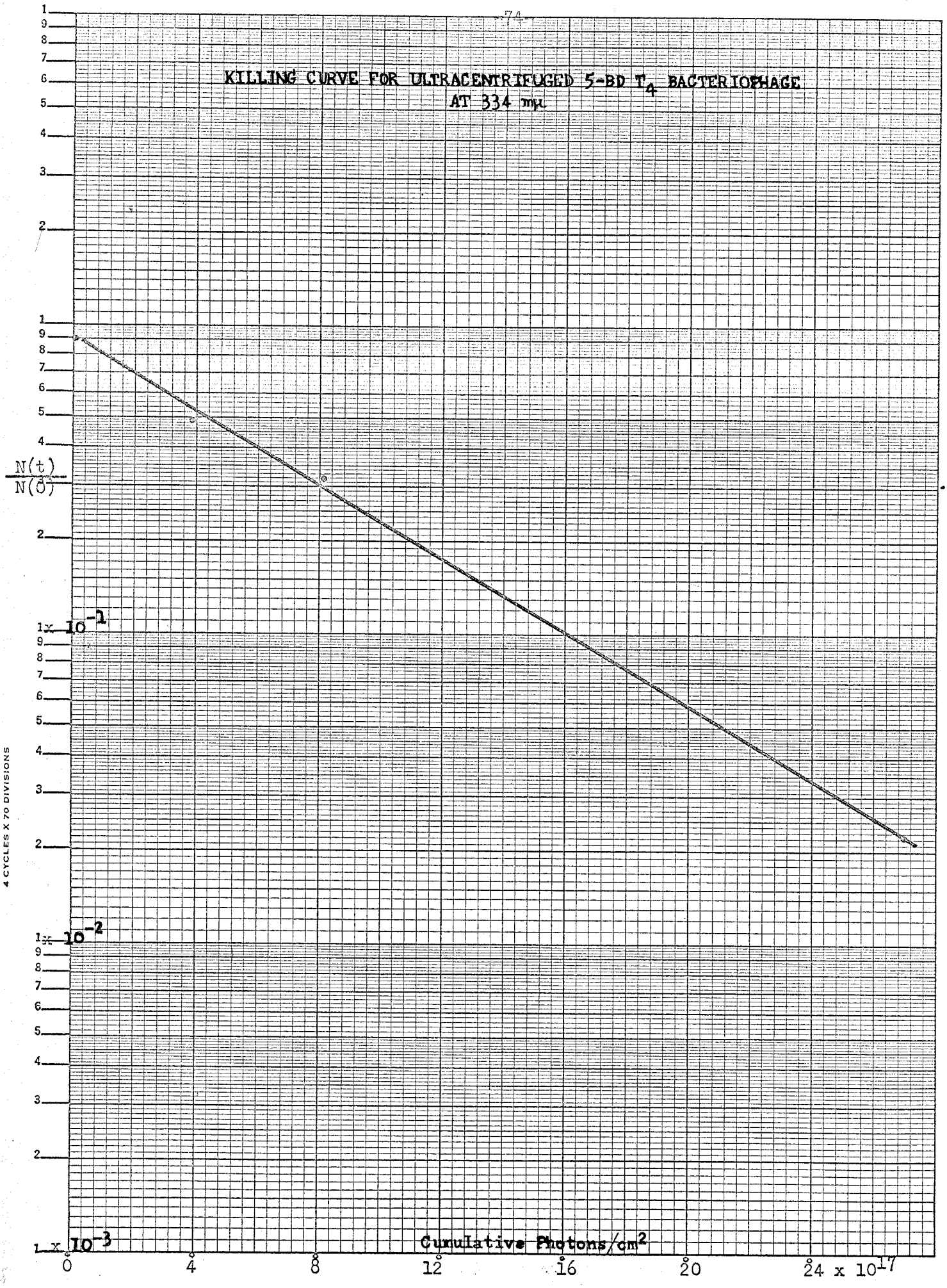
KILLING CURVE FOR ULTRACENTRIFUGED 5-BD T_4 BACTERIOPHAGE
AT 334 mμ
N(t)/N(0)
1 x 10^-1
1 x 10^-2
1 x 10^-3
4 CYCLES X 70 DIVISIONS
0
4
8
12
16
20
24 x 10^17
Cumulative Photons/cm^2

DUPLICATE DETERMINATIONS OF KILLING CURVE OF T_6 BACTERIOPHAGE AT 235 mμ

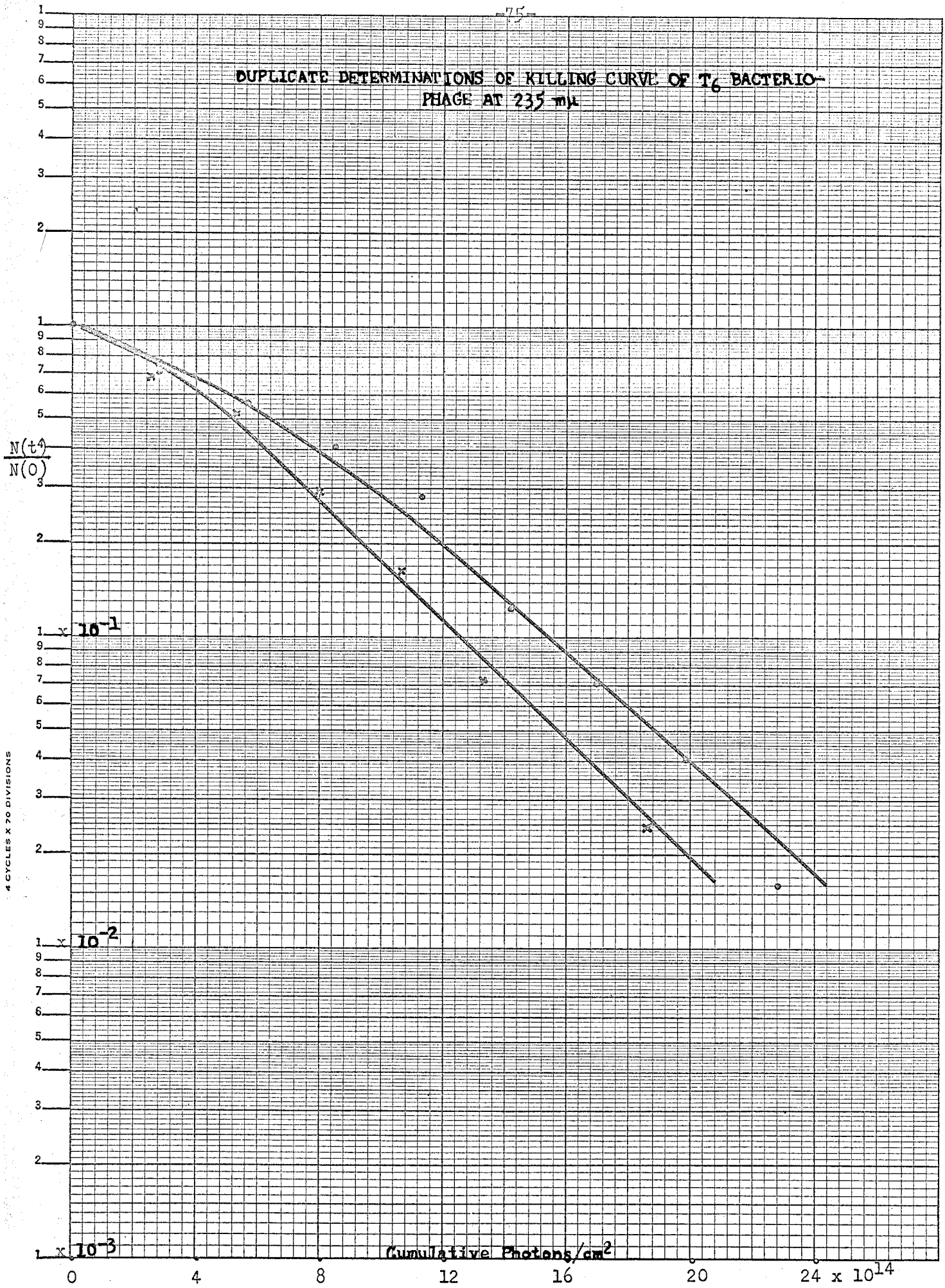

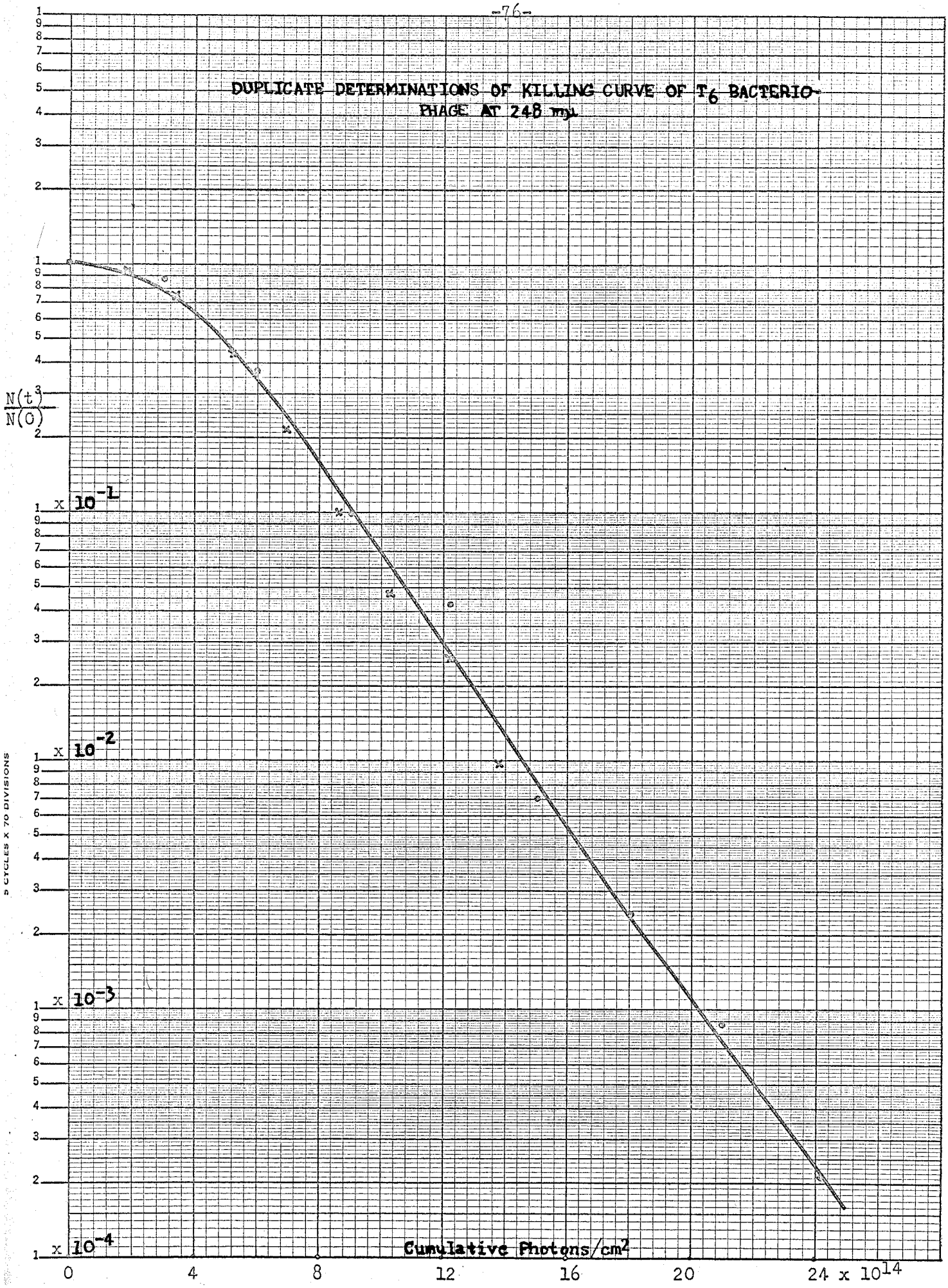
DUPLICATE DETERMINATIONS OF KILLING CURVE OF T6 BACTERIOPHAGE AT 248 mμ
N(t)/N(0)
x 10-1
x 10-2
x 10-3
x 10-4
5 CYCLES X 70 DIVISIONS
Cumulative Photons/cm2
0
4
8
12
16
20
24 x 10^14

DUPLICATE DETERMINATIONS OF KILLING CURVE OF T_6 BACTERIOPHAGE AT 254 mμ

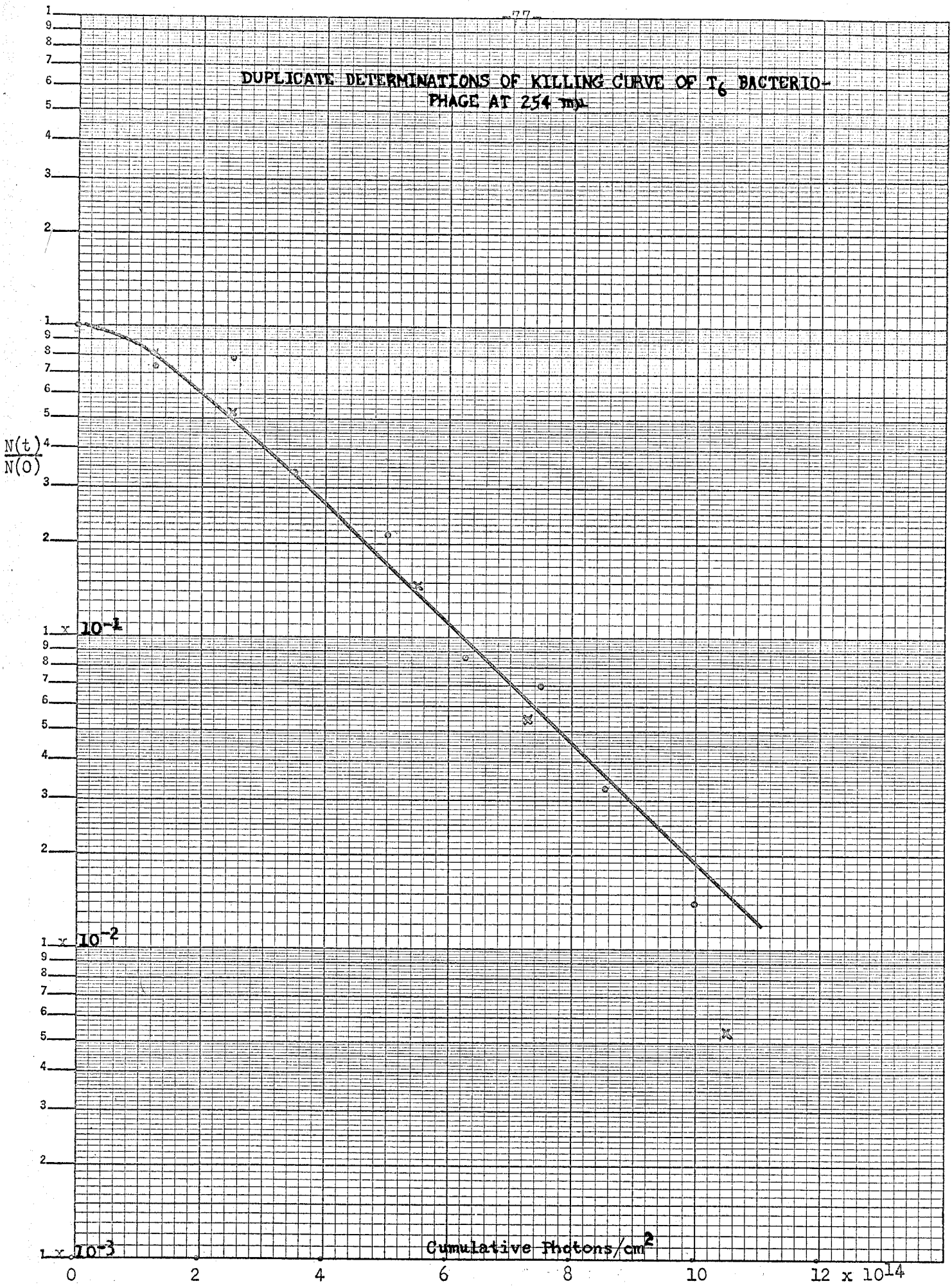

DUPLICATE DETERMINATIONS OF KILLING CURVE OF T_6 BACTERIOPHAGE AT 265 mμ

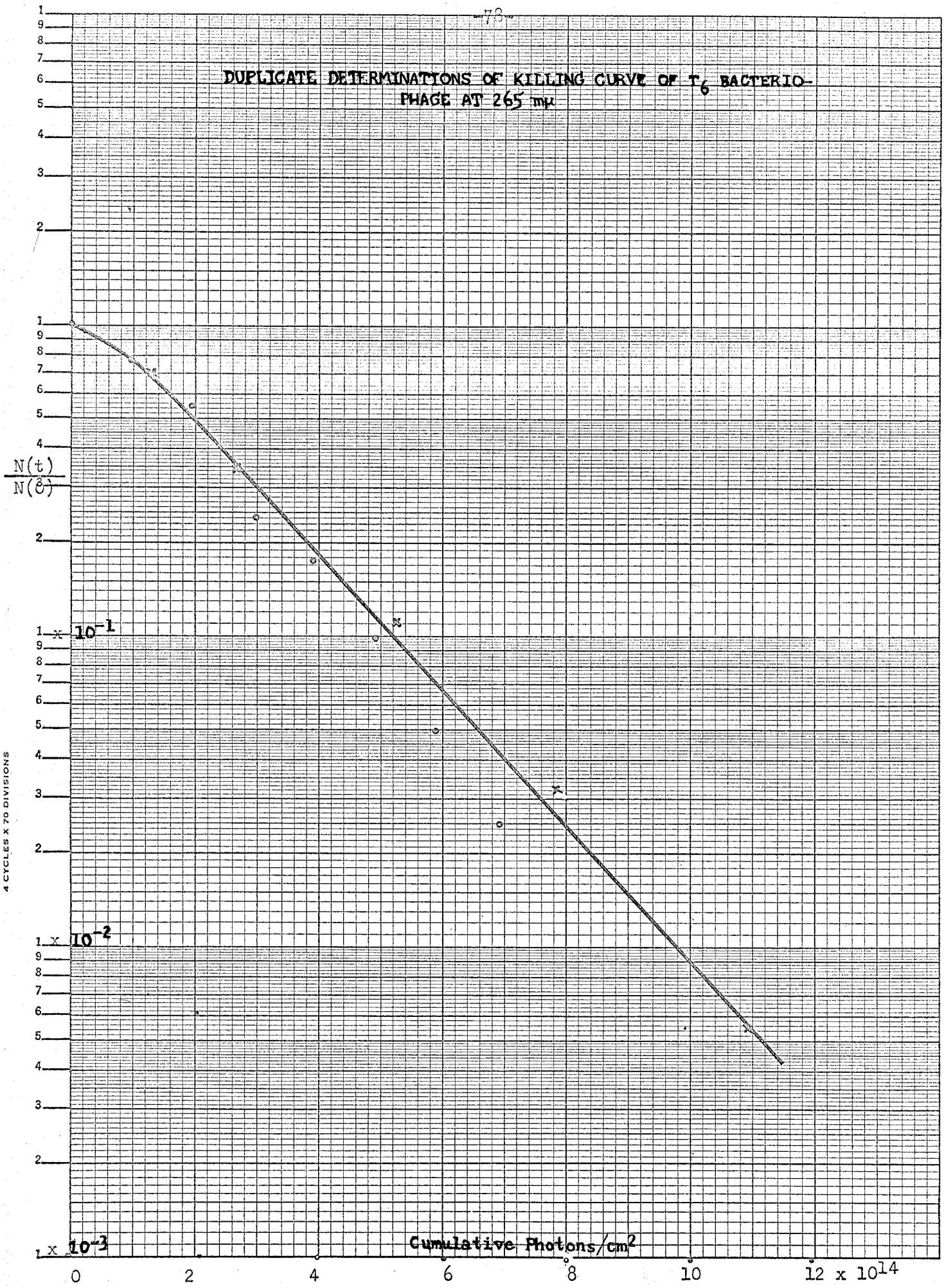

DUPICATE DETERMINATIONS OF KILLING CURVE OF T_6 BACTERIOPHAGE AT 280 mμ

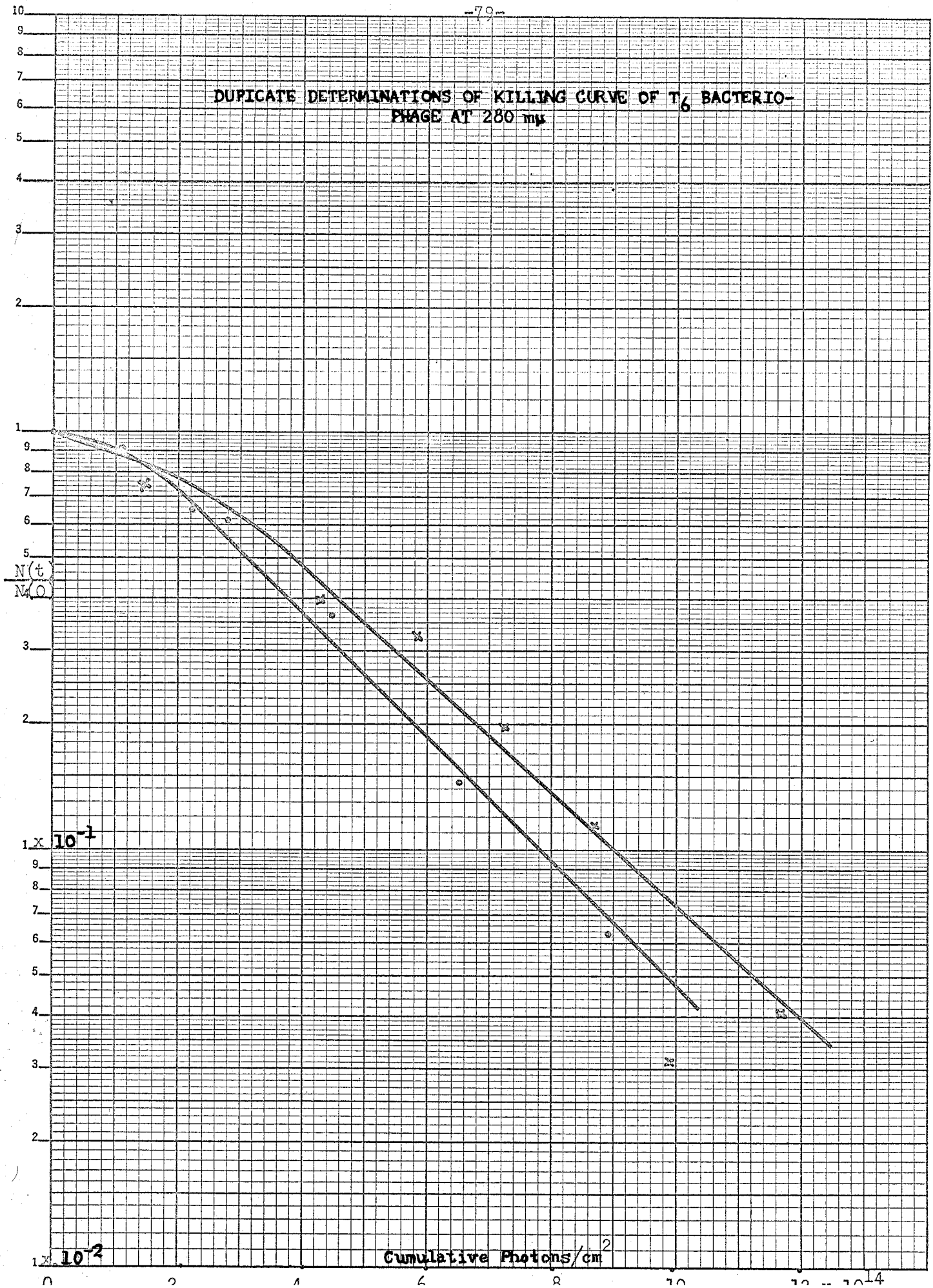

DUPLICATE DETERMINATIONS OF KILLING CURVE OF T6 BACTERIOPHAGE AT 289 mμ

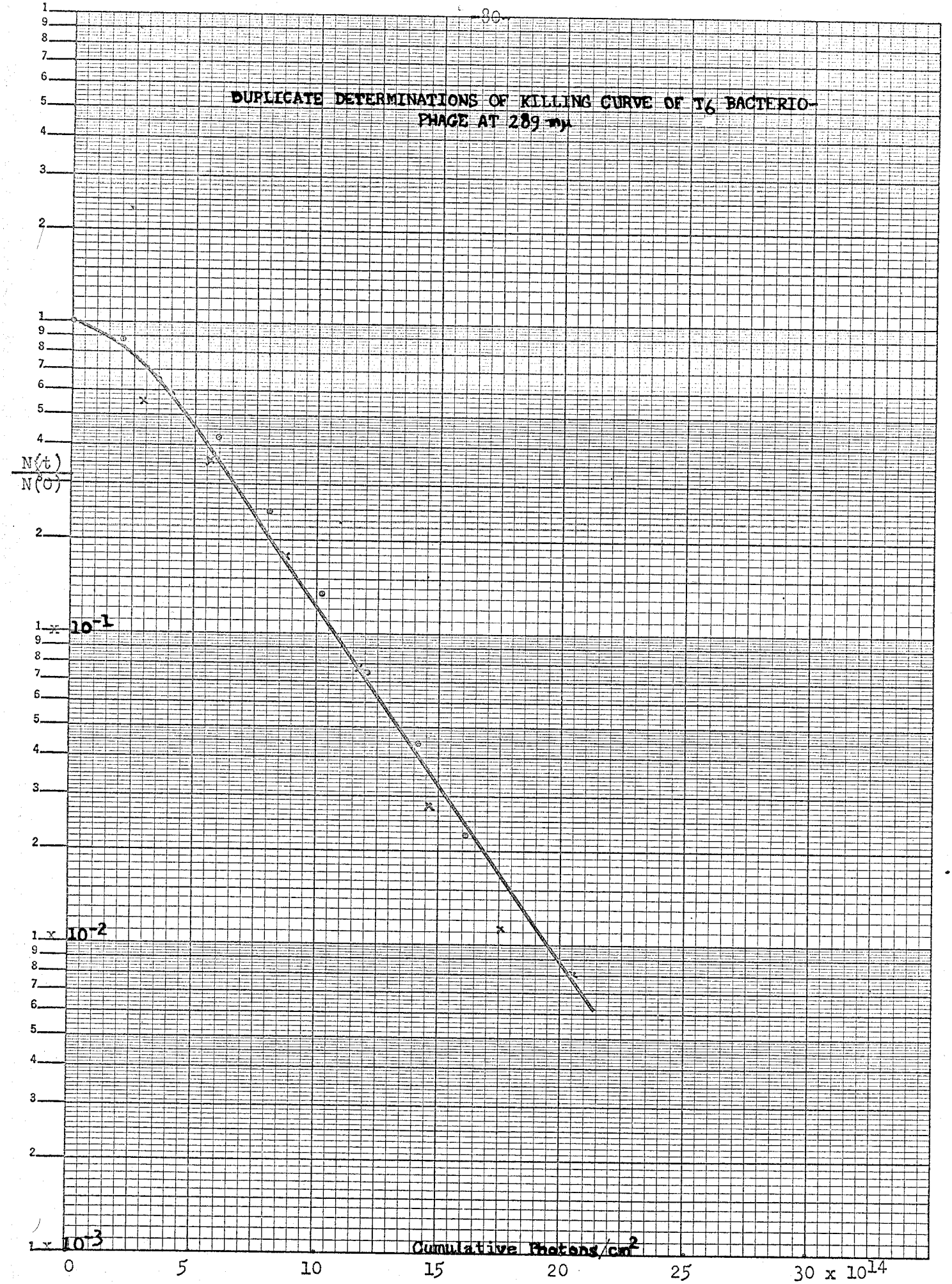

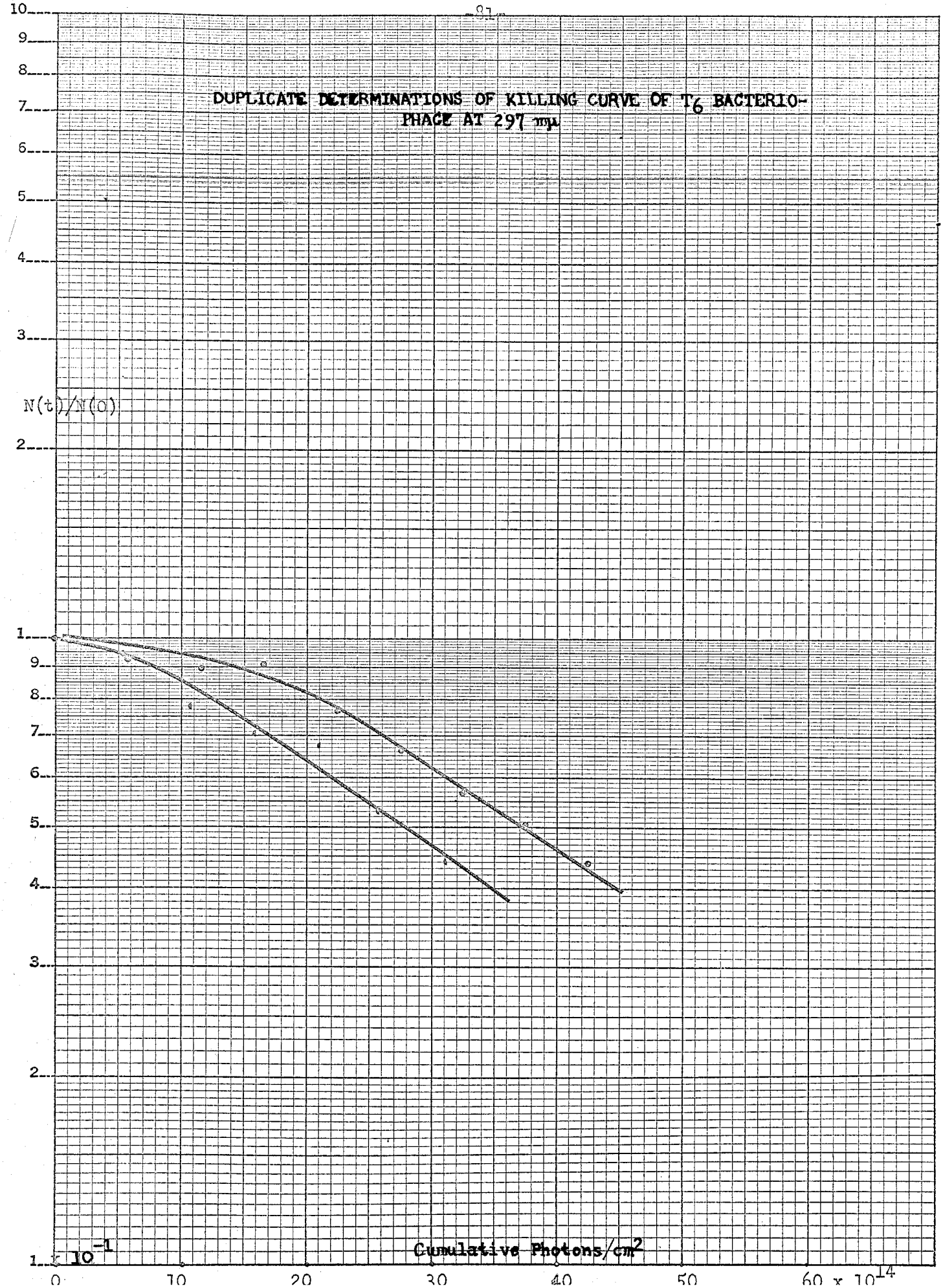
DUPLICATE DETERMINATIONS OF KILLING CURVE OF T6 BACTERIOPHAGE AT 297 mμ
N(t)/N(o)
10
9
8
7
6
5
4
3
2
1
9
8
7
6
5
4
3
2
1 x 10^-1
0
10
20
30
40
50
60 x 10^14
Cumulative Photons/cm^2

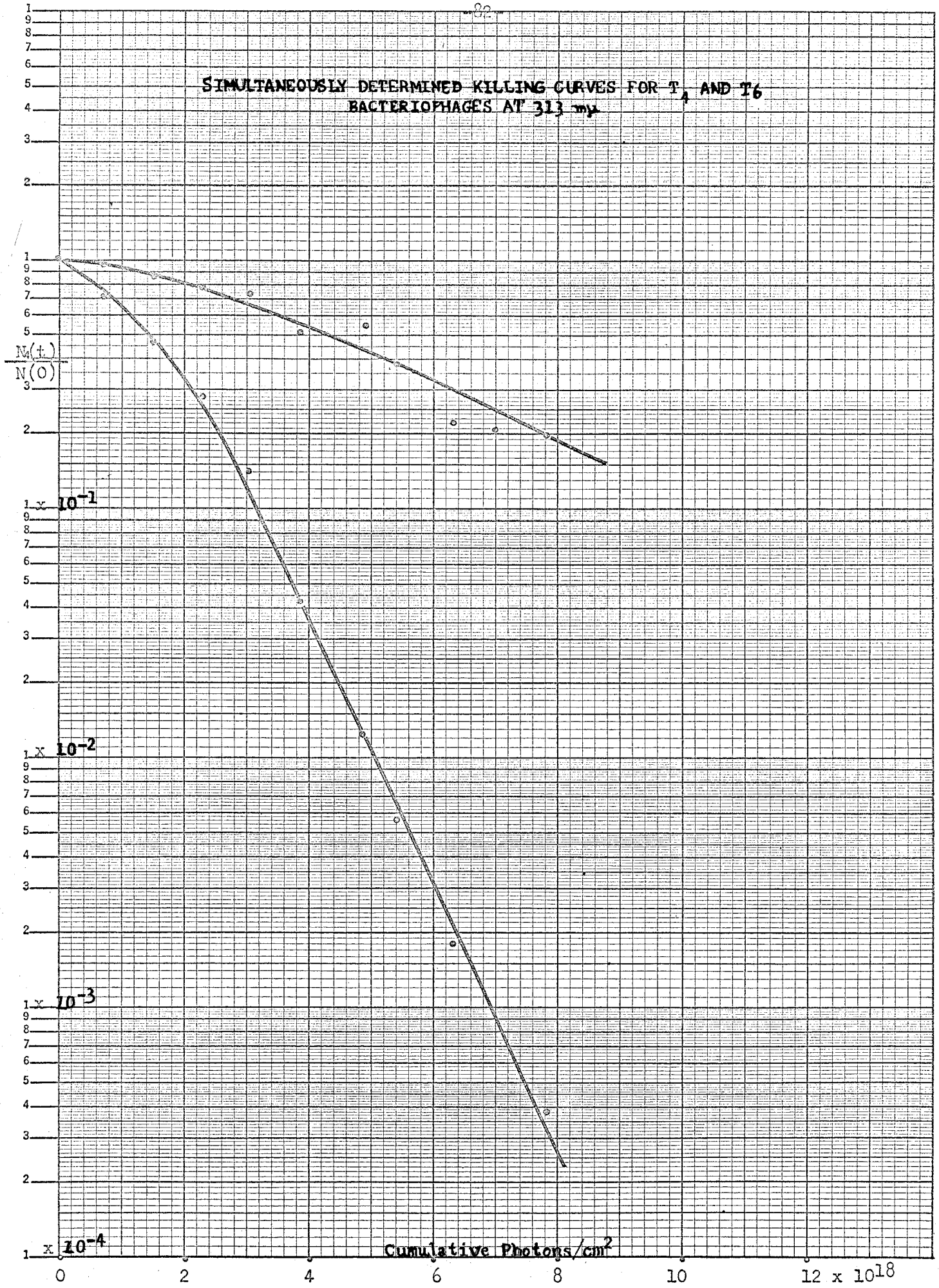
SIMULTANEOUSLY DETERMINED KILLING CURVES FOR T_4 AND T_6 BACTERIOPHAGES AT 313 mμ
N(t)/N(0)
1 x 10^-1
1 x 10^-2
1 x 10^-3
1 x 10^-4
Cumulative Photons/cm^2
0
2
4
6
8
10
12 x 10^18

SIMULTANEOUSLY DETERMINED KILLING CURVES FOR T_4 AND T_6 BACTERIOPHAGES AT 334 mμ

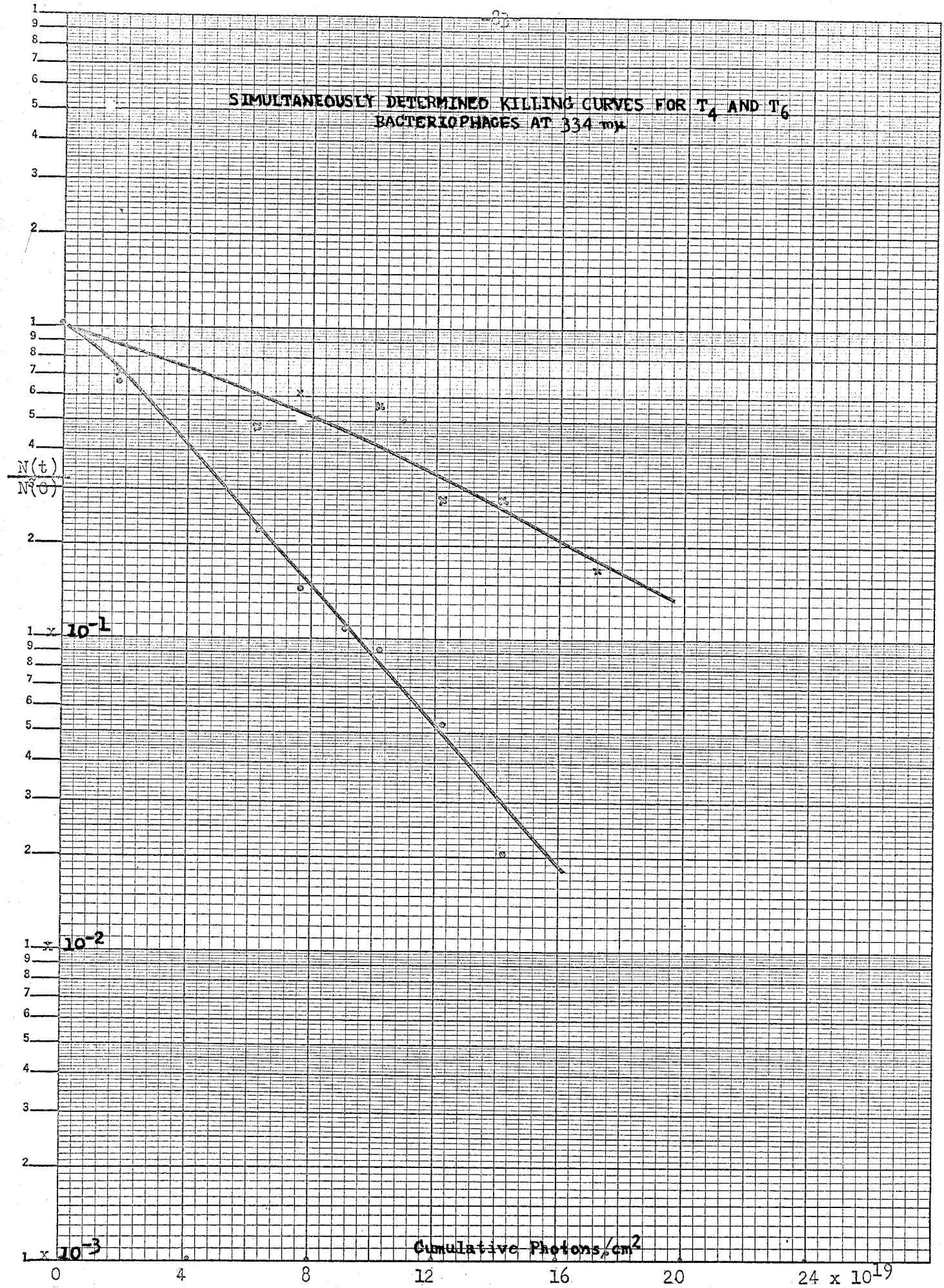

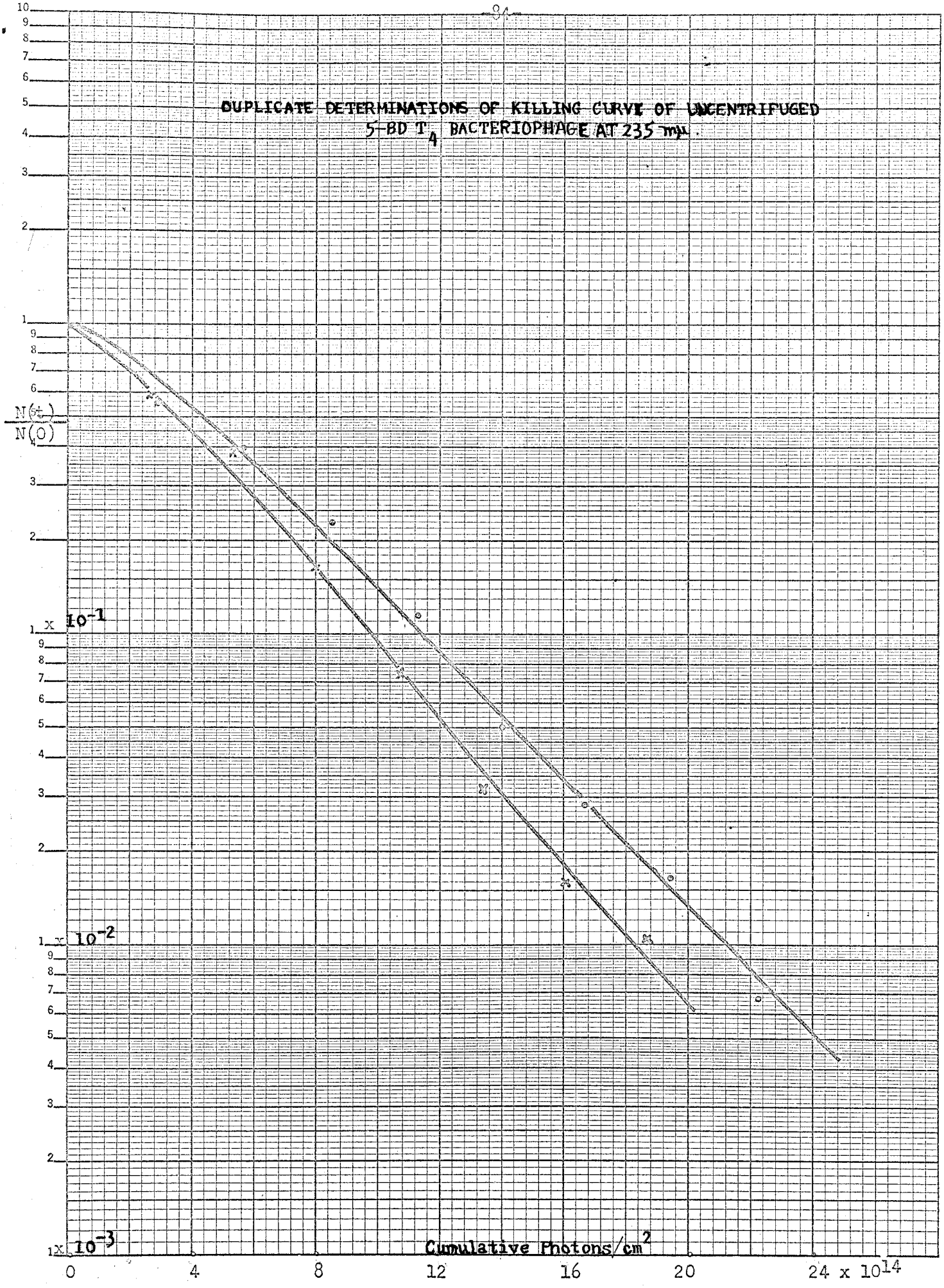
DUPLICATE DETERMINATIONS OF KILLING CURVE OF UNCENTRIFUGED 5-BD T_4 BACTERIOPHAGE AT 235 mμ.
N(t)/N(0)
Cumulative Photons/cm^2
0
4
8
12
16
20
24 x 10^{14}
1 x 10^{-1}
1 x 10^{-2}
1 x 10^{-3}

DUPLICATE DETERMINATIONS OF KILLING CURVE OF UNCENTRIFUGED 5-BD T_4 BACTERIOPHAGE AT 248 mμ

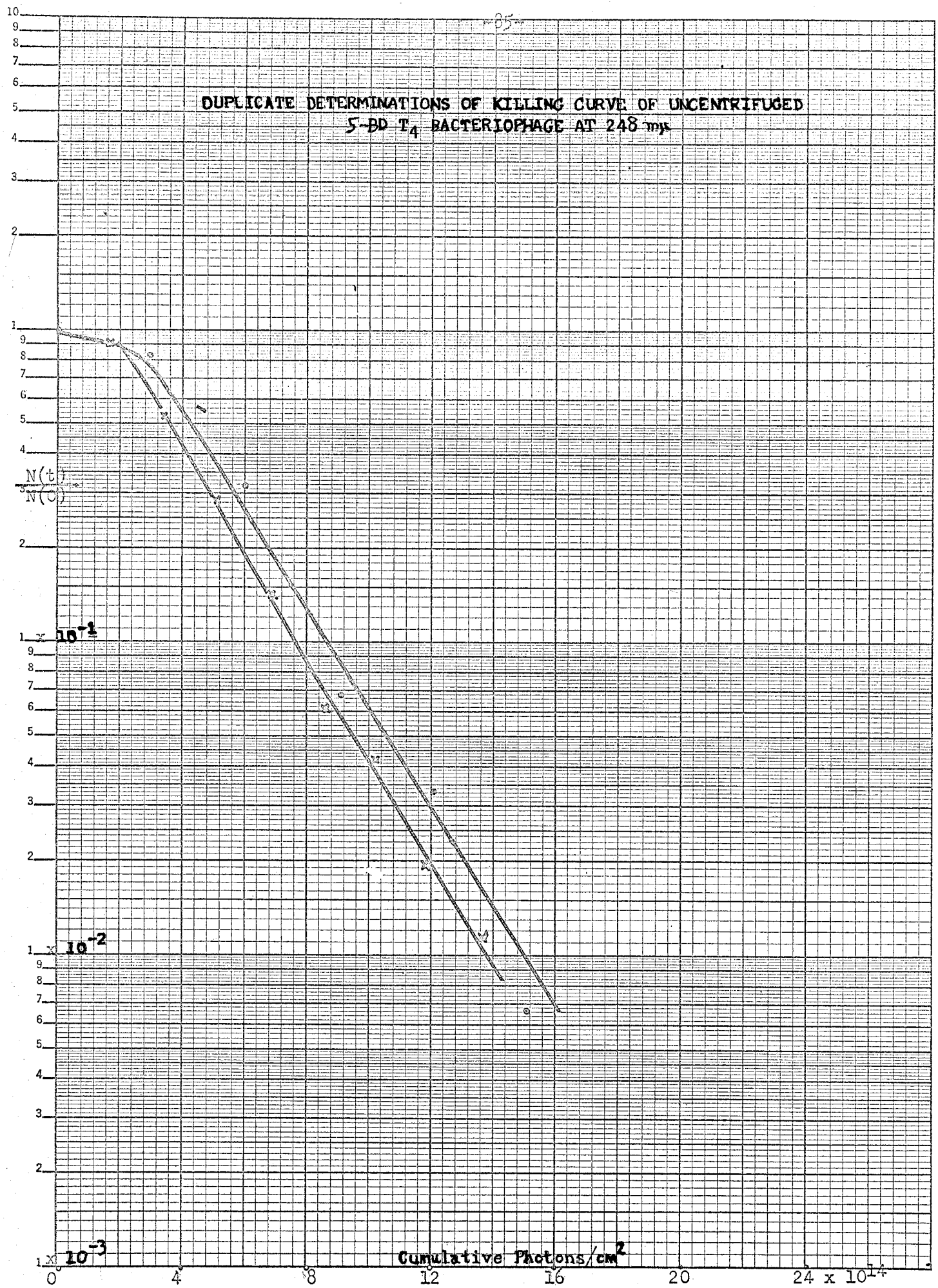

DUPLICATE DETERMINATIONS OF KILLING CURVE OF UNCENTRIFUGED 5-BD T_4 BACTERIOPHAGE AT 265 mμ

$\frac{N(E)}{N(0)}$

1×10^{-1}

1×10^{-2}

1×10^{-3}

Cumulative Photons/cm^2

0 2 4 6 8 10 12 x 10^{14}

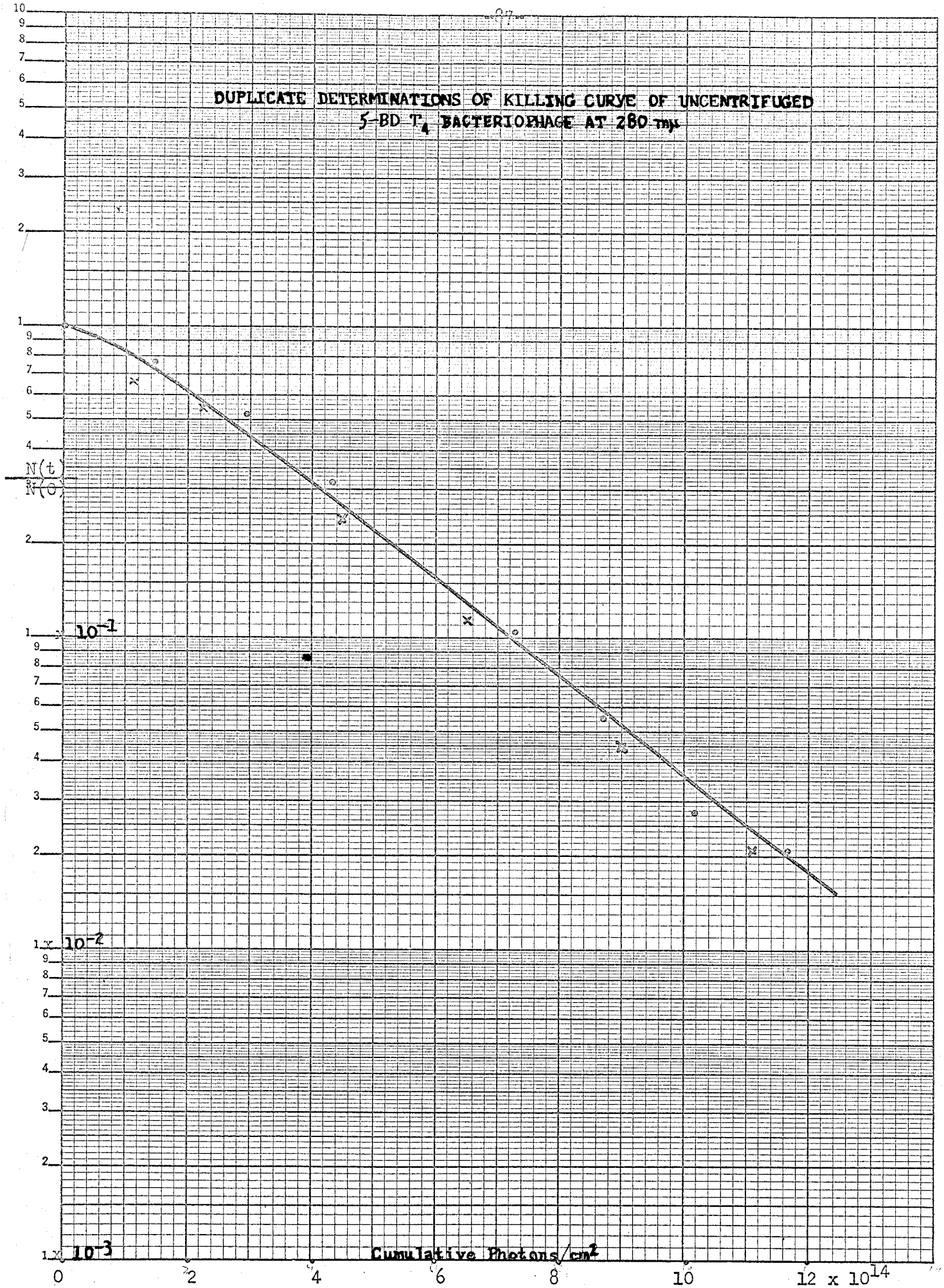
DUPLICATE DETERMINATIONS OF KILLING CURVE OF UNCENTRIFUGED
5-BD T_4 BACTERIOPHAGE AT 280 mμ
N(t)/N(0)
10^{-1}
1×10^{-2}
10^{-3}
Cumulative Photons/cm²
0
2
4
6
8
10
12 x 10^{14}

DUPLICATE DETERMINATIONS OF KILLING CURVE OF UNCENTRIFUGED 5-BD T_4 BACTERIOPHAGE AT 280 mμ

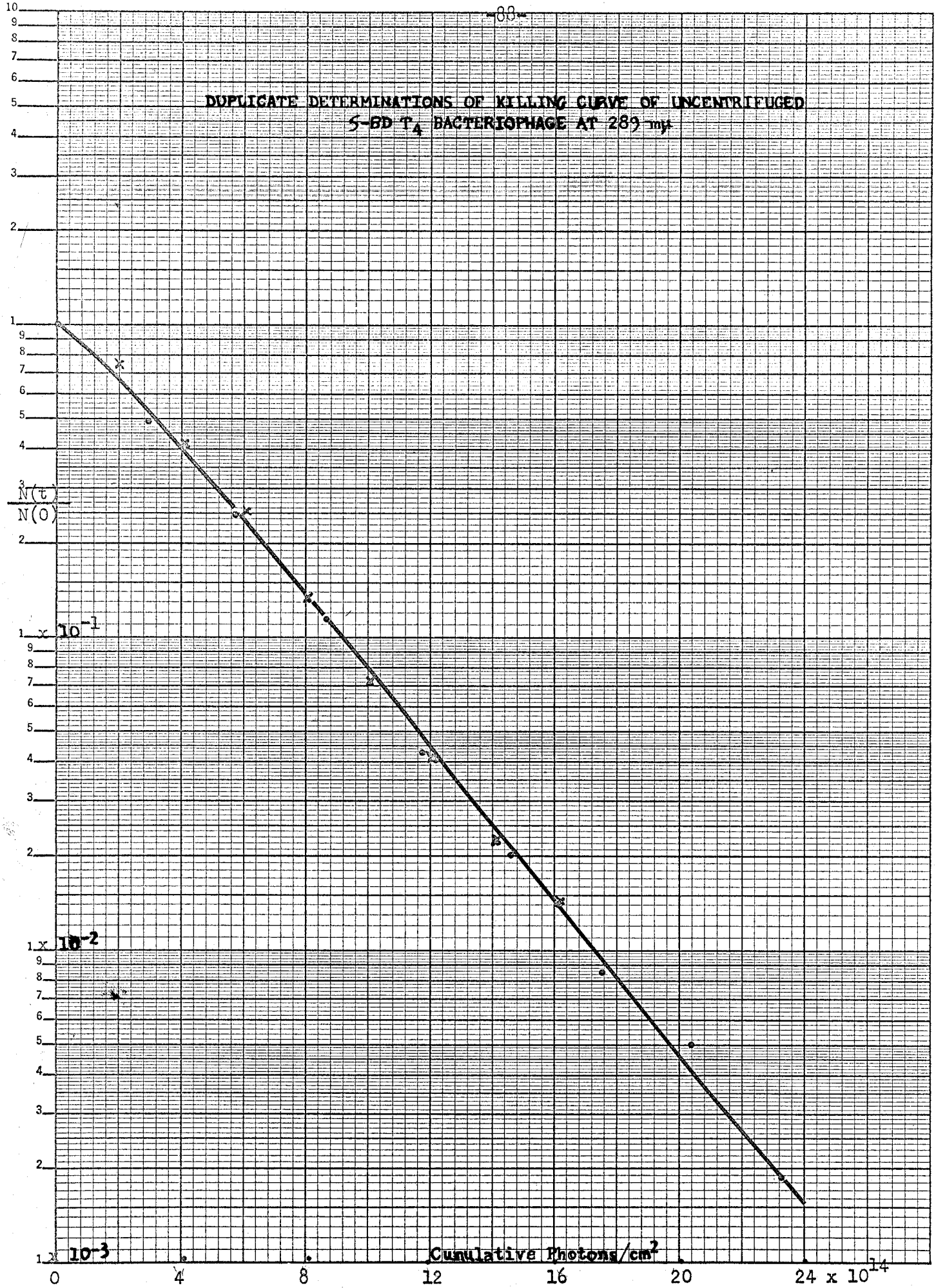

DUPLICATE DETERMINATIONS OF KILLING CURVE OF UNCENTRIFUGED 5-BD T_4 BACTERIOPHAGE AT 297 mμ

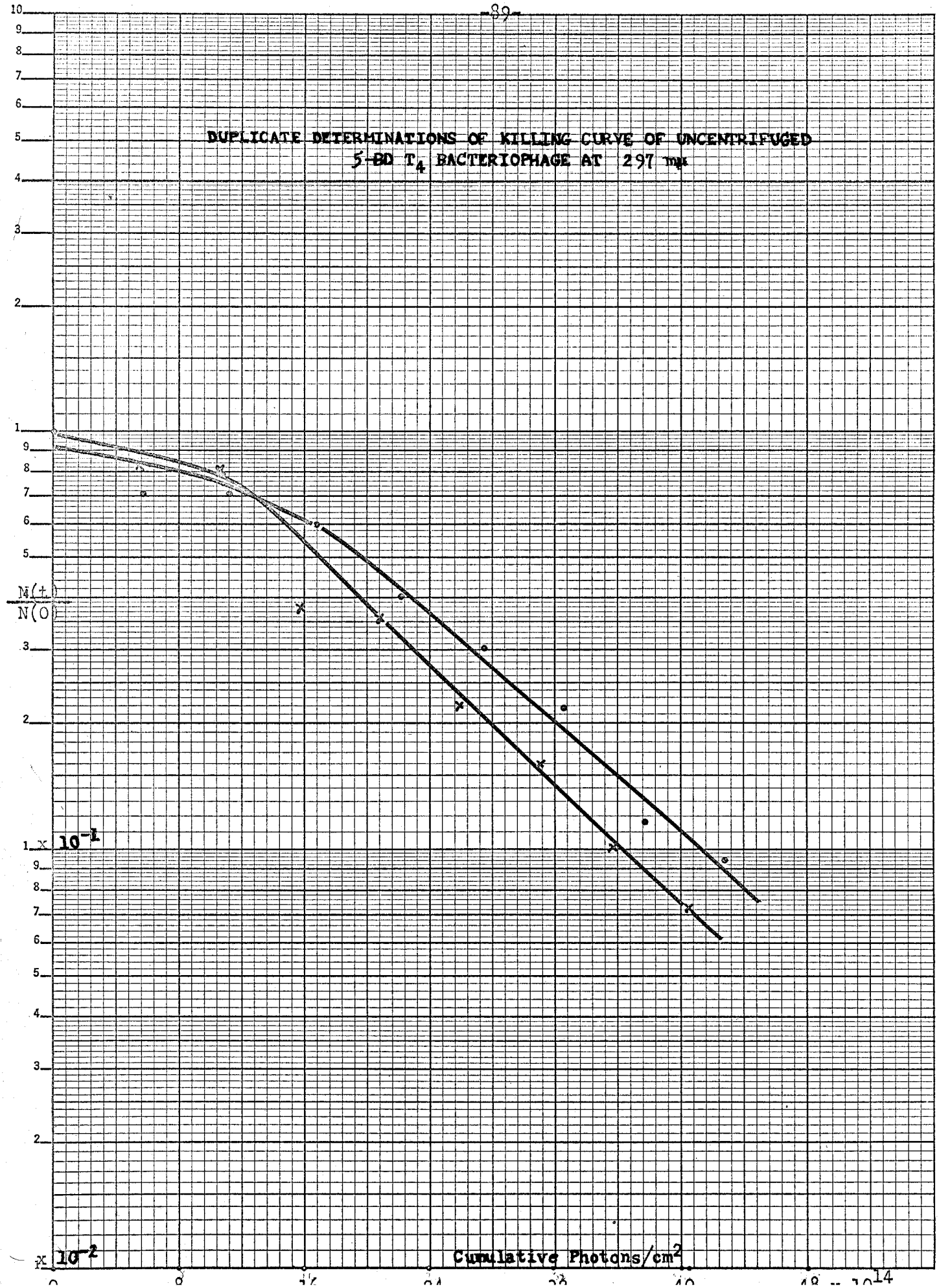

DUPLICATE DETERMINATIONS OF KILLING CURVE OF UNCENTRIFUGED 5-BD T_4 BACTERIOPHAGE AT 302 mμ

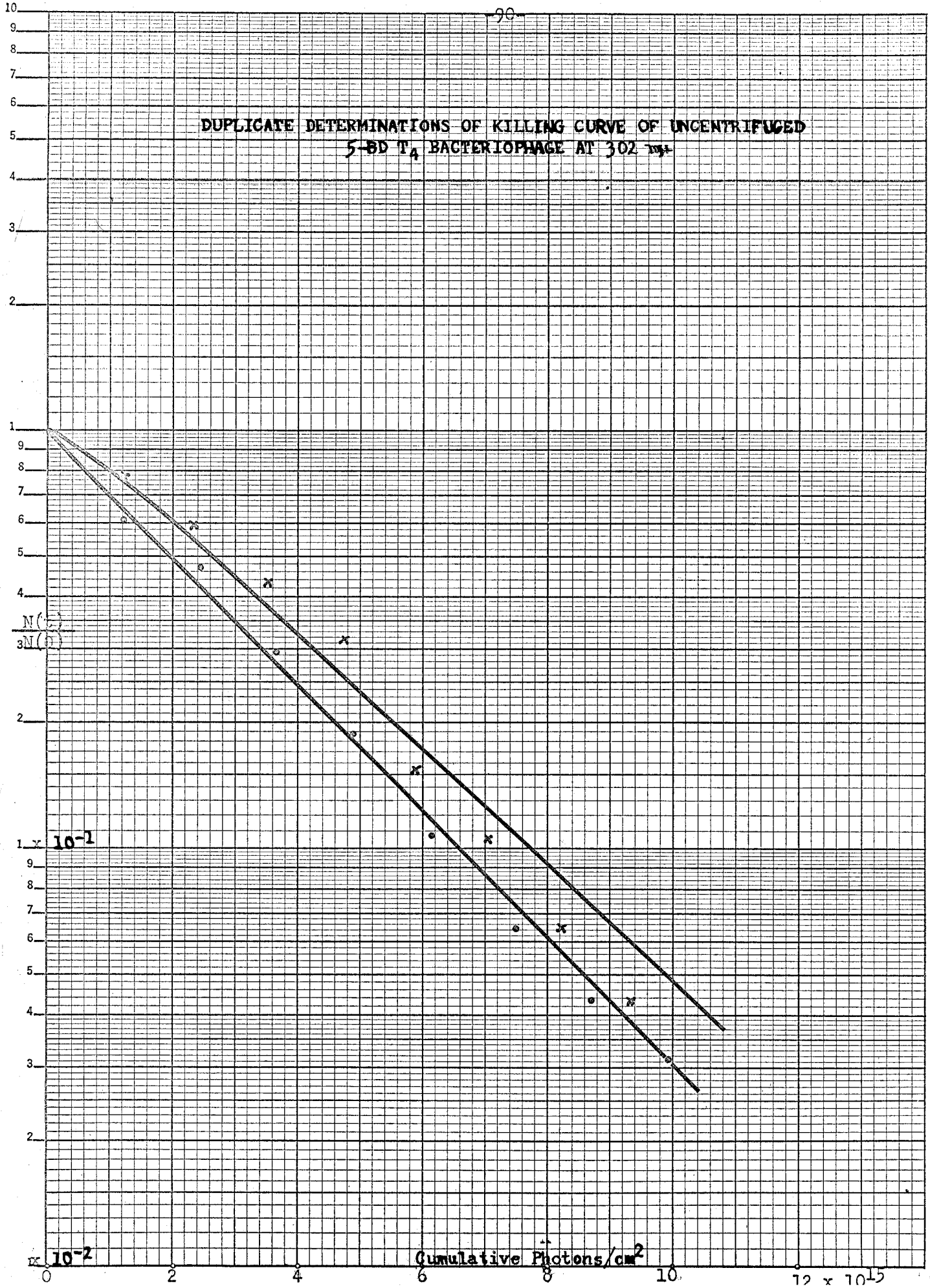

DUPLICATE DETERMINATIONS OF KILLING CURVE OF UNCENTRIFUGED 5-BD T_4 BACTERIOPHAGE AT 313 mμ

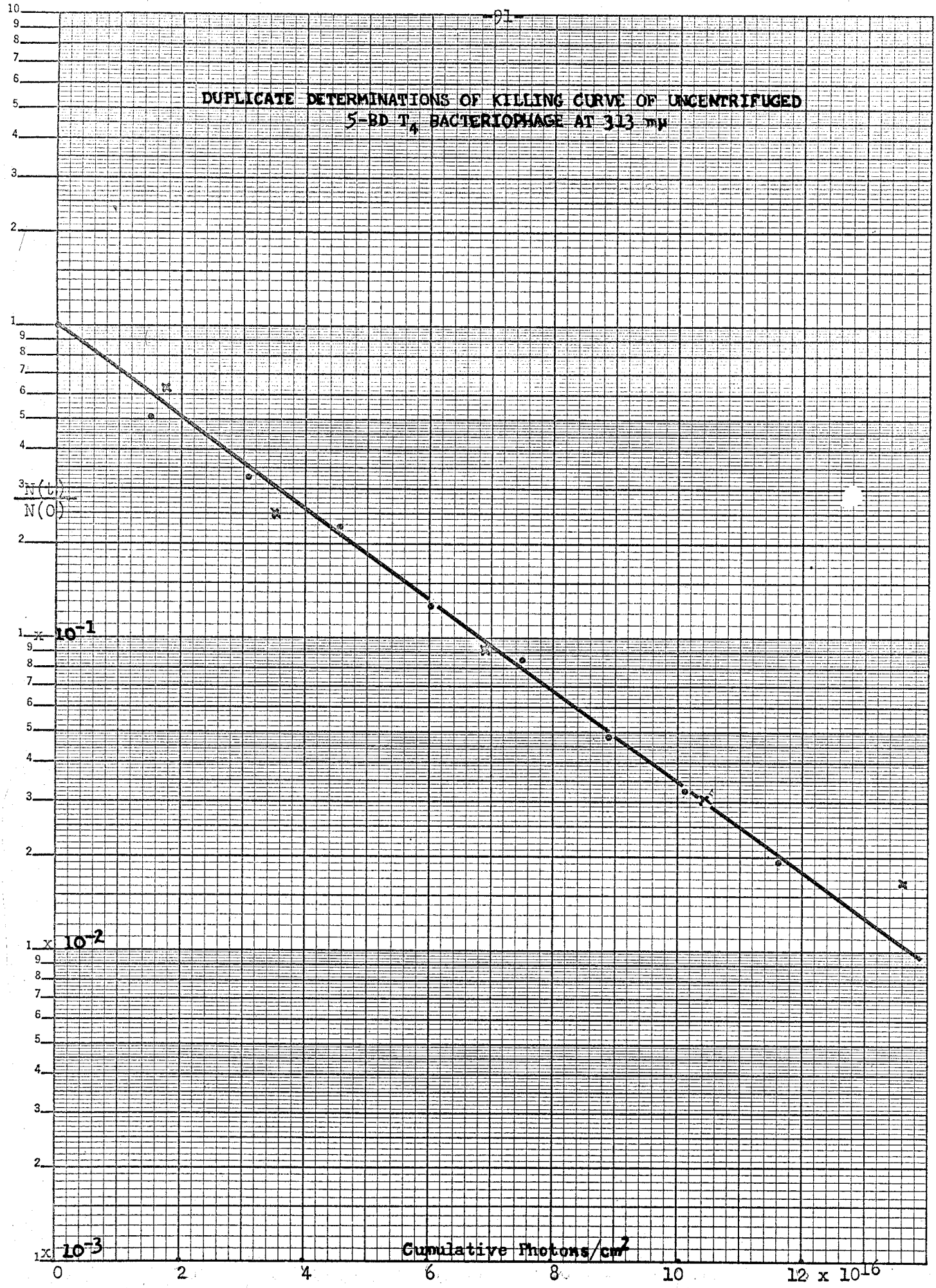

DUPLICATE DETERMINATIONS OF KILLING CURVE OF UNCENTRIFUGED 5-BD T_4 BACTERIOPHAGE AT 320 mμ

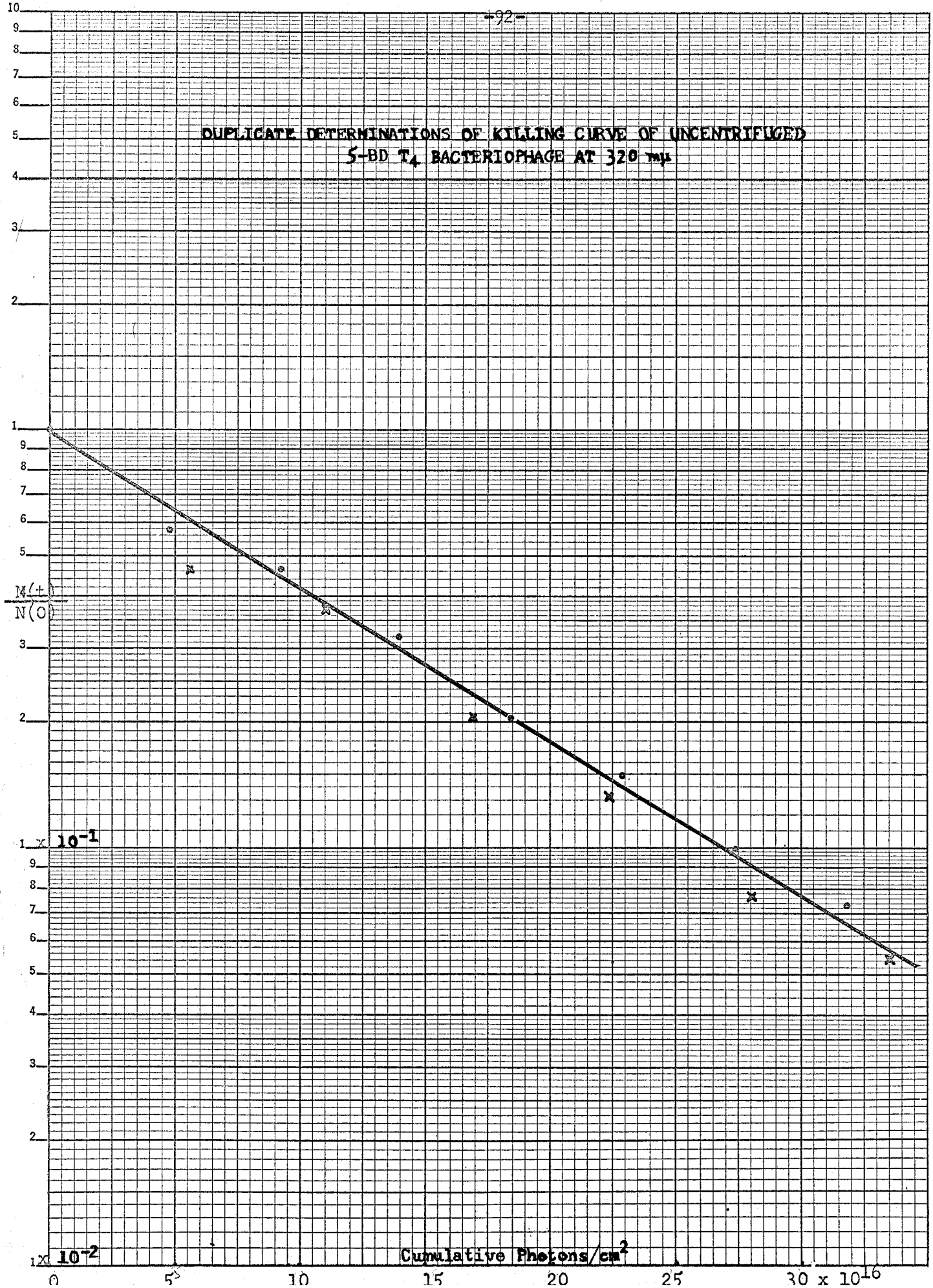

DUPLICATE DETERMINATIONS OF KILLING CURVE OF UNCENTRIFUGED 5-BD T_4 BACTERIOPHAGE AT 334 mμ

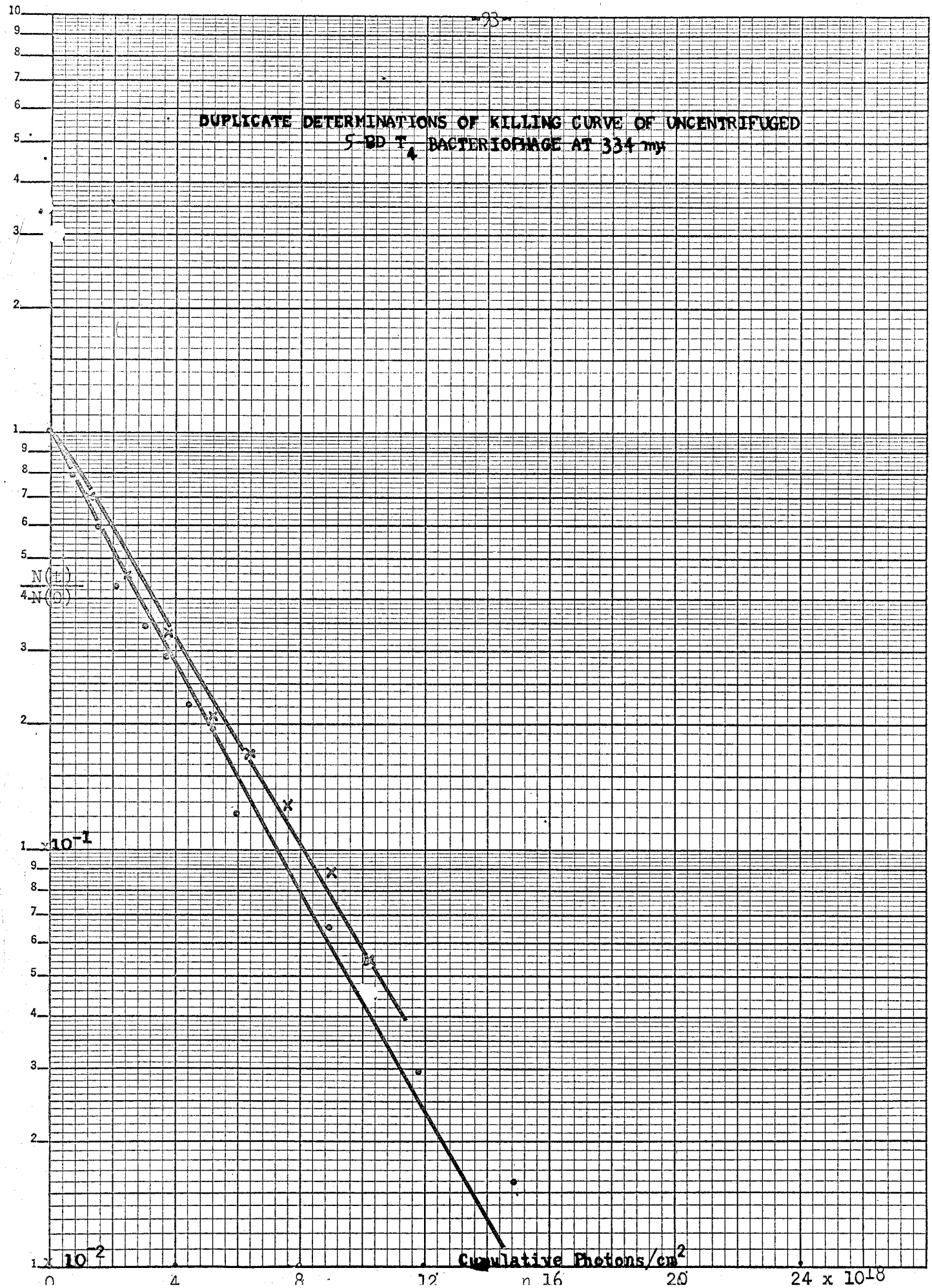

APPENDIX

APPENDIX A: Young-Thollon Prism Analysis*

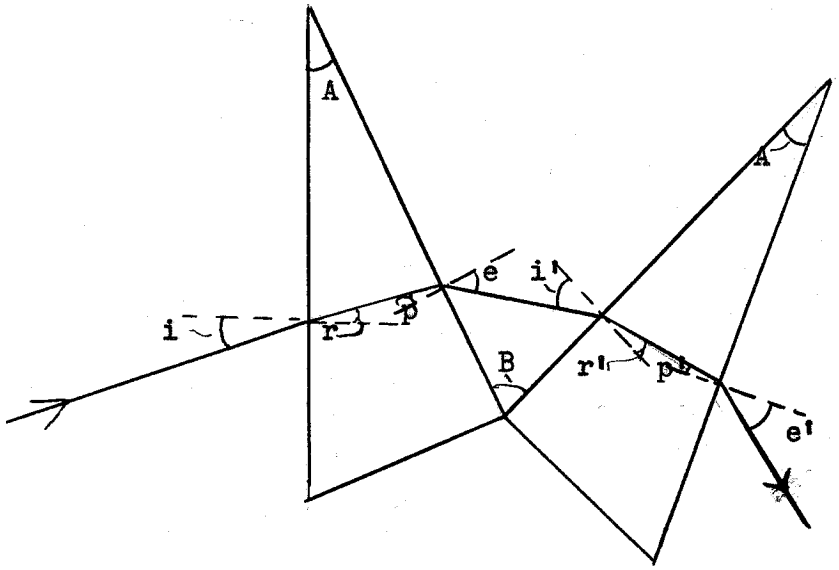

i = angle of incidence to first prism encountered by light

e = angle of emergence from first prism encountered by light

p = angle refracted ray makes with normal to second air-quartz interface encountered by light

r = angle refracted ray makes with normal to first prism surface encountered by light

Primed quantities refer to corresponding angles for second prism encountered by light. Angles i and e are measured relative to normals to the prism surfaces.

$$B = e + i'$$

$$A = p + r$$

Assume another ray passes through the system and that this ray makes a small angle a with the above described ray. Its angles of incidence and emergence are then given by $(i-a)$, $(e+a)$, $(i' - a')$, and $(e' + a')$ whereas the angles corresponding to r and p of the original

*This analysis is that of Thollon (15) as modified to fit the particular operating conditions under which the monochromator was used.

ray are now given by (r - c) and (p + c).

By Snell's Law,

$$\sin (i - a) = n \sin (r - c)$$

$$\sin (e + a') = n \sin (p + c)$$

or $-\sin a \cos i + \cos a \sin i = n (\sin r \cos c - \sin c \cos r)$

or, since a and c are small,

$$a \cos i = n (\cos r)\, c$$

$$a' \cos e = n\, c \cos p$$

so $a' = a \cos i \cos p/(\cos e \cos r)$. (1)

Likewise for the second prism, if a" is the amount the angle of emergence e' is changed,

$$a'' = a' \frac{\cos i' \cos p'}{\cos e' \cos r'}$$

$$= a \frac{\cos i \cos p \cos i' \cos p'}{\cos e \cos r \cos e' \cos r'}.$$

Formula for Dispersion of a Single Prism:

Consider the first prism encountered by the light ray above.

$$\sin e = n \sin p = n \sin (A - r) = n (\sin A \cos r - \sin r \cos A)$$

$$= \sin A\, (n^2 - \sin^2 i)^{\frac{1}{2}} - \sin i \cos A$$

since $n \sin r = \sin i$.

Differentiating,

$$(\cos e)(de/dn)_i = n \sin A/(n^2 - \sin^2 i)^{\frac{1}{2}}$$

$$(de/dn)_i = \sin A/(\cos e)(1 - \sin^2 i/n^2)^{\frac{1}{2}}$$

$$= \sin A/(\cos e \cos r). \quad (2)$$

The dispersion produced by the couple may be considered to consist of two parts: the dispersion produced by the first prism, de/dn, which is further increased by the second prism by the same factor given in eq. (1)

above plus the dispersion of each ray produced by the second prism alone which is given by eq. (2) above:

$$(de'/dn)_{total} = (de'/dn)_{\substack{2nd\ prism \\ alone}} + (de'/de)(de/dn)_{\substack{1st\ prism \\ alone}}$$

that is to say, a ray is first deviated by the first prism by an amount de given by eq. (2) and this deviation is then increased by the factor cos i' cos p'/(cos e' cos r') as found in eq. (1); this ray is next deviated by a further amount given by eq. (2) so that the total deviation is:

$$(de'/dn)_{total} = (\sin A)/(\cos e \cos r) \times (\cos i' \cos p'/(\cos e' \cos r')) + \sin A/(\cos e' \cos r')$$

$$= \frac{\sin A\ (\cos i' \cos p' + \cos e \cos r)}{\cos e' \cos r' \cos e \cos r}.$$

Here the system is operated such that i = e' = 0, so that

sin i = n sin r = 0 or r = 0 so p = A - r = A

sin e' = n sin p' = 0 or p' = 0.

Also n sin p = n sin A = sin e

n sin r' = n sin A = sin i'.

Therefore,

$$(de'/dn)_{total} = 2 \tan A. \qquad (3)$$

Mechanism of Adjustment of Prisms

The prism assembly was adjusted by turning a screw which moved the two prisms simultaneously in opposite directions as the arms connecting the two prism holders with the drum of the screw were increased in length. (See diagram on next page.) The prisms are turned through a very small angle (about 5° over the 100 mμ range used). In doing this a ray emerging from the last prism surface at a slight angle with the optical axis

of the monochromator due to the dispersion given by eq. (3) is made to emerge along it by rotation of the prisms through an angle h given by

Mechanism for Turning Prisms

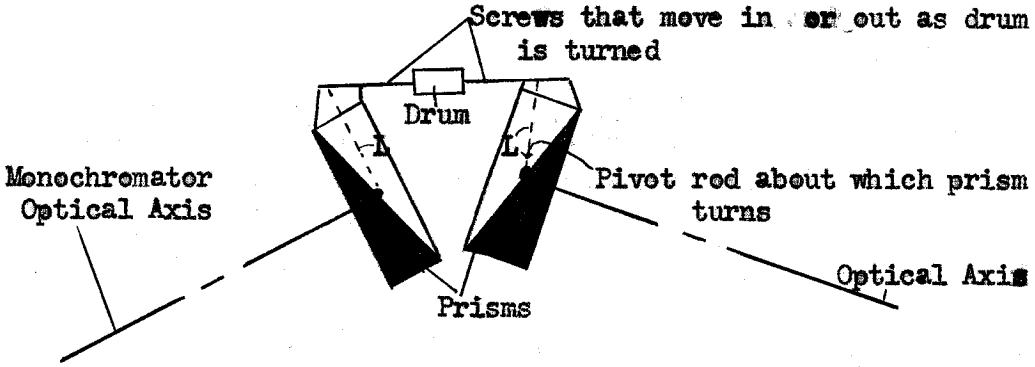

$h = \Delta x/L$, where Δx is the increase in length of the lever arm from the drum to the prism holder due to turning the drum and L is the distance from the rod about which the prism is pivoted to the place of attachment of the screw to the prism holder. (See figure above.)

This angle h must be equal to de' as given by eq. (3) . Thus

$$\Delta x/\Delta\lambda = (\text{const.})\ \Delta n/\Delta\lambda\ ,$$

and the calibration curve for the linear drum scale should be parallel to the plot of the index of refraction of quartz against wavelength.

The calibration curves for the collimating lens settings were also noted to have a similar shape to a plot of index of refraction vs. wavelength for quartz. This should be approximately the case since the linear scales are calibrated in terms of y where $(f_o - y(\lambda))$ = focal length of collimating lens at wavelength λ and f_o is the focal length at some particular wavelength and since by the simple lens formula

$$1/f = (n - 1)(1/r_1 + 1/r_2) = (\text{const.})\ (n - 1)$$

so $$df/d\lambda = - f^2\ dn/d\lambda = - dy/d\lambda\ .$$

Since f varies only about 3 cm over the entire range used and is of the order of 40 cm, f^2 is approximately constant and the slope $dy/d\lambda$ should approximate the slope $dn/d\lambda$.

Calculation of Dispersion of Monochromator

By eq. (3) above $de'/dn = 2 \tan A = 1.154$ since $A = 30^\circ$. Since the exit slit is approximately 38 cm from the second prism, an angle that would subtend 1 mm at the exit slit would correspond to $de' = 1/380$; by the above the corresponding change in index of refraction would be $dn = 1/1.154 \times 1/380 = 2.28 \times 10^{-3}$. From a plot of index of refraction of quartz vs. wavelength it is found that $d\lambda/dn = 1.6 \times 10^3$ mμ at 235 mμ and 5.4×10^3 at 334 mμ so that the wavelength band passed per millimeter of exit slit is $2.28 \times 10^{-3} \times 1.6 \times 10^3 = 3.6$ mμ at 235 and 12.3 mμ at 334 mμ.

APPENDIX B: Relation of Actinity Coefficient to Quantum Yield

Considering a small volume element of depth Δx and using the above defined symbols (p. 21 et seq.), we may write for the photochemical events in time dt:

$$\phi = -dc/(I_o - I)\, dt \qquad \text{by definition.}$$

$$= -a\, c\, I\, dt / I\,(10^{-D\Delta x/L} - 1)\, dt$$

since $-dc/dt = a\, c\, I$

and $I = I_o\, 10^{-D\Delta x/L}$.

$$= +a\, c\, /D \log_e 10$$

since Δx is assumed small.

So $\phi = 2.303 \times 10^{-3}\, a\, e$ from the definitions of D and e.

REFERENCES

1. Khorana, H. G. (1960). The Nucleic Acids, v. 3, E. Chargaff and J. Davidson, ed. Academic Press.

2. Beukers, R., and Berends, W. (1960). Biochim. biophys. Acta, 41, 550.

3. Wulff, D. L., and Fraenkel, G. (1961). Biochim. biophys. Acta, 51, 332.

4. Wang, S. Y. (1961). Nature, 188, 844.

5. Wacker, E., Dellweg, H., and Weinblum D. (1960). Naturwissenschaften, 20, 477.

6. Johns, H. E., Rapaport, S. A., Delbruck, M. (1962). J. Mol. Biology, 4, 104.

7. Smith, J. D., and Markham, R. (1952). Biochim. biophys. Acta, 8, 350.

8. Smith, J. D., and Markham, R. (1952). Nature, 170, 120.

9. Michelson, A., and Todd, A. (1955). J. Chem. Soc., 2632.

10. Lane, B., and Butler, G. (1959). Cand. J. Biochem. and Physiol., 37, 1329.

11. Khorana, H. G., and Gilham, P. (1959). J. Am. Chem. Soc., 80, 6212.

12. Levene, R. and Tipson, R. (1935). J. Biol. Chem., 109, 626.

13. Khorana, H. G. , and Vizsolyi, J. (1961). J. Am. Chem. Soc., 83, 675.

14. Sober, H. and Peterson, E. (1956). J. Am. Chem. Soc., 78, 751.

15. Thollon, L. (1878). Comptes Rendus, 86, 595.

16. Elenbaas, W. (1951). The High Pressure Mercury Vapour Discharge. Amsterdam, North-Holland Pub. Co.

17. Harris, L. , and Kaminsky, J. (1935). J. Am. Chem. Soc., 57, 1151.

18. Harris, L., and Kaminsky, J. (1935). J. Am. Chem. Soc., 57, 1155.

19. Calvert, J., and Rechen, H. (1952). J. Am. Chem. Soc., 74, 2101.

20. Stair, R. and Johnston, R. (1954). J. of Research of the National Bureau of Standards, 53, 211.

21. Leighton and Leighton, (1936). J. Chem. Phys., 36, 1882.

22. Greer, J. (1960). J. of Gen. Microbiology, 22, 618.

23. Stahl, F., Crasemann, J., Okun, L., Fox, E., and Laird, C. (1961). Virology, 13, 98.

24. Litman, R. and Pardee, A. (1956). Nature, 178, 529.

25. Benzer, S., and Freese, E. (1958). Proc. Nat. Acad. Sci., 44, 112.

26. Dunn, J. B., and Smith, J. (1954). Nature, 174, 305.

27. Dunn, J. B., and Smith, J. (1957). Biochem. J., 67, 497.

28. Zamenhof, S. and Griboff, G. (1954). Nature, 174, 307.

29. Barbos, T., Levin, G., Herr, R., and Gordon H., (1955). J. Am. Chem. Soc., 77, 4279.

30. Adams, M. (1950). Methods in Med. Research, 2, 1.

31. Herriott, R. and Barlow, J. (1957). J. Gen. Physiol., 40, 809.

32. Fluke, D. and Pollard, E. (1949). Science, 110, 2714.

33. Franklin, R., Friedman, M., and Setlow, R. (1958). Arch. Biochem. and Biophys., 44, 259.

34. Setlow, R. and Doyle, B. (1953). Biochim. biophys. Acta, 12, 508.

35. Setlow, R. and Boyce, R. (1960). Biophysical J., 1, 29.

36. Winkler, U., Johns, H., and Kellenberger, E. Virology (1962), in press.

37. Gates, F. (1934). J. Exptl. Med., 60, 179.

38. Rivers, T. (1928). J. Exptl. Med., 47, 45.

39. Hollaneder, A. and Olipan, J. (1944). J. Bact., 48, 447.

40. Price, W. C., and Gowen, J. W. (1937). Phytopath., 27, 267.

41. Gates, F., Sturn, E. and Murphy, J. (1932). Proc. Nat. Acad. Sci., 55, 441.

42. Wahl, R. (1946). Ann. Inst. Pasteur, 72, 284.

43. Wahl, R. and Latarjet, R. (1947). Ann. Inst. Pasteur, 73, 957.